Understanding fire histories: the importance of charcoal morphology

Submitted by Alastair James Crawford to the University of Exeter
as a thesis for the degree of
Doctor of Philosophy in Geography (Physical)
In December 2015

I certify that all material in this thesis which is not my own work has been identified and that no material has previously been submitted and approved for the award of a degree by this or any other University.

Signature: ……..

Abstract

Quantifying charcoal particles preserved in sedimentary environments is an established method for estimating levels of fire activity in the past, both on human and geological timescales. It has been proposed that the morphology of these particles is also a valuable source of information, for example allowing inferences about the nature of the vegetation burned. This thesis aims to broaden the theoretical basis for these methods, and to integrate morphometric study of sedimentary charcoal with its quantification. Three key questions are addressed: firstly, whether the elongation of mesocharcoal particles is a useful indicator of fuel type; secondly, whether different sedimentary archives tend to preserve different charcoal morphologies; and finally, the critical question of how morphology affects charcoal quantification.

The results corroborate the idea that grasses and trees produce mesocharcoal with distinctly different aspect ratios. However, the application of this as an indicator of vegetation change is complicated by the inclusion of species which are neither grasses nor trees, and by considerations of the effects of transportation. Charcoal morphotypes in diverse sedimentary environments are shown to be influenced by vegetation types, transportation history, and nature of the fire that produced them.

Previous research has treated charcoal quantification and charcoal morphology as separate issues. Here it is shown that understanding morphology is essential for the accurate quantification of charcoal, since it affects the relationship between volumes and the two-dimensional areas from which measurements are taken. Understanding this relationship could allow such measurements to be used not just as relative measures of past fire activity, but to enable the accurate quantification of the charcoal sequestered in soils and sediments. This has important implications for our ability to understand the effects of fire on carbon cycling, and the role that fire plays in the Earth system.

Acknowledgements

I would like to express my gratitude to Claire Belcher for her advice and guidance throughout the course of this research, and also to Tim Lenton, Dan Charman and Anne Le Brocq, who all provided valuable guidance in the early stages of the project.

I have benefitted greatly from discussions with many researchers in this field, but would like to particularly thank Sarah Baker, Margaret Collinson, Vicky Hudspith and Luke Mander for many helpful exchanges.

Among the numerous technical staff who have helped me over the last three years, I especially thank Angela Elliot and Mark Grosvenor for their advice and assistance.

I thank the following for their permission to collect peat and vegetation samples: Norman Baldock (Dartmoor National Park Authority), Andy Guy (Natural England), Tom Stratton (Duchy of Cornwall), Penny Warren (Gidleigh Commoners' Association), and Iain Park and Peter Greenwood (University of Exeter). I am also grateful to those researchers from whom I have directly or indirectly procured fossil material, including Steve Grimes, Patrick Herendeen and Stephen Hesselbo, in addition to others mentioned above.

I thank Hong Chang and Peter Splatt for their assistance with SEM and CLSM microscopy respectively, and Jeremy Metz for his valuable advice on image analysis methods.

Finally, I am enormously grateful to Emma for her support over the last three years and more, and for putting up with this nonsense.

Contents

List of Figures

Chapter 4

Chapter 5

Chapter 6

List of Tables

List of Formulae

Chapter 1

Chapter 5

List of Symbols and Abbreviations

a	Years
A	The projected area of a charcoal particle
ANOVA	Analysis of Variance
BP	Before Present
C	A factor which accounts for differences in shape when calculating the volume of a charcoal particles from their projected area
cal.	Calibrated (^{14}C date)
CHAR	Charcoal Accumulation Rate
CLSM	Confocal Laser Scanning Microscopy
F	F-ratio; the ratio of variation explained to variation not explained by a model
H_o	Null hypothesis
ka	Thousands of years
Ma	Millions of years
n	The number of individuals in a sample
P	P-value; the probability of obtaining a value as extreme as that found, given the null hypothesis
r	Pearson's product-moment correlation coefficient
r^2	Coefficient of determination (for a least-squares linear model; the square of r)
R^2	Coefficient of determination (multiple regression)
s	Standard deviation (of a sample)
SEM	Scanning Electron Microscopy/Microscope/Micrograph
TIFF	Tagged Image File Format
ρ	Spearman's ρ (nonparametric correlation coefficient)
σ	Standard deviation (of a population)

Chapter 1: Introduction to Palaeofire Reconstruction

1.1 Applications of palaeofire reconstruction

Early work on palaeofire reconstruction (e.g. Iversen, 1964) focused on its role as a driver of, or in relation to, vegetation dynamics, with microcharcoal (typically < 125 μm) being quantified as an adjunct to palynological studies. This remains a widespread application of sedimentary charcoal analysis (Rhodes, 1998). The ability to identify past fire activity is also valuable in archaeological studies; for example due to the occurrence of fire and vegetation change coincident with settlement of upland areas of Britain by prehistoric peoples, which is often interpreted as evidence of fire being used as a land management tool (Simmons & Innes, 1988). Understanding of fire regimes on timescales exceeding the historical record may also be necessary for informed environmental management (Gavin et al., 2007); for example by establishing reference conditions for fire regimes prior to anthropogenic influences, and in planning for fire regimes under future climatic change, based on statistical modelling of fire frequency (Gavin et al., 2007). In all these applications, the effects of fire are understood at the landscape scale.

Palaeofires have less often been studied in relation to global processes. However, wildfire is increasingly seen as an integral component of the Earth system, both affecting and affected by atmospheric composition, climatic change, vegetation dynamics and other factors (Bowman et al., 2009). Quantifying the prevalence of wildfire at different times in the Earth's history therefore has relevance for several branches of the Earth sciences.

Ignition and spread of wildfire are known to be controlled by the level of atmospheric oxygen (Belcher et al., 2010a) and by climate (Belcher et al., 2010b) – implying a global component to variation in fire activity – and fire is in turn a controlling factor in terrestrial carbon balance (Flannigan et al., 2009), land productivity (Watson & Lovelock, 2013), weathering rates and hydrological and mass movement behaviours (Shakesby & Doerr, 2006). In principle, reconstructions of past levels of fire activity could inform understanding of each of these areas.

One question in Earth system science to which the reconstruction of palaeofire activity is especially pertinent is the regulation of atmospheric oxygen content. The persistence of sedimentary charcoal over the last 350 Ma has been used as evidence for a minimum atmospheric O_2 content of c. 15% throughout that time (Lenton, 2001), on the basis of experimental evidence that fire cannot be sustained at lower partial pressures of O_2 (Watson et al., 1978). Lovelock (1988), Kump (1988) and Lenton & Watson (2000) have all proposed fire-linked negative feedback processes for the stabilisation of atmospheric oxygen. Reconstructions of past fire activity have the potential to corroborate such hypotheses. Glasspool & Scott (2010) use fluctuations in inertinite (charcoal) content of coals to model atmospheric oxygen content over the Phanerozoic. It is also necessary to develop a quantitative understanding of levels of palaeofire activity if its role in biogeochemical cycling is to be understood. The incorporation of pyrogenic carbon into soils may be a large component of the global carbon cycle, acting as both carbon sink and oxygen source (Zimmerman, 2010).

1.2 Methods of identifying fire in the palaeoenvironmental record

1.2.1 Charcoal

Analysis of charcoal remains, preserved in lake and marine sediments, peats, soils and terrestrial sedimentary rocks, is the dominant method for reconstructing ancient fire activity, on timescales ranging from the historical to hundreds of millions of years. A number of features make charcoal an especially valuable fire proxy. Firstly, it is universal, because it is always formed in some quantity when wildfire occurs; though this does not mean that it is necessarily preserved. Secondly, it is generally unambiguous as a product of wildfire. Volcanism (specifically lava flows or pyroclastic flows) can also produce charcoals, but these may be distinguished by the larger size of fully charcoalified pieces, and potentially by their situation and resistance to shattering (Scott, 2010). Losiak et al. (2015) have argued that charcoal preserved in the ejecta of a large meteorite impact may have been formed by

the heat of the impact, without fire necessarily occurring; but if this is correct, such events would be extremely rare, and accompanied by widespread evidence of the impact. Thirdly, because charcoal is generally inert by comparison with the parent material from which it is formed, both in the biosphere and in sedimentary environments, the signal is persistent through geological time (Scott & Damblon, 2010), and it may be relatively easily extracted from rocks or sediments for quantification (Mooney & Tinner, 2011). The amount of charcoal in a known quantity of sediment is normally quantified optically, either as a measure of areal coverage on a microscope slide, or as a number of particles in one or more size classes.

Charcoal also has a number of other uses as a palaeoenvironmental indicator. Plant anatomy is preserved in particles of more than a few µm in size (Scott, 2010), and many studies have therefore used charcoal to reconstruct the presence of vegetation types (e.g. Collinson et al., 1999). Where used for this purpose, scanning electron microscopy (SEM) is usually employed for identification (Scott, 2010). Larger pieces of wood charcoal can preserve growth rings, which may convey information on climate (Falcon-Lang, 1999), while density of stomata may be related to atmospheric CO_2 concentration (McElwain, 1998). Carbon isotope composition of charcoal has been used to infer the dominance of C3 or C4 plants, as well as moisture availability (Turney et al., 2001). Charcoal may also be used for ^{14}C dating up to a maximum limit of around 60 ka (Scott & Damblon, 2010), though accuracy is very limited beyond about 40 ka (Moore et al., 1996).

It has been suggested that the reflectance of charcoal is determined by temperature and duration of heating at formation (Scott & Glasspool, 2005). Reflectance measurements have thus been used as a proxy for minimum temperature of formation (e.g. Hudspith et al., 2014). However recent work suggests that this is more likely related to the duration of heating than the temperature (Belcher & Hudspith, in review). The distribution of reflectance values in an assemblage has also been used to differentiate wildfire charcoals from those used as fuel by humans (McParland et al., 2009).

Sedimentary charcoal is conventionally divided into microcharcoal and macrocharcoal fractions, though definitions vary and some authors also use a

mesocharcoal fraction. Whitlock & Larsen (2001) define macrocharcoal as that >100 μm, and Mooney & Tinner (2011) identify "macroscopic charcoal" as "typically >100 μm in length", while Scott (2010) defines particles of 180-1000 μm as mesocharcoal, and those over 1000 μm as macrocharcoal.

1.2.2 Biological indicators

Palynological evidence comes from evidence of fluctuations in vegetation, which may be associated with fire (Whitlock & Larsen, 2001). Such methods are favoured by the co-preparation of microcharcoal particles with pollen. Pollens associated with burning include common heather (*Calluna vulgaris*), *Melampyrum* species, and *Myrica* species (Blackford et al., 2006). Non-pollen-producing plants indicative of fire include bracken (*Pteridium aquilinum*) and club-mosses (family *Lycopodiaceae*) (Tolonen, 1983). Several taxa of fungal spores have also been identified as indicators of fire (Innes et al., 2004; Blackford et al., 2006).

In addition to these species which have a positive association with fire, decline in tree and other pollens may be related to burning (e.g. Tolonen, 1983; Blackford et al., 2006). Swain (1973) used the 'conifer/sprouter ratio' as a fire indicator: species which reproduce vegetatively will recover rapidly following a fire, while conifers, which reproduce only by seed, will take anything between 10 and 40 years to return to abundance in the pollen record. The ratio of conifers to sprouters should therefore be a more sensitive index of fire activity than any individual pollen profile.

Insect, mollusc, and vertebrate remains have also been used as palaeofire proxies (Conedera et al., 2009), and Tolonen (1983) refers to changes in diatom assemblages as evidence of fire.

As well as the presence of indicator organisms, and changes in abundance, forest structure can also be used for more recent timescales. Indirect evidence of fire comes from the "mosaic character of forest stands, which are usually in homogeneous patches with abrupt but irregular boundaries" (Rowe & Scotter, 1973), while age structure can also be interpreted as indicative of periodic

disturbance (Rowe & Scotter, 1973). Even-aged stands are indicative of fire (Zackrisson, 1977). While these measures are insufficient to establish fire histories on their own, they may be used to corroborate other evidence.

1.2.3 Lithological evidence

Lithological fire proxies may include both evidence of pyrogenic erosion, and the presence of fire-altered soil minerals (Whitlock & Larsen, 2001). Swain (1973) assumed charcoal to be of local origin only where accompanied by a rapid increase, then more gradual decrease, in varve thickness – a presumed consequence of pyrogenic sediment influx. Cwynar (1978) also considered concurrent rapid increases in varve thickness as evidence that increases in charcoal represented major fires within the watershed. In these cases, geomorphological evidence is combined with charcoal analysis to improve the record. Conedera et al. (2009) count “fire cracked rocks” and “fire-induced surface weathering of stones” as evidence of fire.

Alteration to soils may be indicative of fire. Reddening of soil in burned areas is associated with depletion of carbon and nitrogen, and is dependent on both temperature and duration of heating (Ketterings & Bigham, 2000). Where present, this effect provides evidence of the autochthonous origin of charcoal within the soil (Jull & Geertsema, 2006).

1.2.4 Magnetic methods

High temperatures and a reducing soil atmosphere cause the formation of ferrimagnetic oxides in topsoil, and post-fire erosion may lead to the formation of a persistent, magnetically distinct layer within lake sediments (Rummery, 1983). The use of magnetic parameters as palaeofire proxies was demonstrated by Rummery (1983) but subsequently neglected (Gedye et al. 2000).

Not all fires will be detectable by this method. Soil temperature must reach around 400 °C (Rummery, 1983). Surface or canopy fires are unlikely to

produce the necessary heating (Gedye et al., 2000). In conjunction with other evidence, magnetic parameters may therefore be used to infer fire type as well as to distinguish between fires of different temperatures. They could also be used to establish whether charcoal originates from within the hydrological catchment (Rummery, 1983). However, Gedye et al. (2000) found evidence for the degradation of the magnetic signal at depth, and false positives may arise from weathering processes or airborne sources (Conedera et al., 2009).

Gedye et al. (2000) conclude that the complexity of the magnetic response to fire dictates "a comprehensive suite of [magnetic] measurements" as no single parameter can be relied on in isolation. The value of magnetic measurements consists in their rapidity and non-destructive nature (Rummery, 1983), and their use in combination with other methods, or for the initial detection of areas of interest (Conedera et al., 2009).

1.2.5 Chemical markers

Molecular markers of combustion have only recently been used as palaeofire proxies (Conedera et al., 2009). Many compounds are potential fire indicators; including direct products of burning, and second degree proxies deriving from the decomposition, diagenesis or other subsequent transformations of fire products (Conedera et al., 2009).

Particularly useful are the isomeric monosaccharide anhydrides levoglucosan, mannosan and galactosan, which derive only from pyrogenic sources (Kirchgeorg et al., 2014). These exhibit low volatility and tend to be absorbed by, or adsorbed onto, aerosols, and may be subject to long-distance atmospheric transport (Kirchgeorg et al., 2014). They may be persistent in ice cores and sediments on millennial timescales, though are quickly destroyed in solution (Kirchgeorg et al., 2014). The ratios of these three species may indicate changes in vegetation burned (Kirchgeorg et al., 2014), at least at low temperatures (Hammes & Abiven, 2013). In any case, the three together are likely a more reliable proxy than levoglucosan alone (Hammes & Abiven, 2013).

Conedera et al. (2009) warn that there remain uncertainties over the stability and longevity of usable compounds, as well as methodological problems involving the measurement of the very low quantities which are often required.

1.2.6 Elemental carbon determination

Another chemically-based method is the determination of elemental carbon content as a proxy for charcoal quantity. Winkler (1985) used nitric acid (HNO_3) digestion to remove organic carbon (along with carbonates and pyrite) before igniting samples (at 450-500 °C for 3 hours) and calculating charcoal content as loss on ignition. Mooney & Tinner (2011) note that this technique is the most commonly used chemical digestion method; but also that it produces distinctly different results to other measures of charcoal content, and has rarely been successfully related to independent fire histories. This is to be expected, as although the quantity measured by this technique may be termed charcoal (Winkler, 1985) or 'Winkler charcoal' (Mooney & Tinner, 2011), the method specifically quantifies elemental carbon, in the form of microcrystalline graphite, which may be only a minor (and highly variable) part of what is termed charcoal in optical quantifications (Winkler, 1985). Thus while 'Winkler charcoal' is a measure of fire activity in itself, it will not allow easy comparison with the results of optical techniques.

Problems associated with chemical digestion methods include inadequate digestion of fibrous, peat-rich sediments (Rhodes, 1998), an inability to resolve small changes in carbon content (Rhodes, 1998), potential error due to thermal decomposition of clay minerals (Whitlock & Larsen, 2001) and an inability to distinguish between the products of biomass burning and fossil fuel burning (Rhodes, 1998). Whitlock & Larsen (2001) note that the results of the chemical digestion method seem unreliable, and Mooney & Tinner (2011), while maintaining their potential, note that chemical digestion methods are little used.

1.2.7 Dendrological methods

Fire scars on living or dead trees, using dendrochronology for dating, often allow the time of burning to be established with an error margin of ±1 year, though in some cases up to ±10 years (Zackrisson, 1977). This method has the clear advantage that the (partial) location of the fire can be determined exactly, where the tree is in situ. Methods based on dendrochronology thus allow high spatial and temporal resolution. However, forest stands suitable for such studies are extremely scarce (Zackrisson, 1977). Dendrological methods are particularly suited to the reconstruction of low-intensity surface fires, and least suited to the high-intensity crown fires which will tend to kill the trees (Whitlock & Bartlein, 2004). Tolonen (1983) notes that they tend to give higher fire frequencies than sedimentary sources.

Caldararo (2002) describes fire histories derived from tree-ring analyses as "unreliable" and "applied without rigorous scientific methods" because scars may originate from injury to the tree from any source. This criticism appears to ignore the specific signs of fire scarring identified by Zackrisson (1977): elongate or triangular shape, usually widest at the base of the trunk; accompanied by a dramatic change in ring width; and showing flecks of charcoal, and a black crust at the edges of the scar. In addition, fire scars form only on the leeward side of trees (Gutsell & Johnson, 1996). Conedera et al. (2009) imply that similar orientation of scars at one location will therefore also be indicative of their formation by fire, and note that it is generally agreed that fire scars do provide a useful proxy. Whitlock & Bartlein (2004) suggest that dendrochronological methods are limited to the lifetimes of the trees used. However, Conedera et al. (2009) add that subfossil wood, e.g. from peat bogs, may also reveal fire history from fire scars viewed in cross-section; though this approach has rarely been used.

1.2.8 Summary of palaeofire reconstruction methods

The diverse records of palaeofire which exist are indicative of the extent to which fire has modified both the biotic and abiotic environment in the past. Conedera et al. (2009) note that "every element of the combustion products

continuum in every sedimentary situation" has potential for reconstructing palaeofires. In addition to this there are the effects which persist in living matter (fire scars, homogeneity of stand ages, species composition) as well as documentary sources for those fire events which occurred in historical times. It is therefore unsurprising that a wide range of approaches have been taken, both in selection of proxies and in choice of methods to quantify them. As in other fields of palaeoenvironmental research, the most successful approach is to use a combination of indices (Tolonen, 1986).

Nonetheless, quantification of sedimentary charcoal has been used more widely than other methods. Variations in the abundance of sedimentary charcoal have been used as an indicator of changes in fire activity at about 1000 sites globally (Mooney & Tinner, 2011), and correlation with charcoal records is often used as a measure of the viability of less well-established methods (e.g. Gedye et al., 2000; Kirchgeorg et al., 2014).

1.3 Formation and nature of charcoal

Combustion comprises two key phases; pyrolysis and oxidation. If both occur, combustion is complete, leaving only mineral ash; but where pyrolysis is not followed by oxidation, pyrolysis products (charcoal) are the result. Charcoal may be formed in wildfires by the sufficient heating of any biomass. In a flaming fire, the surface of the fuel is depleted of oxygen by the flame; thus the solid fuel is pyrolysed to produce charcoal, while the pyrolysate gases are oxidised in the flame. In a smouldering fire, where there is no flame, both pyrolysis and oxidation of the solid fuel occur; the heat penetrates the solid fuel ahead of the oxidation reaction, and although the pyrolysed material formed is subsequently oxidised, a thin layer of charcoal will be left when the oxidation front ceases to advance. All wildfires will therefore produce charcoal in some amount. While microcharcoal is created by any wildfire, significant macrocharcoal production is dependent on fuel type and whether the fire is flaming or smouldering. Grassland fires and smouldering peat fires tend to produce little macroscopic charcoal, while flaming heathland fires and surface fires in forests may produce a lot (Scott, 2010; Rein, 2013).

The process of charcoalification involves the reorganisation of the basic atomic structure to become independent of that of the parent material, but with the preservation of the larger scale morphology (Harris, 1999). Charcoal consists of two phases arranged in a mosaic-like structure; an 'organised' phase consisting of graphitic layers, and a 'disorganised' phase consisting of complex aromatic and aliphatic structures (Cohen-Ofri, 2006). This basic structure was established by Franklin (1950) applying x-ray diffraction to high-temperature (1000 °C) laboratory-created chars of > 99% carbon. Cohen-Ofri et al. (2006) use transmission electron microscopy (TEM) to establish that Franklin's model is applicable to wildfire charcoals, albeit that they have a higher proportion of the non-organised phase due to the lower temperature of formation. The molecular structure of charcoal is still not well understood (Harris, 2013). However, the recent discovery of fullerenes, in which pentagonal carbon rings provide curvature to otherwise planar graphitic structures, has led to new, but not universally accepted, models (Harris, 2013).

Charcoal is part of a continuum of pyrolysis products, dependent on peak temperature (Antal & Grønli, 2003; Figure 1.1). While it is the peak temperature reached which largely determines the nature of the solid residue, including its volatile matter content and other properties, the rate of heating and the duration for which peak temperature is maintained also matter (Antal & Grønli, 2003).

Based on laboratory experiments using a furnace, Jones & Chaloner (1991) consider the pyrolytic transformation of wood to consist of three phases. At temperatures of 180-220 °C, wood is scorched or charred but not charcoalified. At 230-340 °C, true charcoal is formed, while at higher temperatures the charcoal becomes fragile and preservation is unlikely. Scott & Glasspool (2013) have questioned the accuracy of these reported temperatures, on the basis that an external temperature probe was used. Despite this potential source of inaccuracy, Jones & Chaloner's (1991) argument that charred wood should be distinguished from charcoalified wood is important. Although scorched/charred plant material does not have the same resistance as true charcoal, it does have greater resistance to biological degradation and diagenetic alteration (Jones & Chaloner, 1991), and therefore increased preservation potential, as well as

providing evidence of wildfire in its own right. Scorched/charred wood corresponds to retified or torrefied wood as defined by Antal & Grønli (2003).

Solid products of biomass pyrolysis may be termed 'charcoal', 'char', 'coke' and 'soot', but these terms have not always been used consistently. Franklin (1951) established that pyrolysis of organic matter could produce carbons of two distinct types. Graphitising carbons were those which could be converted to graphitic forms by heating to high temperatures (1700-3000 °C), while non-graphitising carbons could not. Harris (2013) identifies these with the prior classification of carbons from organic pyrolysis into soft, dense cokes (graphitising), and hard, low-density chars (non-graphitising). Coke is formed by condensation from the fluid phase, while char remains solid throughout the formation process. 'Coke' may be considered an industrial term, as it is formed in abundance under non-natural conditions, and is not typically used as a term in wildfire science. Combustion residues that are condensed from the gas phase are more commonly termed 'soot' (e.g. Preston & Schmidt, 2006; Hammes & Abiven, 2013).

In a narrow sense, 'charcoal' may be identified with char (Harris, 1999; Hammes & Abiven, 2013), but in a broader sense may encompass both char and coke. Antal & Grønli (2003) term char 'primary charcoal' and coke 'secondary charcoal', and note that many researchers wrongly assume the 'charcoal' composed of these to be the product only of solid-phase reactions[1].

In general, the charcoal studied in palaeoenvironmental archives will fall under the broader definition of Antal & Grønli (2003) (i.e. the products of both solid-phase and gas-phase reactions). However as taphonomic processes may result in differential preservation of the two forms, they need not always be found together; for example fossil charcoals found in Cretaceous-Paleogene terrestrial sediments (Belcher et al., 2003) and 'soot' found at the Cretaceous-Paleogene boundary marine sediments (Wolbach et al., 1990).

The properties of charcoal vary according to the parent material and the charring process. Parent material has been shown to affect density,

[1] In palaeoenvironmental studies, the terms 'primary charcoal' and 'secondary charcoal' are more likely to refer to differences in transport and sedimentation processes, as described in Section 1.4.

mechanical properties, ignition properties and elemental composition (Antal & Grønli, 2003). Peak temperature and heating rate influence the mechanical properties of wood charcoal, and temperature strongly affects its ignition properties and electrical resistivity (Antal &Grønli, 2003).

A notable property of charcoal is that despite reconfiguration of the molecular structure, anatomical features are well preserved (Scott, 2010). Charring does however result in shrinkage of the material (Sander & Gee, 1990)[2]. In addition, the cell wall structure becomes homogenised, such that the layers of adjacent cell walls become indistinguishable (Sander & Gee, 1990). This homogenisation depends on both temperature and duration of heating (Antal & Grønli, 2003). It occurs when the fuel is maintained at a temperature of around 325 °C or higher (Scott, 2010), but this does not directly translate into fire (i.e. flame) temperature or fire intensity (Belcher and Hudspith, in review).

Charcoalification is therefore a process by which the fuel material is altered to obtain a more stable configuration at a molecular level while preserving much of its physical form. The information potentially encoded within a piece of charcoal at its formation includes:

1. The fact of its creation in a wildfire
2. Such taxonomic information as is contained in its form
3. Such environmental information as can be inferred
    a. Indirectly from its taxonomic affiliation
    b. Directly from its anatomy
4. The degree of heat transformation which has occurred
    a. At the anatomical level
    b. At the molecular level
5. Elemental and isotopic information deriving from the parent material

[2] Though Antal & Grønli (2003) note that some types of wood actually swell during pyrolysis.

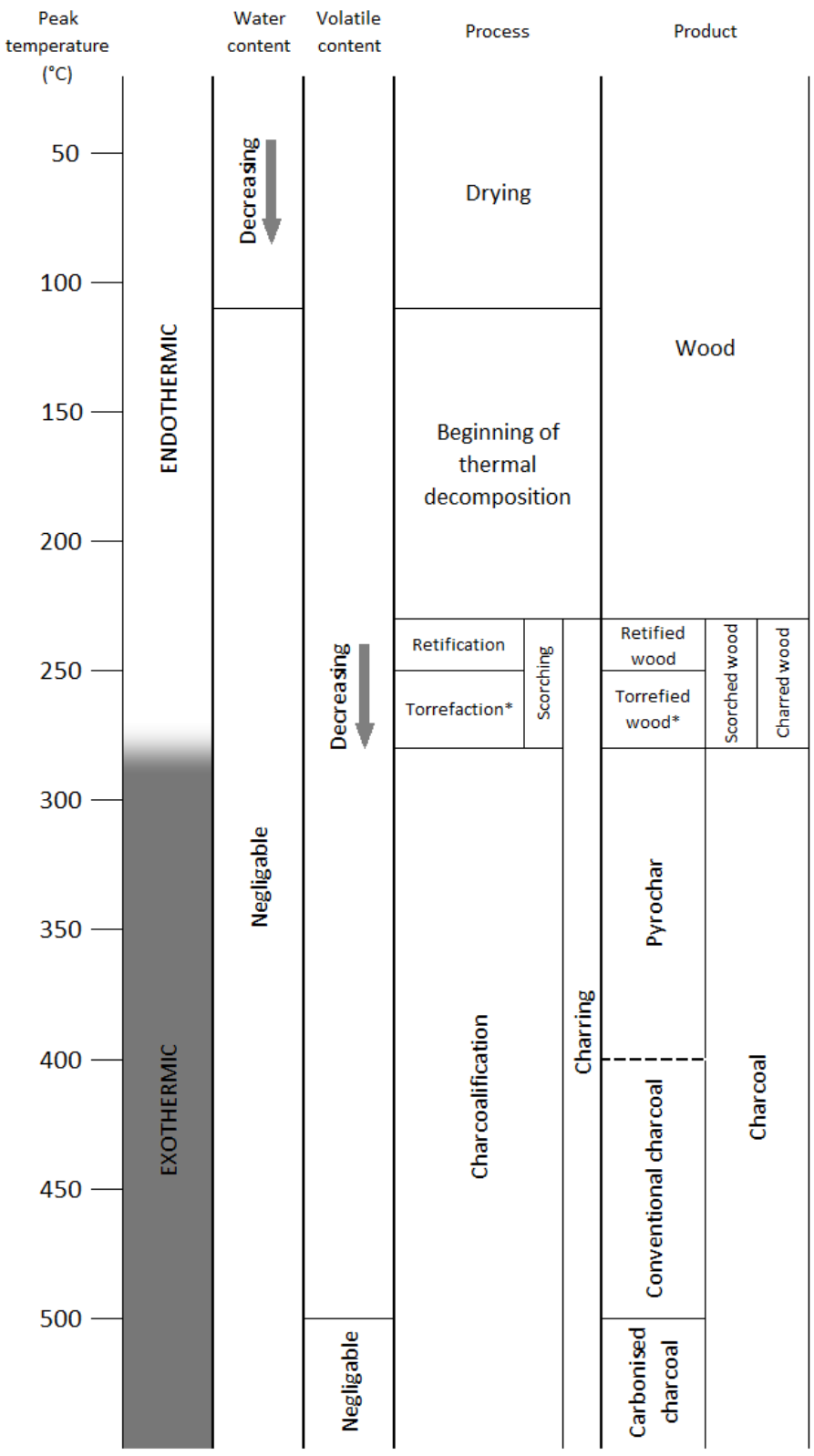

Figure 1.1: Processes and products resulting from the heating of wood to different peak temperatures (sustained for a minimum period). Temperatures based on FAO (1985) and Antal & Grønli (2003); nomenclature additionally based on Jones & Chaloner (1991). Temperatures are based on furnace experiments, and thus refer to the temperature sustained within the fuel itself. This will not in fact correspond to flame temperature in a wildfire. [* Torrefaction occurs only at low rates of heating.]

1.4 Transportation and taphonomy

Between its production and its extraction for palaeoenvironmental analysis, charcoal may undergo transportation by air, water and potentially biota, and be altered by physical, chemical and biological processes. Understanding transportation mechanisms is essential to understand the origin of a charcoal assemblage, while taphonomic changes must be accounted for before making inferences about fuel material or fire from its features.

Empirical evidence from a number of studies (Conedera et al., 2009) shows that microcharcoal (c. 10–200 µm) mostly derives from within 20-100 km of the sampling site, and macrocharcoal (usually defined as > 100-200 µm) mostly derives from within a few hundred metres. It has become normal practice to take microcharcoal to be representative of 'regional' fires, and macrocharcoal to be representative of 'local' fires, though quantifying the exact scale is problematic (Mooney & Tinner, 2011). The difference in transportation distance is related to the fact that microcharcoal is often air-transported while macrocharcoal typically is not.[3]

Clark (1988) created a simple model of aeolian charcoal transport, which predicted downwind distribution of particles as a function of a single injection height, wind speed, and the size and density of the particles. This predicted that pollen slide charcoal (5-80 µm) and thin section charcoal (50-10,000 µm) will exhibit "fundamentally different" behaviour with regard to air transport. Despite the general result of decreasing rates of deposition with downwind distance, Clark's (1988) model also predicted the existence of 'skip distances' between the source and the location of the nearest deposited particles. Empirical evidence for skip distances is not found, and Peters & Higuera (2007) dismiss this result as an artefact of the unrealistic single injection height in Clark's (1988) model. As well as accounting for this, they develop Clark's one-dimensional (i.e. downwind) model into a two-dimensional one, in which probability of charcoal deposition varies laterally to wind direction according to a

[3] Andreae (1983) found that soot was present in air masses of continental origin over remote areas of the Atlantic, in concentrations comparable to those of rural continental areas. This is interpreted by Tinner et al. (1998) as evidence that "particles of 2-5 µm diameter can have continental to global sources." However (or because of this) particles of this size are not normally utilised in charcoal analyses.

Gaussian function. This two-dimensional model may thus be used to infer probable source areas from a given sampling point. They compared the results with deposition from experimental fire, and reported reasonable agreement (r^2 = 0.67, P < 0.001), but only within the experimental range of 200 m.

Scott (2010) warns against the assumption that macroscopic charcoal relates only to local fires, on the grounds that most macrocharcoal is transported by water. The transportation distance in this case will be affected by size, formation temperature, and the material charred, as well as the effect of fire on soil permeability (Scott, 2010). Fire tends to decrease soil infiltration and therefore increase overland flow, which at the catchment scale leads to increased runoff and reduced response times (Shakesby & Doerr, 2006). Conedera et al. (2009) also note that convective processes associated with high-intensity crown fires may carry significant amounts of centimetre-sized charcoal for several kilometres.

Differential transportation of macrocharcoal by water or wind may create a considerable size bias in the final assemblage (Scott, 2010). Understanding of both differential transportation and differential preservation is therefore essential to the correct interpretation of a charcoal assemblage. Reworking of charcoal may also complicate the interpretation of the assemblage, though it may be possible to identify reworked charcoal based on shape and porosity (Conedera et al., 2009). Charcoal incorporated into the sediment during or shortly after a fire event may be termed ‘primary charcoal’; that introduced “during non-fire years, as a result of surface run-off and lake-sediment mixing” may be termed ‘secondary charcoal’ (Whitlock & Larsen, 2001).

After deposition, charcoal may be altered or destroyed by physical, chemical and biological processes. The brittle nature of charcoal is an important factor in its preservation, causing breakage due to compaction and bioturbation (Lancelotti et al., 2010). Alkaline conditions may result in softening and fragmentation of charcoal (Braadbaart et al., 2009). Charcoal is degraded both chemically and microbially (Zimmerman, 2010), reacting at lower rates with increasing temperature or longer duration of charring (Zimmerman, 2010). Since the proportion of the graphitic or aromatic phase increases with formation temperature (Cohen-Ofri et al., 2006), this evidence is consistent with a model

of char as having a stable aromatic phase, and a less stable aliphatic phase (Zimmerman, 2010). Cohen-Ofri et al. (2006) present evidence contrary to this assumption, showing that the graphitic phase of charcoal appears to undergo greater diagenetic change. They observed a “huge” increase in electrical resistivity in fossil charcoal (from the Iron Age and Upper Palaeolithic of Israel) as compared to modern specimens, implying loss of the electrically conductive graphitic phase. The presence of carboxylate groups indicated that the charcoal had undergone oxidation, and if this had affected the graphitic phase it would be in keeping with the change in resistivity. The relative proportion of the non-organised phase increased ~10%; either due to the breakdown of the graphitic phase, or to the ingress of humic acids from the surrounding soil. They find that the evidence is consistent with the oxidation of the graphitic phase into compounds similar to humic acids. However Ascough et al. (2010) suggest that charcoals produced at lower temperatures (< 400 °C) appear to be more susceptible to oxidation, and findings from several studies indicate increasing stability with increasing temperature or duration of heating (Zimmerman et al., 2010).

***

Transportation, reworking and post-deposition changes seriously complicate the interpretation of sedimentary charcoal, and complex procedures have been designed to overcome this interference (cf. Section 1.8). Study sites are typically chosen based on consideration of taphonomic processes. For lake sites, the characteristics of both lake and hydrological catchment should be considered (Whitlock & Larsen, 2001): a large catchment relative to lake size will maximise the charcoal input from a fire event, but also the input of secondary charcoal. Steep slopes may also increase the input of secondary charcoal, from erosion within the catchment (Whitlock & Larsen, 2001). The morphology of the lake and surrounding landscape should be considered in selecting a site, according to whether local or regional fire reconstruction is the target (Tolonen, 1986). Lakes with large inflowing streams will maximise the input of secondary charcoal (Whitlock & Larsen, 2001). Peats may offer a more precise microcharcoal record of local fires, on account of having smaller source areas and much simpler taphonomic processes than lake sediments (Innes et al., 2004).

Conversely, some features of taphonomic change have uses for interpretation of a charcoal assemblage. The sorting of an assemblage into particles by size is indicative of transport, while a wide range of sizes suggests local origin (Scott, 2010). The presence of fragile morphotypes can be taken as evidence that the assemblage has not undergone high-energy transportation (Mustaphi & Pisaric, 2014). It is therefore important to consider the size distribution and morphometry of the charcoal particles in an assemblage.

1.5 The identification of charcoal

Identification of charcoal in the sedimentary record has been based on a number of visual and physical criteria. Whitlock & Larsen (2001) identify charcoal particles as "opaque, angular and usually planar, black fragments"; distinguished from minerals by their lack of crystalline form, from insect cuticles by their thickness, and from other dark plant matter by their brittleness. According to Scott (2010), charcoal may be identified by its being black with a "lustrous sheen", brittle, leaving a black streak, its preservation of anatomy and absence of conchoidal fracturing. In addition, it often fragments into typical sizes. Mooney & Tinner (2011) state that plant charcoal is generally "black, opaque, brittle and angular" and often but not always with "an elongate-prismatic appearance [and] some cellular structure". In practice, it may be found that particles which are clearly identifiable as charcoal under light microscopy and those which are clearly not charcoal are found in association with apparently intermediate forms in a continuum in which the delimiting point is not clear (Patterson et al., 1987).

No straightforward visual test exists, and charcoal is identified by displaying a number of relevant criteria, and by the absence of others. In reality, charcoal researchers will learn to identify charcoal through practice, rather than by such simply described criteria. Whitlock & Larsen (2001) allude to the necessity of learning charcoal identification over time, and recommend examination of experimentally created charcoal and published photographs. Tolonen (1986) is among those who recommend use of reference slides for comparison of possible charcoal with known charcoal. The problem of charcoal identification

is particularly difficult in pre-Quaternary sediments, in which coalified woody material may have a similar appearance (Glasspool & Scott, 2013).

Boulter (1994) suggested that it is not possible to identify true charcoal by visual methods alone, and that "Unfortunately some authors use the term 'charcoal' (carbonized woody plant tissue) without having obtained scientific evidence that that is what they really have." He therefore recommended that black palynodebris that is "opaque, angular" and with "a sharp outline" be classified simply as 'black debris'; though his description of black debris was subsequently used by Daniau et al. (2013) as justification for their identification of such particles as charcoal.[4]

If visual identification will not suffice, other methods for confirming the identification of charcoal are available. Singh et al. (1981) tested their optical identifications of lake sediment charcoal by boiling some of their samples in concentrated nitric acid (HNO_3) for one hour, before washing them with a 5% ammonium hydroxide (NH_4OH) solution. This should have removed any material which could have been mistaken for charcoal. The lack of significant differences in results between these and the standard samples was taken as evidence that identifications had been sufficiently accurate. However, Patterson et al. (1987) have disputed that the difference was not significant; while Clark (1984) suggests that the method is unreliable, as hot nitric acid treatment can be shown to remove charcoal as well as other dark material, and to a degree that cannot be quantified. Rhodes (1998) recommended digestion with 6% hydrogen peroxide (H_2O_2), to bleach rather than remove non-charred dark organic material, while minimizing chemical or physical alteration of the charcoal assemblage.

One method which can give conclusive results is the use of scanning electron microscopy (SEM) to observe the homogenisation of the cell wall layers (Scott, 2010). However, the time and cost involved mean that this is not ordinarily employed for this purpose, except where taxonomic identification also requires it. It should be noted that taking homogenisation of cell walls to be the marker

[4] Furthermore, they did so in a study of grassland fire, which by Boulter's (1994) definition cannot produce charcoal. In this respect, Boulter is not in agreement with other researchers (e.g. Scott, 2010) who have studied charcoal formed from many types of plant and animal material.

of true charcoal results in a narrower definition than is usual, since charcoal is normally considered to be formed at temperatures as low as around280 °C (Antal & Grønli, 2003; FAO, 1985).

In general, it is evident that the descriptions and definitions given by different researchers are not entirely coextensive. In addition, the idea that charcoal identification must be a learned practice, rather than subject to precise description, implies that an element of subjectivity is inevitable. This must be considered when making comparisons between different studies.

1.6 Development of charcoal quantification methods

Early studies (e.g. Iversen, 1964) used stratigraphic charcoal only to indicate the occurrence of a fire at a particular time. Swain (1973) noted that until recently it had been common to ignore charcoal except where “conspicuous layers are visible”. Such a layer would be indicative of an in situ fire. From the late 1960s, systematic charcoal counting was introduced, resulting in measures of continuously varying charcoal influx (Swain, 1973), which necessarily included transported as well as in situ charcoal. Until the mid-1990s, fire histories were most commonly based on quantifying the microcharcoal present in pollen slides (Mooney & Tinner, 2011), though the methods employed in the quantification increased in complexity. The study of macrocharcoal began in the 1980s (Mooney & Tinner, 2011), and has gained in importance since, especially for deep time studies (Scott & Damblon, 2010). However pollen slide preparations remain the most common method of quantifying microcharcoal (Glasspool & Scott, 2013).

Waddington (1969) introduced the use of particle size classes to determine area (Patterson et al., 1987), and this became the dominant laboratory technique for microcharcoal analysis (Tolonen, 1986). With the aid of an eyepiece graticule, particles are tallied in a series of size classes, with the smallest pieces usually ignored and the largest measured individually (Tolonen, 1986). Total ‘charcoal area’ is then calculated by multiplying the number of particles in each size class by its mean or median diameter, and summing these values for all size classes (Tolonen, 1986). Swain (1973) added a suspension of polystyrene

microspheres, in a known concentration, to the samples. When counted along with the charcoal, these allow calculation of the volumetric concentration of charcoal particles in the sediment.

Many subsequent studies followed the basic methods of Swain (1973) (Tolonen, 1986). Exotic pollens may be used in place of plastic microspheres, to give charcoal area per unit volume, and if the rate of sedimentation is known, this can be converted to a flux value (Tolonen, 1986). The counting may be done along just 10 predetermined cover-slip traverses and using only 2 or 3 size classes, and disregarding the smallest particles (<25 μm in diameter) (Tolonen, 1986).

Clark (1982) established the 'point-count' method of charcoal quantification. A series of points, defined by an ordinary eyepiece micrometer, are checked to determine whether or not they 'touch' a charred particle. The area of charcoal can then be calculated from the ratio of points to touches, and concentration and influx rate can be calculated by the pre-existing methods. This method had in fact been used by Iversen (1964), but it was Clark (1982) who described its theoretical basis and brought it into general use. The method is faster than those following Waddington (1969), but gives only total area, not count or size classes. Tolonen (1986) recommended the method as being "as good as more complicated techniques", and recommended it for both pollen preparations and thin sections, though noted that the absence of number and size distributions can make estimating proximity harder, and that non-random occurrence of very large particles can distort the results. Rhodes (1998) reported that Clark's (1982) method was becoming increasingly popular due to its speed. However, Fægri et al. (1989) maintained that "the only practicable method is to count number of charcoal fragments/number of pollen grains, neglecting pieces below a certain size (2 or 5 μm).... Quantitative measurement by microscope is very time-consuming and the results do not deviate much from those obtained by counting."

Clark (1984) tested for effects of standard laboratory processing on the quantification of charcoal. Thirteen pollen preparation regimes were tested, consisting of different combinations of chemical and physical treatments. Area was then estimated using the point-count method, and number of particles >6

μm^2 counted. Clark (1984) concludes that all types of processing will affect the amount of charcoal recorded. Comparisons should therefore only be made where samples have received identical preparation, but even this will not avoid the problem of differential responses to treatment according to degree of carbonisation (Clark, 1984).

While the focus on microcharcoal had been in part a consequence of the study of charcoal in pollen preparations, techniques subsequently expanded to include larger charcoal fractions. Mooney & Tinner (2011) suggest that the quantitative analysis of macrocharcoal began in the late 1980s, with the study of petrographic thin sections, though this technique proved too complex to become widespread. From the early 1990s macrocharcoal has normally been quantified after wet-sieving (Mooney & Tinner, 2011). In deep time, macroscopic charcoal is the principal means to interpret fire history, though few such studies have been published (Scott & Damblon, 2010). As with microcharcoal, there has been a move away from quantifying macrocharcoal according to size classes. This was a consequence of a number of studies which reported that different macrocharcoal size classes significantly correlated to one another and to total charcoal (Mooney & Tinner, 2011). Mooney & Tinner (2011) recommend using whichever size fraction is easiest, according to the equipment available and the expected concentration of particles.

A range of competing methods of charcoal quantification have therefore developed: counting, area estimation by size class tallying, and stereological point counting, as well as measurement by image analysis (see Section 1.10). Rather than newer or evidently more accurate methods displacing older ones, the question of how best to quantify sedimentary charcoal remains a source of debate.

1.7 Quantification of sedimentary charcoal at different dimensions

Patterson et al. (1987) wrote that methods which assess area were generally considered to give better estimates than particle counts, but that, if count and area are significantly correlated, there may be little benefit in measuring the

latter, even by Clark's (1982) point-count method. More recently, a number of researchers have promoted the idea that areal measurement of charcoal particles may be unnecessarily time-consuming, and that reliable fire histories may be obtained from simply counting particles.

Tinner et al. (1998) used a historical database of fires to calibrate lake-sediment fire reconstructions with fire occurrence and area burned, at Lago di Origlio in Switzerland. Image analysis was employed for measurement of area and other parameters, on both pollen slides and thin sections. By linear regression of pollen-slide data for charcoal area and number, they derived an equation to predict area from number. This was tested on an 11 ka data series, with the result that measured and predicted areas did not differ significantly at a confidence level of 95%. Tinner et al. (1998) suggest that measurements of area or categorisation into size classes may therefore be redundant for regional-scale reconstructions. However, such an equation could not be derived for the larger particles present in thin sections, and so Tinner et al. (1998) favour retaining areal measurement of these.

Extending the work of Tinner et al. (1998), Tinner & Hu (2003) used lake sediment cores from Lago di Origlio and two further lakes in the region, and sought to establish the relationship between number and area of charcoal particles. Area/volume and count/volume for pollen-slide charcoal were highly correlated at all three sites, the covariance even mirroring minor changes in concentration (Tinner & Hu, 2003). Linear regressions were produced for the two new sites, in addition to that of Tinner et al. (1998). Number concentrations accurately predicted area concentrations at all three sites. At each site, number explained 82-83% of area variability (Tinner & Hu, 2003).

Tinner & Hu (2003) also tested whether a number-area model from one site could be used to predict concentrations in another. For each possible paring of their three sites, the model from one was used to predict area from number in the other, and vice versa. Predicted area values matched those measured, with *r* values of between 0.86 and 0.89. They concluded that, for the vegetation types studied ("shrub tundra, boreal and temperate forests") an equation relating count to area derived at one site can be used to estimate area from

count at another, provided that pollen preparation remains the same. Area measurement in standard pollen slides was therefore held to be unnecessary.

Finsinger & Tinner (2005) subsequently addressed the question of how many particles need to be counted per slide to provide an accurate measure. As particle concentration estimates obtained from counts of 200-300 particles (both charcoal and marker grains) were not significantly different from those obtained from counts of 1000 particles, they recommended that a count of 200 particles is sufficient for a 95% confidence level, as long as the charcoal-to-marker ratio is not too high or too low.

Conedera et al. (2009) conclude from these studies that "there is little value in quantification of size-classes or estimation and measurement of areas (e.g. point-count estimation following Clark, 1982; image analysis) of charcoal particles in pollen-slides", while Mooney & Tinner (2011) report that counting methods have been favoured in the last decade.[5]

However, while Tinner & Hu (2003) had identified strong and consistent linear relationships between count and area (r^2 = 0.83, 0.83, 0.82) for microcharcoal in boreal lake sediments, Ali et al. (2009) found that relationships were both weaker and more heterogeneous (r^2 = 0.69, 0.53) for macrocharcoal, and Leys et al. (2013) found that the relationship was weak (r^2 = 0.28) for microcharcoal in a Mediterranean lake record.[6]

***

While there has been extensive discussion of how well correlated records based on count and area may be, very little has been said about how well correlated either record might be with a volumetric measurement of charcoal, if such a measure were to be taken.

[5] While Tinner et al. (1998) and Tinner & Hu (2003) recommended the use of areal measures of charcoal abundance, and proposed the use of particle counts as a quick way to obtain these, the more recent studies (Finsinger & Tinner, 2005; Conedera et al., 2009) recommend the use of particle counts as a measure of fire activity in themselves.

[6] Asselin & Payette (2005a) have also asserted that counts and areas are "highly correlated" for macroscopic charcoal, citing Asselin & Payette (2005b); although the latter paper contains no reference to this correlation.

Weng (2005) has highlighted the problems inherent in using measurements of a lower dimension than the charcoal itself, pointing out that fragmentation of charcoal during processing will lead to an increase in measured area despite the amount of charcoal remaining the same. To account for this problem, Weng (2005) derives a formula to convert areal measurements into volumes:

$$V_t = C \sum_{i=1}^{N} A_i^{3/2} \tag{1.1}$$

where V_t is the volume of charcoal in the sample, C a constant, and A_i the area of a charcoal particle.

Weng's (2005) hypothesis is that correlation between measurable area (e.g. on a slide) and the unmeasured depth of the particles should allow the latter to be estimated from the former. Weng (2005) notes that his volume results remained "relatively stable" as the number and area of particles "increased dramatically" upon breaking up of the charcoal pieces. However, the constant C may vary with fuel, as different fuels may produce particles of different shapes (Weng, 2005), and this would therefore have to be determined experimentally in different situations. The amount of experimental work needed to produce C values for the range of conditions needed is unknown. However, Weng (2005) suggests that even taking C as equal to 1, the method will necessarily be superior to techniques based on particle counts or area estimations. The method has been little used; although the work of McMichael et al. (2012a & 2012b) is an exception.

Ali et al. (2009) noted that there had been no attempt to test whether measurements of number, area or volume actually produce comparable results when used to reconstruct fire histories from macrocharcoal. Although significant correlations have been found between count and area in some studies, Ali et al. (2009) find that the regression functions relating count to area differ according to location "indicating the difficulty in predicting total charcoal area of a sample with a single equation, as suggested by Tinner and Hu (2003) for pollen-slide charcoal." Ali et al. (2009) use two lake sediment records to compare the three approaches, measuring number and area by standard

methods, and using Weng's (2005) formula to derive volumes from the latter. They find that "measuring charcoal accumulation rates by area, number or estimated volume all provide comparable fire-history interpretations when using a locally-defined threshold to infer fire occurrence." This allows legitimate comparisons of data obtained by these three different methods.

The only prior empirical study of the relationships between measured areas and measured volumes of sedimentary charcoal particles was conducted by Belcher et al. (2013b), who apply confocal laser scanning microscopy (CLSM) to measure volumes of c. 100 particles each of modern microcharcoal and mesocharcoal, and Cretaceous mesocharcoal. They warn that the method is not viable for regular quantification of sedimentary charcoal due to the time and cost involved. This study revealed approximately linear relationships between volume and area for both modern and fossil mesocharcoal. A relation of $y = 13x$, where y is volume and x is area, was proposed for the conversion of mesocharcoal area measurements to volumes, dependent on corroboration by further studies, using charcoal of different ages, taxa, organs and size fractions.

There has in general been an assumption that to measure the area of charcoal seen in a sample ought to be a more accurate measure of its amount than to count the number of pieces. Thus arguments for using count methods are based on demonstrating correlation between the results of the two approaches. While the tendency in the last two decades seems to have been toward acceptance of the suitability of count measures, evidence on the nature of these correlations remains equivocal. For practical reasons, the question of how well either type of measure might correlate to measurement of the actual volume of charcoal has been largely ignored. Weng's (2005) formula is of little practical use unless the variation in the value of C can be understood, while the suggestion of Belcher et al. (2013b) that a simple linear relation may pertain between the two measures requires further study both for corroboration and to determine the limits of its applicability.

1.8 Interpretation of charcoal curves

Whichever particular method is used to quantify charcoal, a series of samples from different depths will normally be used, in combination with a dating method, to produce a curve of charcoal influx over time. The charcoal measurements are often converted to a charcoal accumulation rate (CHAR), to account for changes in sedimentation rate.

The interpretation of such a record is complicated. Tolonen (1986) wrote that "Very little is known about the relationship between the charred particle curves and the intensity and/or frequency of fires, but it is usually assumed that relatively high frequencies and/or intensities of fire are expressed by the charred particle peaks". A charcoal curve by itself does not allow differentiation between number, extent and frequency of fires (Innes et al., 2004), and there is no empirical evidence to link magnitude of charcoal peaks to any single characteristic of fire, such as severity or area burned (Marlon et al., 2009).

However, peaks in a charcoal record are often interpreted as individual fires, and series of peaks as indicators of fire frequencies (e.g. Swain, 1973; Cwynar, 1978; Millspaugh et al., 2000). Several problems are inherent in this approach. Firstly, there is the danger that the magnitude at which a peak is held to be distinct from background variation is arbitrary. Although methods have been developed to identify a threshold value which distinguishes peaks from background variation (Section 1.8), the theoretical basis and assumptions underlying such methods are questionable (Section 1.8.5), and strong biases may be introduced by their use (Higuera et al., 2012). Secondly, the 'fire frequency' produced does not have the same meaning as the fire frequency used in other fields of fire science, which is the average number of fires at a given point per unit time (Davies, 2013). Depending on the source area of the charcoal, the different fires used to derive this frequency may not have burned the same area of ground. Also, the temporal resolution of the record must be finer than the fire frequency in order to capture it; otherwise a peak may represent more than one fire. For this reason, some researchers interpret peaks as 'fire episodes', defined as one or more fires occurring during the time spanned by a charcoal peak (Marlon et al., 2009), rather than simply fires. Peak frequency is therefore to be interpreted as 'fire episode frequency' (Marlon

et al., 2009), although this may then be abbreviated back to ‘fire frequency’ (Marlon et al., 2009).

To avoid this confusion, and in recognition that changes in frequency and in biomass burned cannot be separated, some authors interpret changes in charcoal influx as changes in ‘fire activity’, defined by Marlon et al. (2009) as “biomass burned and fire frequency”, though they also note that it can vary with the proximity of the fire. Taking charcoal as a measure of ‘fire activity’ avoids prejudging the contributions of these factors, before that measure is interpreted with reference to other aspects of the palaeoenvironmental record. While this terminology is unspecific, this reflects the nature of the information.

Even regarding fire activity (i.e. charcoal influx) as a combination of frequency and mass burned may be too simplistic. The charcoal influx will also be affected by variability in the proportion of the burned material that is charcoalified (Antal & Grønli, 2003), by transportation processes (Whitlock & Larsen, 2001), and potentially by the decay of charcoal post-deposition (Scott & Damblon, 2010).

1.8 Statistical treatment of charcoal records

A set of statistical procedures has been developed for the purpose of defining specific fire events and frequencies from the variations in charcoal abundance which are revealed by measurement of count or area. The process may consist of up to 6 stages (Higuera et al., 2010):

1. Interpolation: to produce a time series with regular intervals.
2. Transformation: for the purpose of stabilising variance.
3. Smoothing: to define the ‘background’ component.
4. Detrending: to define the ‘peak series’ by subtraction (or sometimes division) of the background component from the original series.
5. Thresholding of the peak series: To separate ‘fire’ and ‘noise’ components.

6. Minimum count screening: to remove peaks formed from a statistically insignificant number of particles

1.8.1 Interpolation & Transformation

While samples taken from a sedimentary sequence may or may not be equally spaced in depth, equal spacing in time is highly unlikely due to changing sedimentation rates. Interpolation is therefore used to produce a time series with regular intervals. Logarithmic or other transformations may then be applied for the purpose of stabilising variance, thus allowing the subsequent use of parametric statistical techniques. Both of these processes are carried out for the purposes of making data handling easier, rather than elucidation of the charcoal record itself.

1.8.2 Smoothing & Detrending

Detrending of charcoal time series is a particular case of the method of time series decomposition (Kendall, 1976), by which a measured quantity varying as the sum of several forces (uniform, cyclical and random) is separated in an attempt to define the magnitude and frequency of these components. In sedimentary charcoal analysis, two constituent components are supposed: a low frequency background component, and a higher frequency peak component (Long et al., 1998). The peak component is of interest as it is considered to consist of individual fire events within or close to the watershed of the lake (Long et al., 1998). The background component derives from charcoal which has undergone a greater degree of transport in space and/or time (Long et al., 1998), and reflects long-term changes in fire regime (fuel characteristics and area burned) and taphonomic and transport processes (Kelly et al., 2011).

Long et al. (1998) first defined the background component by means of a locally weighted moving average. Every point in the time series is replaced by a weighted average of the values within a surrounding window. The weighting assigned to each point within the window is determined according to a tricube

weight function (Cleveland, 1979) centred on the point being replaced. With the high frequency component thus removed, the remaining signal is taken to be the background component, and can be subtracted from the original signal to give the peak series. Subsequent studies have generally followed this approach (Gavin et al., 2006; Marlon et al., 2008; Higuera et al., 2010; Kelly et al., 2011; Finsinger et al., 2014).

1.8.3 Thresholding of peak series

Clark et al. (1996) wrote that "Identification of the peak magnitude that might indicate local fire is implicit in many charcoal studies, but rarely calibrated. This magnitude is critical, however, because it determines the fire frequency...." For thresholding, as for detrending, the selection of an appropriate value can be informed by comparing the results to known fire events (Long et al., 1998). This may be done by reference to historical records or tree ring data (i.e. fire scars or stand ages) but is again limited by the timeframe (Higuera et al., 2010). A number of mathematical methods have therefore been employed to separate the two (supposed) distributions.

Clark et al. (1996) assume that the distribution of peak heights will be bimodal, with high values from fires at the lake edge, and low values from the 'background'. They calculate a 'sensitivity index' designed to return minimal values for the rarer peak heights intermediate between these:

$$s_{\mu C'} = \frac{\delta\mu/\mu}{\delta C'/C'} \tag{1.2}$$

where μ is the mean interval in years between values exceeding C'.

This is calculated for a range of values of C'. Values close to zero should indicate a suitable location for the threshold point between the two distributions, where a change in the exact threshold value does not affect the resultant frequency. However, the peak height distribution may not be bimodal, as was found in one case by Clark et al. (1996).

Gavin et al. (2006) introduced another method (which they used in conjunction with tree ring evidence and assessment of the sensitivity of frequency to threshold value), by modelling the peak distribution as the sum of two Gaussian distributions. One distribution is taken to be the local fire signal, the other to be composed of reworked and long-distance charcoal as well as "analytical noise". These two distributions are defined by Gaussian mixture modelling, using the CLUSTER program of Bouman (2005). This approach assumes that the "noise" component is normally distributed with stationary mean and variance, and that there are enough samples in the data set to characterise this distribution (Higuera et al., 2010). Higuera et al. (2010) argue that normality of the noise distribution is supported by both modelling and empirical evidence, but also suggest that skewing of this distribution is possible, with deleterious effects on the reliability of the method. The problem of homogeneity of variance and mean may be overcome by performing the method only for subsets of the data where these are met (in effect, applying a local threshold rather than a global one), or by defining the peak series in such a way as to produce stable variance (Higuera et al., 2010). That there are enough samples for the modelled distribution to adequately represent the actual data can be tested by using a goodness-of-fit statistic to assess "the probability that the empirical data came from the modelled Gaussian distribution" (Higuera et al., 2010). However, the stationarity of mean and variance becomes less likely the larger the data set is, and so a trade-off exists between this and the assumption that the sample is large enough (Higuera et al., 2010).

1.8.4 Minimum Count Screening

Application of a threshold does not necessarily mean that the peaks identified will differ from the background count by a statistically significant amount (Higuera et al., 2010). Higuera et al. (2010) describe a test[7] to identify those peaks which may be a result of sampling variation, based on a statistic which gives the probability that particle concentrations from two consecutive samples originate from the same Poisson distribution.

[7] Both Higuera et al. (2010) and Finsinger et al. (2014) attribute this method to Gavin et al. (2006), who do not in fact mention it.

Finsinger et al. (2014) introduce a method which can be applied to area measures, as the above applies only to count measures. For each identified peak in CHAR area, a set of synthetic CHAR area peaks is calculated, each having the same number of particles but an area based on random sampling of the real areas of individual particles from within a defined time window around the peak. 10,000 bootstrap samples are generated for each peak, and the peak is accepted if its area exceeds the 95th percentile of the bootstrapped distribution.

1.8.5 Critique of statistical treatments

Interpretation of macrocharcoal records may thus take place after the data have undergone a complex series of transformations, with each step involving certain assumptions and potentially arbitrary decisions. The need to guard against bias in such a process is evident. Issues which must be considered may be summarised as follows:

1. Interpolation of the time-series to obtain values for points in time not actually sampled necessarily introduces a degree of error.

2. Transformation for homoscedasticity has the effect of supressing larger peaks and amplifying smaller ones. The decision of whether and how to transform is thus likely to affect calculation of fire frequency.

3. To regard a time series as the sum of a number of components is to impose a model on the data, which must be rejected if the data do not fit (Kendall, 1976, p. 16). Arguing that a two-component model is suitable, Long et al. (1998) cite work by Whitlock & Millspaugh (1996), who studied the incorporation of charcoal into lake sediments following modern fires. However, while this study demonstrates that charcoal is deposited in sediments both directly and through reworking, this does not amount to a demonstration of a duality between the two types of deposition. It is universally accepted that lake sediment charcoal will contain both particles produced recently and nearby, and others longer ago and further away. If there were an intermediate range from which

they could not originate, it would undoubtedly be legitimate to seek to separate the two. However, the probability that a particle originates from any particular point declines as a continuous function of that point's distance from the sampling site (Peters & Higuera, 2007). A continuous distribution can only be divided into two components on an arbitrary basis. Insofar as the separation of the two components is supposed to be that of local and recent vs. transported and reworked charcoal, the separation must be arbitrary.

4. In applying the locally weighted regression method, a function for the smoothing window, comprising both its width and its shape (i.e. weighting as a function of distance), must be selected, and it is not clear that this can be done on a non-arbitrary basis. Long et al. (1998) state that the use of the tricube function "allows points closer to the center of the window to influence the weighted average more than points near the edges of the window", though Cleveland (1979) notes that decreasing weight with distance is a property of any reasonable function. Long et al. (1998) also state that the window width "can usually be selected by visually comparing the resulting background component with the CHAR time series". Selection of the width is informed by comparison of the results with known (i.e. historical) fire events at the site, or with present-day fire regimes in analogous environments. The robustness of the method to variation in width was assessed by comparison of the results of different window widths with present-day data. The legitimacy of the smoothing record therefore rests on its producing results in conformity with understanding of current and recent historical fire regimes. This incorporates a bias against falsification of any preconceived model of fire history.

5. The use of a sensitivity index to select a threshold point may be an attempt to avoid an arbitrary choice. However, as is seen in the results of Clark et al. (1996), it is successful only where the frequency distribution is indeed bimodal. Where that is the case, the threshold point should be identifiable from a plot of the frequency distribution. Identifying a threshold point by Gaussian mixture modelling necessitates several assumptions about the data distribution (as described above),

and the trade-off between sample size and stationarity of mean and variance (noted by Higuera et al., 2010) suggests a fundamental problem in meeting these.

There is also a lack of consistency as to what the thresholding is intended to remove. While some authors refer to the removal only of "random variability" or "noise" (Kelly et al., 2011; Leys et al., 2013; Finsinger et al., 2014), others include variability caused by "distant fires" and "charcoal redeposition" (Gavin et al., 2006). If the thresholding is intended to remove variability from these sources, it is a tacit acknowledgement that the detrending is inadequate.

6. Finally, the peak screening method described by Higuera et al. (2010) and attributed to Gavin et al. (2006) makes further assumptions about the shape of the data distribution, specifically that the distribution of possible particle counts around the average for a given sediment volume will approximate a Poisson distribution.

1.8.6 Summary

The quantitative treatment of charcoal records over the last two decades has thus become increasingly complex. The program CharAnalysis (Higuera et al., 2009) now allows these steps to be carried out in an automated fashion. However, each step carries some risk of introducing bias to the charcoal record.

1.9 Morphology of sedimentary charcoal

Charcoal morphology has been proposed as a potentially valuable source of palaeoenvironmental information which could be obtained alongside quantification of the charcoal, but without the time and cost associated with SEM. The primary use of this method is likely to be in taxonomic identification, and a number of authors have promoted the idea that the basic morphology of mesocharcoal could be used to indicate the nature of the material from which it was formed. Relationships of morphological features to aspects of fire, and

transportation effects, are also possible. These studies have taken one of two methodological approaches, either using human vision to classify particles according to a set of rules intended to categorise them, or using computerised image analysis to calculate morphometric parameters (such as 'roundness' and 'elongation') which can then be assessed statistically.

Umbanhowar and McGrath (1998) used the image analysis approach to assess differences in morphometrics between laboratory-created mesocharcoal (125-250 µm and 250-600 µm) from eight grass species and the leaves and wood of eight tree species, discovering significant differences in certain morphological parameters between the three material types. They suggested that the length-to-width ratio of charcoal particles might be used to identify their source as either grassland or forest fire; grassland charcoal being more elongate.

Enache & Cumming (2006) suggested that morphology may be important in selecting charcoal particles for fire histories. In a study of charcoal in 20th century lake sediments, they identified seven morphotypes (>150 µm), which were differentially correlated to area burned within 20 km of the lake, as recorded in forestry records. One morphotype ('Type M') was identified as a better indicator of fire events than total charcoal, perhaps on account of its fragility limiting transportation and redeposition. Enache & Cumming (2007) found one of the more robust morphotypes ('Type F') to be correlated to precipitation, not fire, suggesting that it is associated with secondary transport. Enache & Cumming (2009) propose that a "Charcoal Morphotype (CM) fire index" be used, based on a regression model which uses Type M and Type F charcoal as independent variables to predict area burned. They present evidence that both Type M charcoal (as well as the CM index) is correlated with palaeoclimate proxies where total charcoal is not. Moos & Cumming (2012) also found that fire frequency calculated (by peak analysis) from Type M charcoal to be consistent with palaeoclimate proxies, while that derived from total charcoal was not.

Jensen et al. (2007) returned to the effects of plant anatomy on morphology, describing five morphotypes from a minority of particles (125-250 µm) that were morphologically distinctive in a Holocene lake sediment core. They found it was possible to reproduce four of these to some extent by selection of parent

material when producing charcoal under laboratory conditions. Mustaphi & Pisaric (2014) have produced a more extensive classification of macrocharcoal (c. 100 µm to 2 cm) morphologies from a series of Holocene lake sediment cores in British Columbia, Canada. Their classification consists of 7 broad morphological categories and 27 subclasses, based on overall shape, dominant surface texture and other "major features". Unlike earlier studies, this classification includes all of the particles studied, rather than identifying only those with distinctive morphologies. The classification is intended to be adaptable to other environments. Mustaphi & Pisaric (2014) also relate these classifications to morphotypes produced by experimental burns, observing that this is possible for some morphologies but not others.

The idea that basic morphology could be a valuable source of information has been stated many times, but despite the studies noted above demonstrating the effects of fuel type and transportation on morphology, practical applications have been limited. Exceptions to this have been several recent studies (Aleman et al., 2013; Daniau et al., 2013; Lim et al., 2014; Colombaroli et al., 2014) which have used Umbanhowar & McGrath's (1998) demonstration of different aspect ratios between grassland and woodland charcoals to infer changing proportions of grassland and woodland biomass represented in the charcoal record.

1.10 Image analysis

The use of computerised image analysis applied to sedimentary charcoal has been proposed both as a means of rapid (areal) quantification, and for the purpose of taking morphometric measurements. Progress has to date been frustrated by the inability of systems to automatically distinguish charcoal from certain other materials.

Clark (1982) thought contemporary image analysis generally more time-consuming than manual point counting for the measurement of area. Patterson et al. (1987) applied image analysis with limited success, finding that the system employed was unable to consistently distinguish between charcoal and "other black or dark-edged material". They suggested that with suitable pre-treatment

of samples and “appropriate” programming, such a system could provide fast and accurate counting of “suitably pure” samples.

In keeping with other fields of palaeoenvironmental work (Francus et al., 2004), the application of image analysis to charcoal quantification was first used to a significant extent in the 1990s. MacDonald et al. (1991) compared measures of microcharcoal obtained by image analysis, based on the optical density (opacity) of the particles, with those obtained by optical counting using standard methods (Tolonen, 1986; Patterson et al., 1987). Image analysis failed to register one charcoal peak, and produced consistently lower estimates of area, which was accounted for by the exclusion of the smallest fragments, and by the lower optical density of the edges of charcoal particles. Horn et al. (1992) also developed an automated image analysis system based on optical density to determine numbers, areas and size classes of microcharcoal particles. While both MacDonald et al. (1991) and Horn et al. (1992) reported that the results of image analysis were significantly correlated with those of standard methods, this does not provide any information on the utility of one method over the other. Earle et al. (1996) used OPTIMAS image analysis software, using visual identification of charcoal to recalibrate the software for each sample; the software then identifying the number and area of particles with equal or lower luminescence. Thevenon & Anselmetti (2007) used ImageJ software to threshold images and measure their charcoal area, relating the inferred fire history to a number of historical episodes.

Other researchers have attempted to go beyond using image analysis for individual fire histories, and employed it to assess the utility or comparability of different methodologies. Tinner et al. (1998) used image analysis to derive relationships between charcoal area and particle number, which led them to question the need for making areal measurements rather than simply counting, when producing regional histories . Clark & Hussey (1996) applied image analysis for the purpose of allowing retrospective comparison of charcoal estimates obtained by different methods. Particles in thin sections of sediment were visually identified using optical microscopy; then IMAGE image analysis software was used to measure the area, major and minor axis length, orientation, and projected length (as subtended on the sedimentation plane) of

the particles. The data obtained were used to derive correction equations, to allow comparison of charcoal quantifications from different methods.

The potential of image analysis for charcoal determination has developed considerably since it was first applied, though no routine methodology has been established and it has not displaced human-optical methods. Mooney & Tinner (2011) report that image analysis software now allows macrocharcoal to be quantified "with relatively little effort". Mooney & Tinner (2011) recommend a method which uses Scion Image software to quantify macroscopic charcoal. However, three problems which they identify with their method are recurrent ones in the application of image analysis to sedimentary charcoal:

1. The technique cannot distinguish charcoal from other dark materials, and so manual sorting may be necessary.
2. Thresholding is a source of subjectivity, although this can be reduced by use of reference samples.
3. Image analysis is not recommended for the quantification of microcharcoal.

At present, these appear to be fundamental limitations on the use of image analysis in this field, and manual separation of charcoal is likely to cancel out any potential time saving over other areal measurement methods. Where image analysis is used, the fact that it tends to produce lower estimates of charcoal area than optical microscopy (Whitlock & Larsen, 2001) may complicate attempts to draw comparisons between studies.

For morphometry, image analysis is more promising, as it allows complex ideas of shape, which are normally understood visually but are difficult to define, to be quantified as numerical values and therefore subject to statistical interpretation.

1.11 Thesis summary and aims

This thesis aims to extend our understanding of charcoal morphology in three areas. The first two address evident gaps in the published literature on charcoal morphology, while the third goes further by seeking to integrate this

subject with the practice of charcoal quantification. Specifically, the thesis aims to answer three key questions:

1. **Can the aspect ratio of charcoals be used as an indicator of fuel type?**

The morphology of charcoal extracted from sediments has been studied primarily in relation to the identification of different fuel types, most often qualitatively but also quantitatively. Although the effects of transportation in fragmenting charcoal particles have been considered in fossil assemblages, the charcoal particles produced in laboratory experiments on morphology (Umbanhowar & McGrath, 1998) have been fragmented in ways that bear little resemblance to a natural system. There had been no published attempt (prior to Crawford & Belcher, 2014) to study the effects of transportation on the morphology of charcoal particles. In Chapter 2 this is attempted by a laboratory simulation of the effects of fluvial transport on charcoal particles, which are also produced from a wider range of plant materials than has been explored previously. The results of this experiment are used to more rigorously test the basis of the assumption that aspect ratio may be used as an indicator of fuel type, as proposed by Umbanhowar and McGrath (1998).

2. **Do different sedimentary archives preserve different charcoal morphologies?**

The second aim is to extend the range of sedimentary archives in which charcoal morphology has been studied. Nearly all previously published studies of charcoal morphometry have been confined to lake sediments of Holocene age. Since sedimentary charcoal analysis is a technique applicable across a wide range of timescales and sedimentary environments, this risks biasing our understanding of the range of charcoal morphotypes. This could lead to errors both with respect to the interpretation of particular morphotypes and to assumptions regarding the identification and quantification of charcoal in the fossil record. This is addressed in Chapters 3 and 4.

3. **How does charcoal morphology affect the accuracy of its quantification?**

Thirdly, the morphology of charcoal particles is considered with respect to its effect on quantification. It is shown in Chapter 5, in the context of questioning the suitability of particle counts or areal measurements to quantify an essentially volumetric measurement, that morphology is an essential variable which can introduce strong biases if not accounted for. Prior work on the volumetric quantification of charcoal is then extended and refined by incorporating this understanding of the role of morphology. It is proposed that this may lay the groundwork for developing visual quantification of sedimentary charcoal into an absolute volumetric measure.

***

The final section of this introductory chapter describes in more detail the concept of charcoal morphology and describes the approaches and terminology that will be used throughout the remainder of this thesis.

1.11.1 Quantifying the morphology of fossil charcoal particles

Morphology may be among the factors used to visually identify charcoal (Whitlock & Larsen, 2001; Mooney & Tinner, 2011), and preservation of the form of the parent material is what makes charcoal particularly valuable for palaeontological study. The morphology of fossil charcoals is therefore a routine consideration in their analysis, though it is typically understood qualitatively, by textual description.

Attempts to deal with charcoal morphology quantitatively have been fairly limited. Quantitative morphology involves the derivation of numerical measures of morphology, which allows for the statistical analysis of shape. If features of shape can be effectively translated into numerical values, it becomes possible to study correlations between shape and aspects of fuel material, fire and taphonomy, which may allow further information to be derived from a charcoal

record than is available from its quantity and its preserved anatomical features. In addition, as will be shown in Chapter 5, shape is itself of considerable importance in the accurate quantification of sedimentary charcoal.

Although it is understood intuitively, shape is not easily defined. While the size, location and orientation of an object may collectively be termed 'pose', all other features (excepting what it is constituted of) may be termed features of shape (Glasbey & Horgan, 1995). Thus 'shape' is a complex concept, because it covers numerous aspects of an object, whose description is an "open-ended task" (Glasbey & Horgan, 1995). Consequently, the methodological decisions as to how to quantify shape will themselves be a factor affecting the resulting data.

1.11.2 Shape descriptors derived from measures of size

Numerous methods of varying complexity are available for the quantitative description of shape (Zhang & Lu, 2004). Those used in this thesis are of the simplest kind, and are derived from measures of size by simple formulae (Table 1.1). Such metrics are widely used (Glasbey & Horgan, 1995), and in the field of fossil charcoal analysis, authors employing shape descriptors of this type include Clark & Hussey (1996), Umbanhowar & McGrath (1998) and Thevenon & Anselmetti (2007).

Zhang & Lu (2004) broadly classify quantitative methods of shape description according to three parameters; whether contour-based or region-based, global or structural, and derived from the spatial domain or transform domain. The shape descriptors used here are contour-based, as they are defined entirely by information contained in the edge or perimeter of the object (i.e. by the outline of a charcoal particle). They are global because the object is not subdivided into regions, and they are derived from the spatial domain, since the analysis is based on the image itself, without use of the Fourier transform or similar methods. In all these respects, they represent the simplest of a wide range of approaches.

Such methods are subject to criticism. Zhang & Lu (2004) write that, although computationally efficient, such simple global shape descriptors are “very inaccurate". Bookstein (1978, p. 10) writes that “the quantities output are ad hoc, not based in any theory of underlying quantitative information of which the measures used take a sample”. As a consequence, they fail to capture much of the true variance in shape. However, this argument assumes the necessity of ‘describing’ a morphology with some combination of such metrics. This is not necessary for the purposes for which morphological analysis is applied in this thesis. In charcoal analysis, a measure of elongation, for example, is used for the purpose of establishing correlations between morphology and those factors which affect it, such that the metric itself may have predictive capacity for those factors. The fact that the measures taken go little way toward reconstructing the morphology is not relevant here.

What is important for charcoal morphometry is that the method is computationally simple. The fact that these measures can be readily generated by software such as ImageJ (Rasband, 2012), which is used in this thesis, will allow such relationships to be translated into predictive tools which do not require much input in terms of time or expense, and so may be added to existing methodologies easily. This holds the potential to improve our ability to interpret fire histories without substantially increasing the time or resources used in assessing charcoal assemblages.

1.11.2.1 Problems of nomenclature

The limitations of size-derived morphometrics do have repercussions when it comes to relating the metrics to linguistic descriptions of shape. The terms applied to morphometrics can be misleading, and are often inconsistent. The lack of consistency is demonstrated in Table 1.1, which summarises the morphometrics given in several review papers and textbooks, alongside those calculated by ImageJ, along with the names given to them. It can be seen that the same word may be used by different authors to describe different metrics, while identical metrics used in different cases may be named in such a way as to imply that they measure quite different aspects of shape.

In this thesis, shape descriptors are referred to by the names used in the image analysis program ImageJ (Rasband, 2012). This is done for consistency with published results in Crawford & Belcher (2014), and with the literature on ImageJ (e.g. Ferreira & Rasband, 2012). However, as noted below, the names applied to these statistics can be misleading in some circumstances.

Formula*	**Formula definitions**				
	ImageJ	Costa & Cesar (2001)	Glasbey & Horgan (1995)	Gonzalez & Woods (2002)	Zhang & Lu (2004)
$\frac{major\ axis}{minor\ axis}$	Aspect Ratio	-	-	-	-
$4\pi\frac{area}{(perimeter)^2}$	Circularity	Thinness ratio	Compactness	-	-
$4\times\frac{area}{\pi\times(major\ axis)^2}$	Roundness	-	-	-	-
$\frac{area}{convex\ area}$	Solidity	-	-	-	-
$\frac{perimeter^2}{area}$	-	Circularity	-	Compactness	Circularity
$\frac{convex\ perimeter}{perimeter}$	-	-	Convexity	-	-
$4\pi\frac{area}{(convex\ perimeter)^2}$	-	-	Roundness	-	-
$\frac{length}{breadth}$	-	-	Elongation	-	Eccentricity
* 'Major axis' and 'minor axis' in ImageJ formulae refer to the particle's best fitting ellipse.					

Table 1.1: Formulae and names for shape descriptors as used by different authors.

1.11.2.2 Measures of deviation from circularity

A number of statistics exist which measure a shape's circularity, and for which a perfect circle returns a value of 1, while departures from circularity progress toward 0. These metrics can also be considered as measures of complexity, in that they quantify the degree of departure from the simplest two-dimensional geometry. Costa & Cesar (2001) note that while a number of shape descriptors measure complexity, this is itself an ambiguous concept. There is no precise definition of 'shape complexity', but various measures that capture related aspects. These include the metrics referred to as 'circularity', 'roundness' and 'solidity' in ImageJ, which are used in this thesis.

Circularity is defined as the ratio of an object's area to that of a circle with the same perimeter length, and can also be considered as a measure of 'compactness'. While a value of 1 represents a perfect circle, a value of 0 represents an infinitely elongated polygon:

$$circularity = 4\pi \frac{area}{(perimeter)^2} \tag{1.3}$$

Solidity is the ratio of area to convex area, where the convex area is the area of the smallest possible fully convex shape which would contain the shape being measured. This also results in a maximum value of 1 for any convex object, since the convex area cannot be smaller than the area. This statistic is therefore also a measure of convexity:

$$solidity = \frac{area}{convex\ area} \tag{1.4}$$

Roundness is defined as:

$$roundness = 4 \times \frac{area}{\pi \times (major\ axis\ of\ fitted\ ellipse)^2} \tag{1.5}$$

ImageJ calls this statistic 'roundness', though that name is misleading, as a high value can be obtained for a shape that would not intuitively be regarded as round, as shown in Figure 1.2.

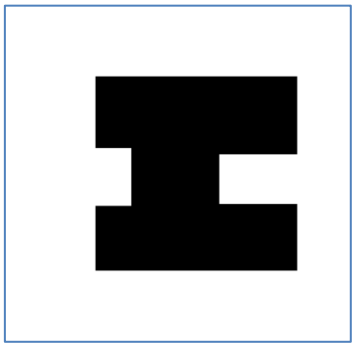

Figure 1.2: A shape which returns a value of 0.913 for 'roundness'.

1.11.2.3 Measures of elongation

The measure of elongation used in this thesis is that which is calculated as 'Aspect Ratio' by ImageJ. This is the ratio of the major and minor axes of the best fitting ellipse:

$$aspect\ ratio = \frac{major\ axis}{minor\ axis} \tag{1.6}$$

There are however numerous measures of elongation (Glasbey & Horgan, 1995; Pirard, 2004). While these are normally ratios of length to breadth, each of those terms may itself be defined in more than one way. The length is normally the Feret diameter (also called 'maximum Feret diameter'), which is the maximum distance between any two points on the perimeter, and therefore also the maximum projected length of the particle. This may be divided by the maximum diameter perpendicular to it, to obtain a measure of 'eccentricity' (Sonka et al., 1999). Alternatively, the Feret diameter can be divided by the sum of the maximum perpendicular distances between it and the perimeter on either side (Glasbey & Horgan, 1995); this being equivalent to the aspect ratio of the smallest bounding rectangle (Sonka et al., 1999).

Other measures of elongation include the ratio of the maximum and minimum Feret diameters (where the latter is the minimum projected length of the particle) (Pirard, 2004):

$$elongation = \frac{maximum\ diameter}{minimum\ diameter} \tag{1.7}$$

Alternatively, the reciprocal may be used to constrain the resulting value between 0 and 1 (Pirard, 2004):

$$elongation = \frac{minimum\ diameter}{maximum\ diameter} \tag{1.8}$$

1.11.2.4 Limiting the number of shape descriptors

There are numerous ways to measure the departure from circularity to increasing complexity of shape, and numerous ways to measure inequality of size with respect to orientation. Simple shape descriptors based on measures of size generally fall into one of these two categories, and different measures in either category will necessarily be correlated with one another. Since such descriptors are easily generated once particle measurements have been obtained, it is possible to produce large quantities of morphological data; yet the information added by each additional descriptor will rapidly diminish. If shape descriptors are subsequently used in statistical analysis, this is likely to be problematic. If a statistically significant effect is sought between shape descriptors and some potentially causative agent, larger numbers of shape descriptors will increase the false positive discovery rate, while reducing the acceptable level of significance to compensate would increase the false negative rate. In this thesis, where statistical testing is required, only one measure of elongation and one measure of complexity are used together, and specified prior to analysis.

1.11.2.5 Choice of shape descriptors in this thesis

Elongation is of interest in the study of fossil charcoal particles because this is the measure of shape which has been used as an indicator of changes in vegetation type, following Umbanhowar & McGrath (1998). Aspect ratio as defined in ImageJ is the most suitable measure of elongation, since it is the measure used by Umbanhowar & McGrath (1998).

Circularity/complexity is of particular interest as regards changes in morphology through transport. Charcoal particles, being derived from living organisms, may show complex structure. The longer the duration of transport they undergo, and the greater the energy of the transport environment, the less complexity the particles would be expected to show, with the particles tending toward sphericity over time. Circularity as defined in ImageJ (Equation 1.3) is used in this thesis as the appropriate measure of this process. This metric is criticised by Pirard (2004) as "lack[ing] clear physical significance", and returning identical values

for entirely different shapes. Pirard (2004) demonstrates the deficiency of this measure by presenting three shapes (A1, B1 and C1 in Figure 1.3) which return the same value, despite being evidently of very different shape. However, this is not a deficiency as the measure is to be used here. The measure is used here not for the purpose of differentiating between categorically different forms (A1 from B1 and C1), but to measure progressive change from any initial morphology (e.g. A1 → A2→ A3). As shown in Figure 1.3, the circularity statistic increases as the initial morphology is degraded, and the shape approaches circularity.[8]

The relevance of this metric is that it is the ratio of the particle's projected area to that of a sphere projecting the same perimeter length. As particles are expected to degrade toward sphericity under ongoing transport, this ratio is a simple and intuitive measure of the extent of that process.

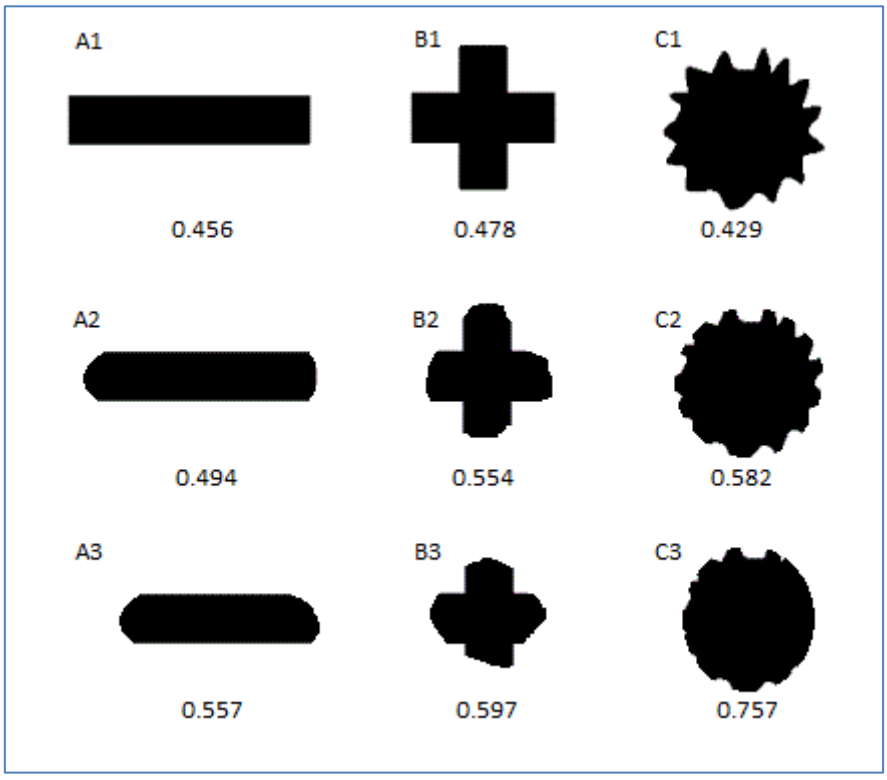

Figure 1.3: Demonstration of the utility of a measure of circularity. Shapes with circularity values as calculated in ImageJ. Adapted from Pirard (2004).

[8] A1, B1 and C1 are reproduced from Pirard (2004). The difference in circularity values between A1, B1 and C1 is most likely due to loss of resolution during this process. Pirard gives a value of 0.436 for each shape.

Chapter 2: A laboratory study of the effects of fuel material and transportation on charcoal shape

The research presented in this chapter has been published in:

Crawford A.J. & Belcher C.M. (2014) Charcoal morphometry for paleoecological analysis: the effects of fuel type and transportation on morphological parameters. *Applications in Plant Sciences*, vol. 2, doi:10.3732/apps.1400004.

2.1 Introduction

The morphology of sedimentary charcoal particles is widely understood to be influenced by the transportation which they may undergo prior to deposition in the sedimentary environment, but this process has only been inferred from particles recovered from the site of deposition (Enache & Cumming, 2006, 2007). Morphometric studies of charcoal particles have been conducted on freshly produced charcoal (Umbanhowar & McGrath, 1998) and on particles extracted from sediments (Mustaphi & Pisaric, 2014), but the effects of the intervening processes have not previously been studied in themselves.

This chapter describes an experiment in which the forces acting upon charcoal particles during transport are simulated in the laboratory, and their effects on particle morphology quantified for varying fuel materials and increasing degrees of transportation.

2.1.1 What determines particle morphology?

Charcoal morphology may be influenced by the parent material (Umbanhowar et al., 2006) and by the nature of the fire (Enache & Cumming, 2006). Since subsequent processes of transportation and burial may cause breakage of charcoal particles, it seems likely that these too will affect morphology.

The speed of heating may determine whether charcoal preserves the structure of the parent material (Enache & Cumming, 2006). Kurosaki et al. (2003)

showed that flash heating of powdered wood removed all evidence of cell structure, while gradual heating maintained it. This could translate into morphological differences at a larger scale. Lancelotti et al. (2010) found that when charcoal formed at 200 to 400 °C from a variety of tree woods was fragmented under pressure, the particle sizes (< 1 mm, 1-2 mm and > 2 mm) were correlated to temperature, and varied between species. According to Théry-Parisot et al. (2010), charcoal formed at 1200 °C or higher is not recognisable on the basis of its structure. In addition, the moisture content of the parent material may affect structure due to boiling of fluids bursting cell walls (Nichols et al., 2000), and may have effects on shrinkage (Enache & Cumming, 2006). Healthy wood has been shown to produce charcoal with greater mechanical resistance than decayed wood (Théry-Parisot et al., 2010). It should be noted however that the majority of experiments on charcoal structure and morphology are based on oven-formed charcoal, and are unlikely to fully recreate the processes of charcoal formation in fire.

It has been demonstrated that the morphology of charcoal particles is influenced by the vegetation from which they are derived, and that morphometric measurements of fossil charcoals may therefore convey information about their parent material (Jensen et al., 2007). As an example of the practical application of this, Umbanhowar & McGrath (1998) suggested that charcoal from grassland sources is more elongate than that from woodland sources. The principle was demonstrated using 8 grass species and 8 angiosperm tree species, all from the vicinity of Northfield, Minnesota, USA. This experiment was inspired by the “consistently higher” aspect ratios seen in lake sediment charcoal from the Great Plains as compared to forested regions of eastern North America.

Establishing the use of aspect ratio as a general indicator of vegetation type based on this principle requires that several issues be addressed. Firstly there is a question over the range of taxa for which grass charcoals are distinctly more elongate than those from tree leaves or wood. Umbanhowar & McGrath (1998) demonstrated the difference using 16 species from a narrow geographical area, after observing the trend in regions of North America. It may be that the difference in elongation does not extend to all species. In particular, the tree species used by Umbanhowar & McGrath (1998) were limited to the

angiosperms; and all specimens were limited to those growing in the study area. As the technique has been applied globally on the basis of these results (Aleman et al., 2013; Daniau et al., 2013; Lim et al., 2014; Colombaroli et al., 2014) this issue should be addressed.

In addition, the extent to which particle morphology is influenced by the method by which larger charcoal pieces are broken down, as opposed to the parent material, is unknown. Charcoal crushed in a mortar and then sieved, as in Umbanhowar & McGrath (1998), may display different morphological features to that broken down by natural processes (as described in Section 1.4).

To give the theory of Umbanhowar & McGrath (1998) a firm grounding, therefore, the principle that grasses produce more elongate charcoal than trees should be demonstrated with further species, and under a more realistic simulation of charcoal fragmentation.

The only previously published study on the effects of simulated transport on the breakdown of charcoal particles was by Nichols et al. (2000), who simulated the effects of bedload transport by placing charcoal produced from *Pinus sylvestris* L. twigs, sieved to between 3.3 and 9.5 mm, with sand and water in a cylindrical motorised tumbler, and then determined the weights of different size fractions. No consistent relationship was found between the period of abrasion and degree of breakdown. Most breakdown occurred rapidly, and appeared to consist largely of the removal of bark, after which particles remained generally stable. Increasing the proportion of sand increased the abrasion rate only moderately, while the tendency for charcoal to break down did not vary notably between charring temperatures of 450, 600 and 800 °C, but was notably reduced at 250 °C.

The aims of the experiment described in this chapter are to determine the effects of a realistic method of charcoal fragmentation (simulating the effects of fluvial transport) on the morphologies of charcoal particles derived from a range of plant materials, and specifically:

1. To establish whether different fuel types display distinctive morphological features under this type of fragmentation.

2. To determine the extent to which any distinctive parameters are persistent under increasing degrees of breakdown.

3. To further test the hypothesis that the aspect ratio of charcoal particles can reveal whether they originate in grassland or woodland fire.

2.2 Methods

Specimens of 26 plant materials (Table 2.1) were obtained from 14 species, consisting of 2 pteridophytes, 8 conifers, 2 grasses, and 2 other angiosperms, one weedy and one arborescent. In most cases, both foliage and stems or branches were sampled. Native species were sampled from locations in south-west England and north Wales, and exotic species from the botanical collection at the University of Exeter. Specimens were dried to constant weight at 50°C before samples were removed. Samples generally consisted of 1 cm lengths of stems, twigs or long narrow leaves, or 1 x 1 cm squares of broad leaves. The morphology of the specimen determined the exact size and shape of the samples removed. These are given in detail in Table 2.1.

Samples were tightly wrapped in aluminium foil, and placed in batches of eight in 75 ml stainless steel crucibles. The crucibles were then filled with clean mineral sand of grain size ≤ 500 µm in order to exclude oxygen from the combustion process. The crucibles were placed in the centre of a Carbolite GLM3 furnace at 550°C for 20 minutes, causing the samples to pyrolyse. The samples were then removed from the furnace and allowed to cool to room temperature in the crucibles. For five samples, the temperature of the furnace was recorded at 15 second intervals to establish the actual temperature profile under this methodology (Figure 2.1). This indicated that the temperature remained within the range 547–553°C for the duration.

This method produced samples of pure charcoal from leaves, with no material left uncharred, and with only very slight ash production at the edges of some samples. Non-charcoalified material may have remained at the centre of some woody samples.

Species	Description of specimen from which samples were cut	Description of samples
Abies nordmanniana (Steven) Spach	needles	5 needles
Abies nordmanniana	twig 6.5–7 mm diameter	1 cm length
Cedrus libani A. Rich.	needles 1–2 cm long	5 needles
Cedrus libani	twig 3–5 mm diameter	1 cm length
Cephalotaxus fortunei Hook.	twig 3–4 mm diameter	1 cm length
Cephalotaxus fortunei	leaves 3 x 80 mm	1 cm length
Cunninghamia lanceolata (Lamb.) Hook.	needles 2–4 cm long	1 needle
Elymus repens (L.) Gould	leaf	1 cm length
Elymus repens	stem	1 cm length
Equisetum telmateia Ehrh.	stem 1 cm diameter	one eighth of a single nodal section; cut lengthways
Equisetum telmateia	branches	2 x 1 cm lengths
Pinus sylvestris L.	twig 2.5 mm diameter	1 cm length
Pinus sylvestris	needles	2 needles; each in 3 pieces
Poa trivialis L.	leaf	1 cm length
Poa trivialis	stem	1 cm length
Prumnopitys andina (Poepp. & Endl.) de Laub.	needles 1–2 cm long	2 needles
Prumnopitys andina	twig 5 mm diameter	5 mm length
Pteridium aquilinum (L.) Kuhn	stem 2 mm diameter	1 cm length
Pteridium aquilinum	frond 1 cm wide	1 cm length
Quercus robur L.	twig 6–7 mm diameter	1 cm length
Quercus robur	leaf 9 x 6 cm	1 x 1 cm from centre
Rubus fruticosus L.	stem 7 mm diameter	1 cm length
Rubus fruticosus	leaf	1 x 1 cm piece from centre
Torreya californica Torr.	needles 2–4 cm	1 needle
Wollemia nobilis W.G. Jones, K.D. Hill & J.M. Allen	leaves 5–7 cm x 5–7 mm	single leaf in 3 or 4 pieces
Wollemia nobilis	stem 4–5 mm diameter	1 cm length

Table 2.1: Material types and descriptions of samples used for the production of charcoal

Each charcoal sample (mass 0.0008 – 0.1068 g; σ = 0.0255) was placed in a 40 ml polypropylene tube (30 x 70 mm) with a polyethylene screw-cap. Approximately 10 g (9.71 – 10.36 g; σ = 0.10) of silicate gravel (mass 0.07 – 1.02 g; *s* = 0.17) was added, and the tube filled with tap water. Sample tubes were affixed to an electric motor (Figure 2.2), at 10 cm from the axis of rotation and aligned tangential to the direction of rotation, and turned over at 47

revolutions per minute for periods of between one and eight hours. The speed of rotation is arbitrary, but low enough to avoid any inertial displacement of the contents of the tube.

Samples were sieved at 125 µm, and the gravel removed. The charcoal particles retained on the sieve were dispersed in water in 55 mm petri dishes, and left at room temperature for the water to evaporate.

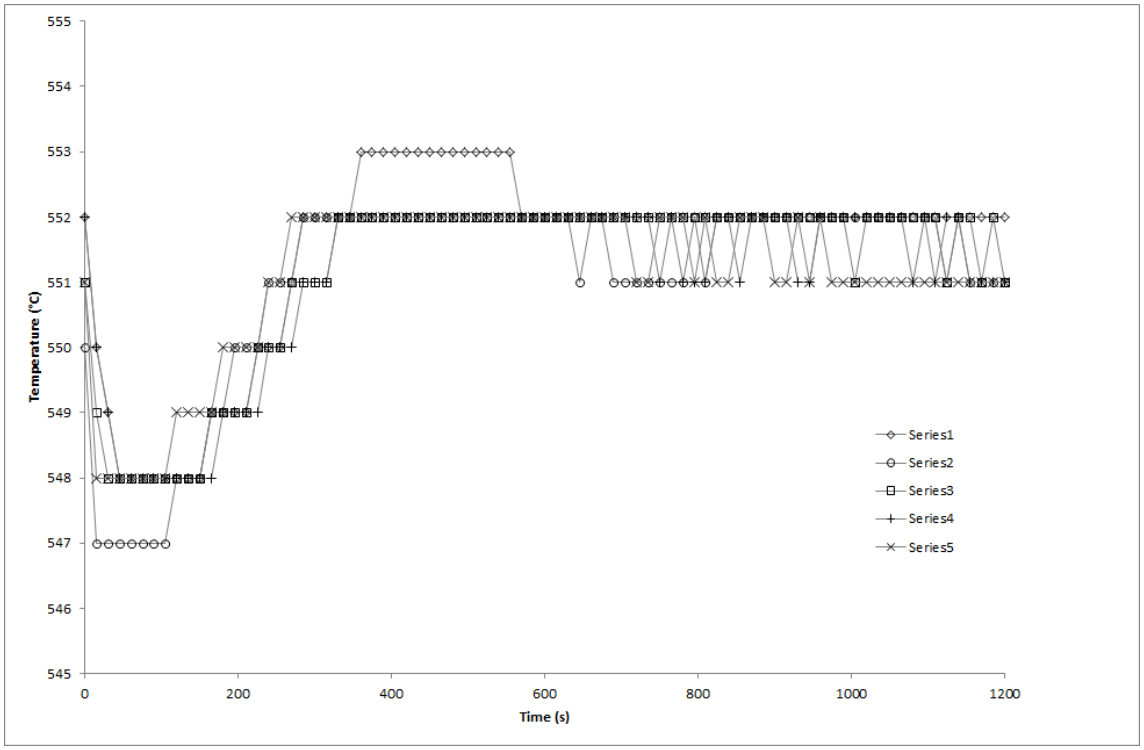

Figure 2.1: Furnace temperature profiles recorded for 5 samples.

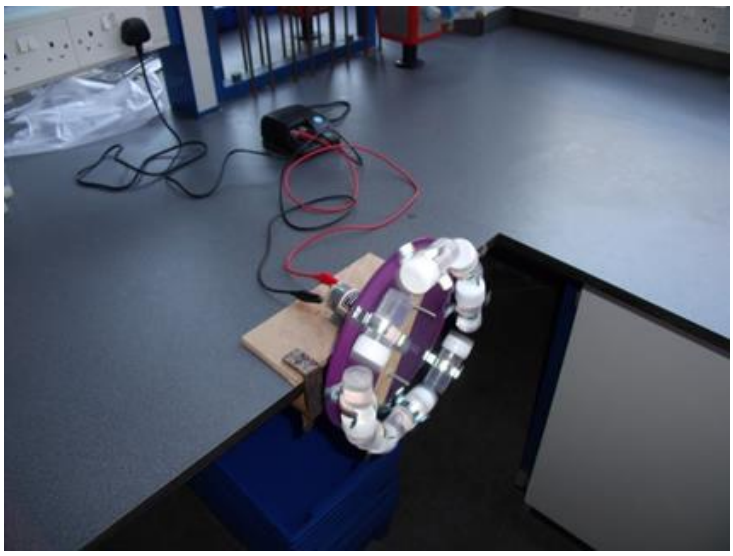

Figure 2.2: Apparatus for simulating effects of fluvial transport on charcoal.

The particles were then imaged using a dissecting microscope and Microtec 5.0MP digital camera, and View version 7.1.1.7 imaging software. Where the original woody particle remained largely intact, this was removed prior to imaging, as the aim was to measure fragmented mesocharcoal particles. An area of 16 cm^2 was photographed as 16 overlapping images, using transmitted light, and the images saved in tagged image file format (TIFF).

Images were processed using ImageJ 1.47t. Each image consisted of a 1 x 1 cm square, and adjacent areas overlapping with other images from that sample. Most images contained some areas in which particle morphology was obscured, either by the density of the particles causing them to touch or overlap, or in some cases due to other material being present in the sample, or faults with the image itself. A region of interest, in which no distorted particle images were apparent, was therefore defined within each 1 x 1 cm square, and the remainder of the image deleted. The edited images were converted to 8-bit greyscale, and then binarised using the default IsoData algorithm (Ridler and Calvard, 1978), adjusting the maximum threshold value manually to distinguish the charcoal particles, and with the minimum threshold value set at 0. All stages of the image processing are shown in Figure 2.3 for a representative image. Shape descriptors (including projected area, circularity and aspect ratio) were generated for all the resulting particle images. Circularity and aspect ratio were calculated according to the formulae given in Section 1.11.

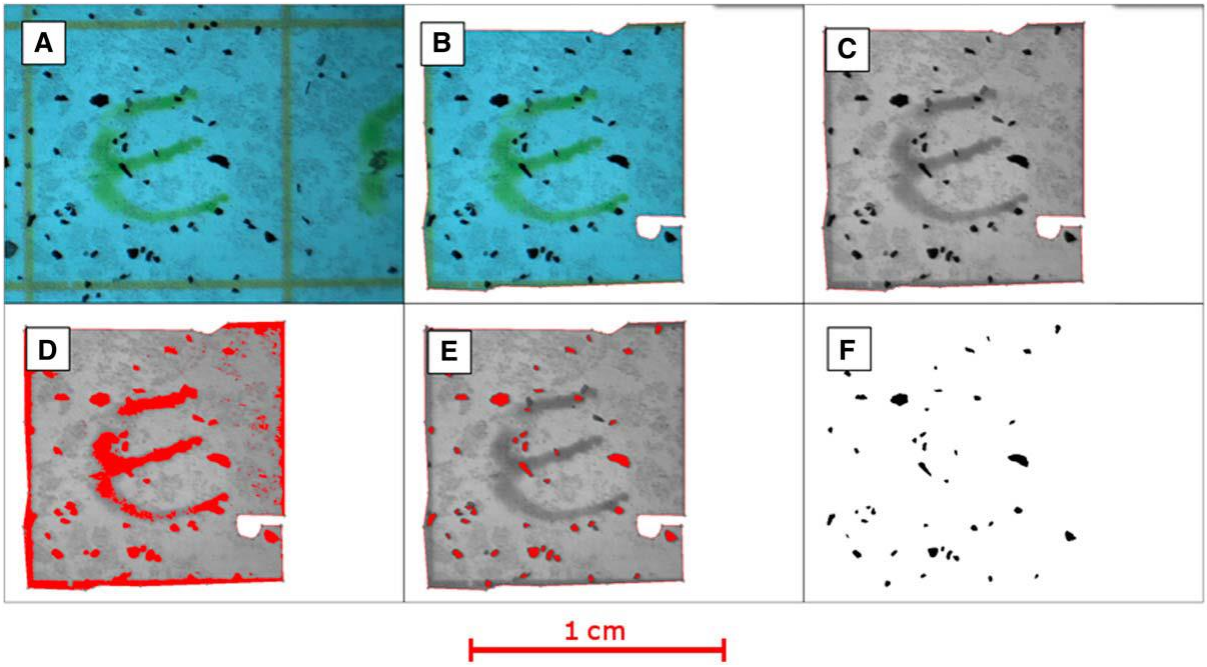

Figure 2.3: Stages of image processing – a raw image overlapping with other images from the same sample (A); cropped to remove overlap with other images and overlapping particles (B); converted to 8-bit grayscale (C); with automatic thresholding applied (D); with threshold manually adjusted (E); and final binary image (F).

Particles of less than 315 μm^2 or greater than 1,000,000 μm^2 were excluded from the analysis. The lower limit serves to remove data derived from images of between 1 and 9 pixels, below which meaningful information is unlikely to be obtained even for the most basic parameter of area (Francus and Pirard, 2004). It is also likely that images of this size would not have been easily visible during selection and thresholding, and they may not represent actual charcoal particles. The upper limit, which coincides with the distinction between mesocharcoal and macrocharcoal as defined by Scott (2010), is essentially arbitrary. Particles at the high end of the size distribution were not present in sufficient numbers to produce statistically meaningful data, and their morphology may largely reflect the size and shape of the original sample cut, rather than effects of internal structure and breakdown regime with which this study is concerned.

2.3 Results

2.3.1 General observations

Variation in particle morphology was evident between samples from different vegetation sources prior to measurement. Figure 2.4 provides an indication of the variation in particle morphology visible to the naked eye. An average of 322 particles were measured from each sample, with a minimum of 30 and a maximum of 659.

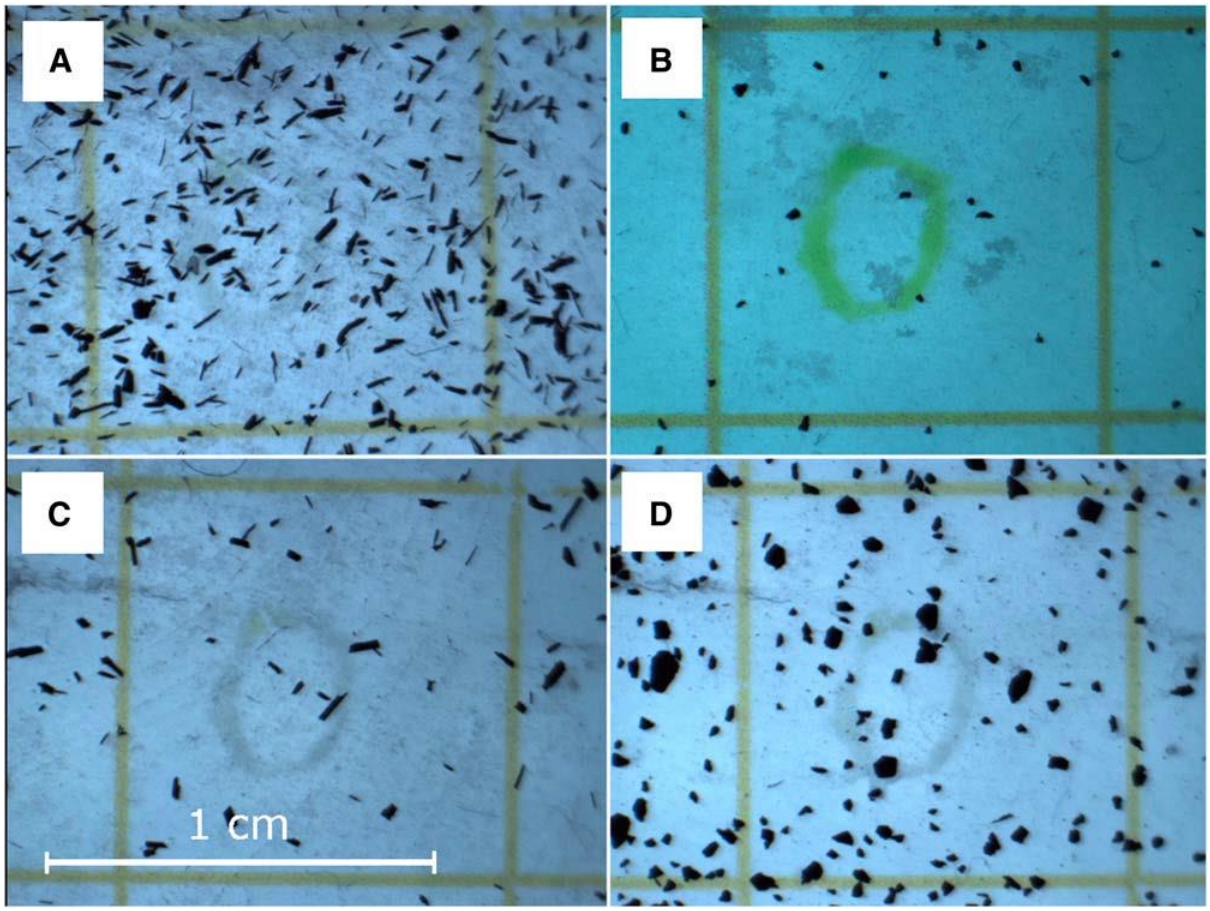

Figure 2.4: Charcoal particles after four hours of simulated transport, showing variations in morphology visible to the naked eye – *Equisetum telmateia* stem (A), *Cedrus libani* wood (B), *Elymus repens* stem (C), and *Rubus fruticosus* leaf (D).

2.3.2 Effects of transport time on particle size

All specimens were found to exhibit a decrease in mean particle area with increasing time of simulated transport (Figure 2.5). Mean particle area is plausibly modelled as a logarithmic function of transportation time ($r^2 > 0.8$) for the leaves of all species, with the exception of *Poa trivialis* L. A marked decrease in the rate of attrition is generally evident between 1 and 2 hours. The branches of *Equisetum telmateia* Ehrh. also follow this trend. The mean particle areas of charcoal produced from stems or wood display generally low r^2 values when a logarithmic function is fitted; below 0.8 with the exceptions of *Cephalotaxus fortunei* Hook. and *Elymus repens* (L.) Gould. This apparent divergence of r^2 values between leaves (including *Equisetum telmateia* branches) and stems (including woody samples) was highly significant ($P < 0.001$; independent samples Mann-Whitney test).

2.3.3 Effects of transport time on particle morphology

All the leaf samples display an increase in mean circularity with increasing transport time (Figure 2.6). This tendency is less distinct than was the case for mean area; some r^2 values are low; and the *Equisetum* branches, which appear to follow the trend for leaves regarding area, tend to decrease in circularity, though without a convincing model fit. Wood and stem samples display no apparent trends (Figure 2.6). Logarithmic models give r^2 values of < 0.3 for all conifer woods, 0.7111 for *Quercus robur* L., 0.7323 for *Elymus repens*, and < 0.4 for all other stem samples. Divergence in r^2 values between the two groups was significant ($P = 0.002$).

Aspect ratio generally decreases with time for leaf samples; the exceptions being *Cedrus libani* A. Rich. and *Quercus robur*, both of which display consistently low aspect ratios (Figure 2.7). Stem and wood samples display little consistency in relationships of aspect ratio to time. Few samples in either group display apparent trends in aspect ratio with transportation time. When logarithmic models are fitted, divergence in r^2 between groups is not significant at 95% confidence ($P = 0.095$).

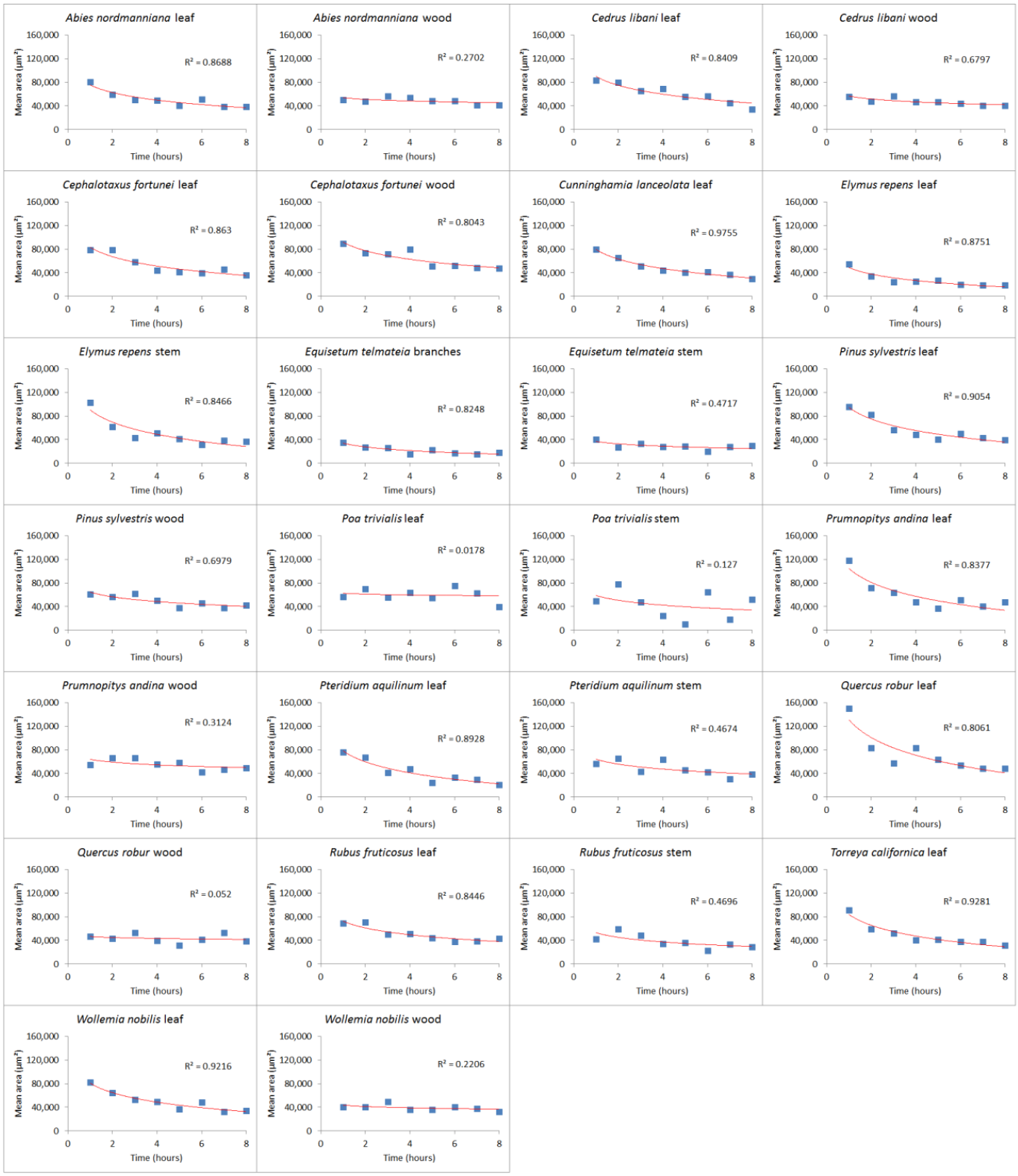

Figure 2.5: Relationships between mean projected area and duration of simulated transport for mesocharcoal particles produced from different plant materials.

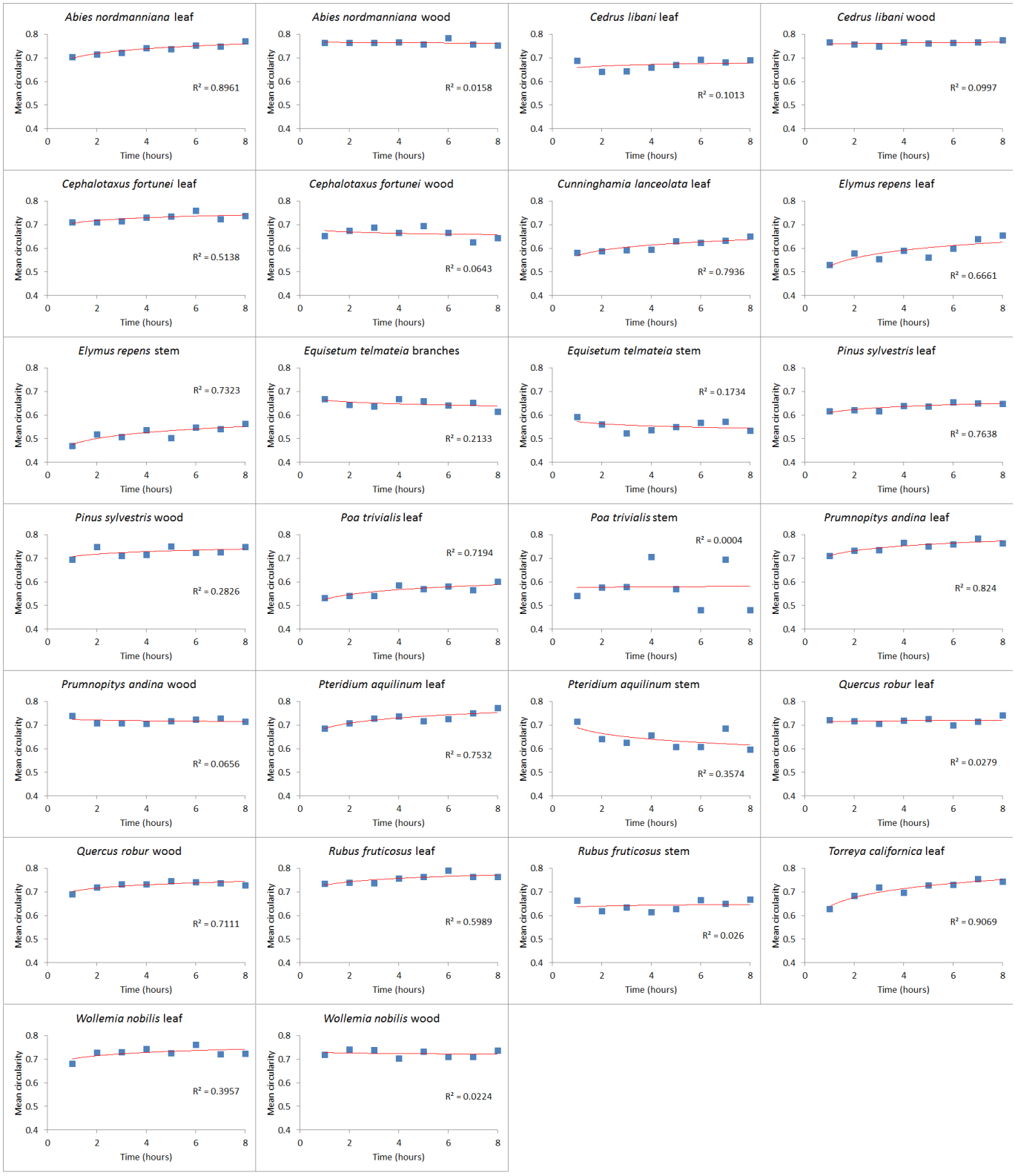

Figure 2.6: Relationships between mean circularity and duration of simulated transport for mesocharcoal particles produced from different plant materials.

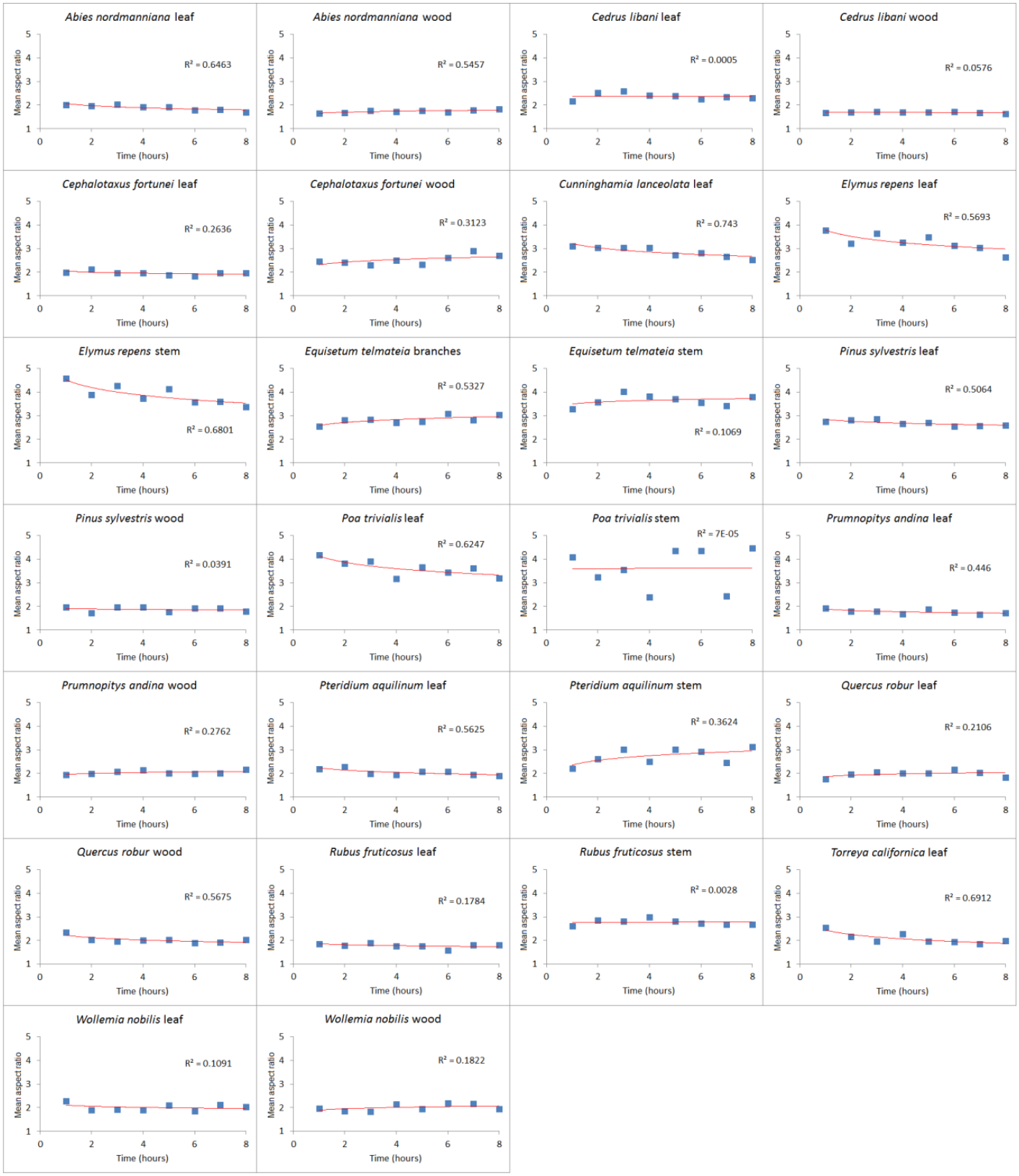

Figure 2.7: Relationships between mean aspect ratio and duration of simulated transport for mesocharcoal particles produced from different plant materials.

2.4 Discussion

The natural transportation processes undergone by charcoal particles will be wide-ranging in terms of their intensity as well as their duration, and may include aeolian as well as hydrological transport. The degree to which this laboratory process replicates the forces acting upon the charcoal will therefore be highly variable. The effects produced in this study will most likely correspond to those in charcoal particles that have undergone vigorous fluvial transport. During fluvial transport, it is to be expected that particles would be subject to attrition (reduction in particle size by friction) as would any other material. Collisions with entrained sediment will cause abrasion of the surface, and impart stresses in the charcoal which may lead to fracturing. The effect of abrasion would be dependent on the concentration, hardness and kinetic energy of the sediment (Summerfield, 1991). Hydraulic action and cavitation may also act upon the particles in a high-energy fluvial environment; but these are not expected to have had any effect in the laboratory simulation here, as tests without gravel in the samples resulted in no discernible breakdown of the charcoal. The floating or suspension of charcoal results in minimal abrasion during hydrological transport (Nichols et al., 2000). In this study, charcoal particles did not float after breakdown, with the exception of *Quercus* leaf charcoal, though the charcoal pieces typically did float before undergoing any simulated transport. In a natural situation, the kind of breakdown process simulated here might be initiated after a period of relatively non-destructive transportation; but having been initiated, the effect of the breakdown on buoyancy would serve to keep the particles submerged, and therefore subject to further breakdown.

The majority of macroscopic (> 1 mm) charcoal undergoes transportation by water (Scott, 2010), and it is also likely to be a common process for smaller particles. Likelihood of fluvial transport is increased by the effects of wildfire in altering hydrological behaviour. Fire tends to decrease soil infiltration and increase overland flow, while at the catchment scale increasing runoff and reducing response time (Shakesby and Doerr, 2006), all of which will assist in carrying the charcoal produced into fluvial systems. However, to the extent that the morphology of broken-down particles reflects internal structure of the charcoal, results may be applicable to charcoal assemblages which have

undergone quite different transportation processes, such as aeolian transport, mass movement of dry material, or a combination of processes. Regardless of the type of transportation that a real charcoal assemblage has undergone, the effect in modifying particle morphology will vary according to the length of time spent in that environment. No attempt is made to relate length of simulated transport in this study to any measure of transportation time or distance of wildfire charcoal. However, the logarithmic changes in projected area and circularity which are generally evident in the leaf charcoal samples indicate that the period of substantive change has been captured in these cases.

The kinetic energy imparted to each sample remains constant through time. The emergence of a logarithmic decrease in mean area, which is evident for the leaf samples, therefore implies a decrease in the susceptibility of the particles to breakdown, implying that the material abraded from the larger particles early on is simply more fragile than the underlying material. In this respect, the results mirror those of Nichols et al. (2000), who attributed the decline in breakdown of their samples to the removal of bark, leaving the less fragile wood charcoal beneath remaining much in its original shape. Since the logarithmic decrease was evident primarily in our leaf charcoal, a comparative distinction between two parts of the material cannot be drawn. However, some other source of variability in the resistance of the leaf charcoal could explain this pattern. It is also possible that the size itself determines the susceptibility of the particles to breakdown under this regime, so that as they are reduced in size the rate of attrition declines regardless of the other physical properties of the charcoal.

It is to be expected that circularity will increase as area decreases. Similarly, aspect ratio should also decrease with decreasing particle size, since a particle is more likely to break across its longest axis than along it. However, no simple relationship was identifiable between aspect ratio and time. The failure to find such a relationship may be a consequence of imaging and measurement biases which affect this parameter in particular. Aspect ratios may be underestimated from images composed of a small number of pixels (Francus and Pirard, 2004). In addition, particles of very high aspect ratio may be lost during thresholding, where those of lower aspect ratio but similar size are retained.

The lack of an identifiable relationship between either area or circularity and transport time for wood or stem samples recalls the results of Nichols et al. (2000) in the simulated transport of *Pinus sylvestris* wood charcoal at a larger size fraction. This may reflect a more heterogeneous nature of wood charcoal as opposed to leaf charcoal. It is notable however that the same results were obtained for rigid but non-woody stems (*Equisetum*, *Pteridium aquilinum* (L.) Kuhn and *Rubus fruticosus* L.) as for the wood charcoal; while the *Equisetum* branches, which were the only non-rigid samples charcoalified other than leaves, followed the logarithmic trend for mean area. The *Equisetum* branches did not follow the logarithmic trend for circularity, but in this case some leaf samples did not either. This suggests that the factor determining whether a simple mathematical relationship exists between these morphological parameters and degree of breakdown may be related more to the physical characteristics of the plant organ than to its function.

2.5 Relevance to interpretations of the fossil record

Umbanhowar and McGrath (1998) concluded that the mean aspect ratio of the best fitting ellipse was a usable indicator of whether an assemblage of charcoal particles (125 – 250 µm) originated from a grassland fire or a forest fire. This conclusion was based on data from 16 species of grasses and deciduous trees native to Minnesota, USA, and is not necessarily applicable in other environments supporting different species. We divided our samples into four groups based on broad material type (grass, tree leaves, wood, and other), regardless of degree of simulated transport, in order to assess differences in aspect ratio. Our results show distinct variability in the range of aspect ratios between the four groups (Figure 2.8). In keeping with the findings of Umbanhowar and McGrath (1998), it is the grass charcoal that displays the most distinctive distribution, with the highest aspect ratios.

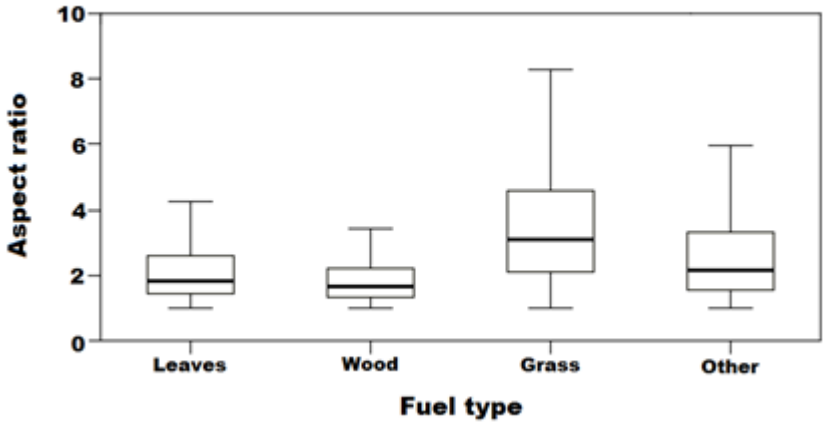

Figure 2.8: Boxplot showing differences in distribution of aspect ratios of charcoal particles (315-1,000,000 μm²), grouped into four broad material types. Outliers are not shown.

Umbanhowar and McGrath (1998) specifically identified the mean aspect ratio of the 125–250 μm fraction as indicative of fuel type, based on the significance of the differences in distribution. The particles in this study were not physically sieved into different fractions, and so identifying this specific size fraction within these data is not possible. Differences in aspect ratio were therefore compared between groups at each of 10 size fractions, according to Feret diameter (the maximum diameter within each particle image), from 0-100 μm to 900-1000 μm. The differences in mean aspect ratio between the four groups remain similar across the range of particle sizes (Figure 2.9), though they are noticeably more closely grouped at the ≤ 100 μm range. The significance of the differences in aspect ratios between the four groups was tested with a one-way Kruskal-Wallis test for each of the size ranges. The overall difference across the groups was highly significant ($P < 0.001$) at every size range (Table 2.2). Pairwise comparisons are also highly significant in most cases, with only 7 out of 60 P-values exceeding 0.001 (Table 2.2). Only one of these comparisons included grass charcoal; paired with other materials, this yielded a P-value of 0.021 at the 900-1000 μm range. While this is in any case sufficient to retain the hypothesis of distinct distributions at the 95% confidence level, it is noted that the higher P-value is likely to be the result of the low number of particles present in this size range; the comparison in question involving a total particle number of 173.

Feret diameter (μm)	Significance	Pairwise comparison	Pairwise significance
≤ 100	< 0.001	Wood–Leaves	< 0.001
		Wood–Other	< 0.001
		Wood–Grass	< 0.001
		Leaves–Other	0.877
		Leaves–Grass	< 0.001
		Other–Grass	< 0.001
100 – 200	< 0.001	Wood–Leaves	0.32
		Wood–Other	< 0.001
		Wood–Grass	< 0.001
		Leaves–Other	< 0.001
		Leaves–Grass	< 0.001
		Other–Grass	< 0.001
200 – 300	< 0.001	< 0.001 for all pairs	
300 – 400	< 0.001	< 0.001 for all pairs	
400 – 500	< 0.001	< 0.001 for all pairs	
500 – 600	< 0.001	< 0.001 for all pairs	
600 – 700	< 0.001	< 0.001 for all pairs	
700 – 800	< 0.001	Wood–Leaves	0.097
		Wood–Other	< 0.001
		Wood–Grass	< 0.001
		Leaves–Other	< 0.001
		Leaves–Grass	< 0.001
		Other–Grass	< 0.001
800 – 900	< 0.001	Wood–Leaves	< 0.001
		Wood–Other	< 0.001
		Wood–Grass	< 0.001
		Leaves–Other	0.021
		Leaves–Grass	< 0.001
		Other–Grass	< 0.001
900 – 1000	< 0.001	Wood–Leaves	0.188
		Wood–Other	< 0.001
		Wood–Grass	< 0.001
		Leaves–Other	0.004
		Leaves–Grass	< 0.001
		Other–Grass	0.021

Table 2.2: P-values obtained from Kruskal-Wallis tests on aspect ratios of four different fuel types, at each of ten particle size ranges.

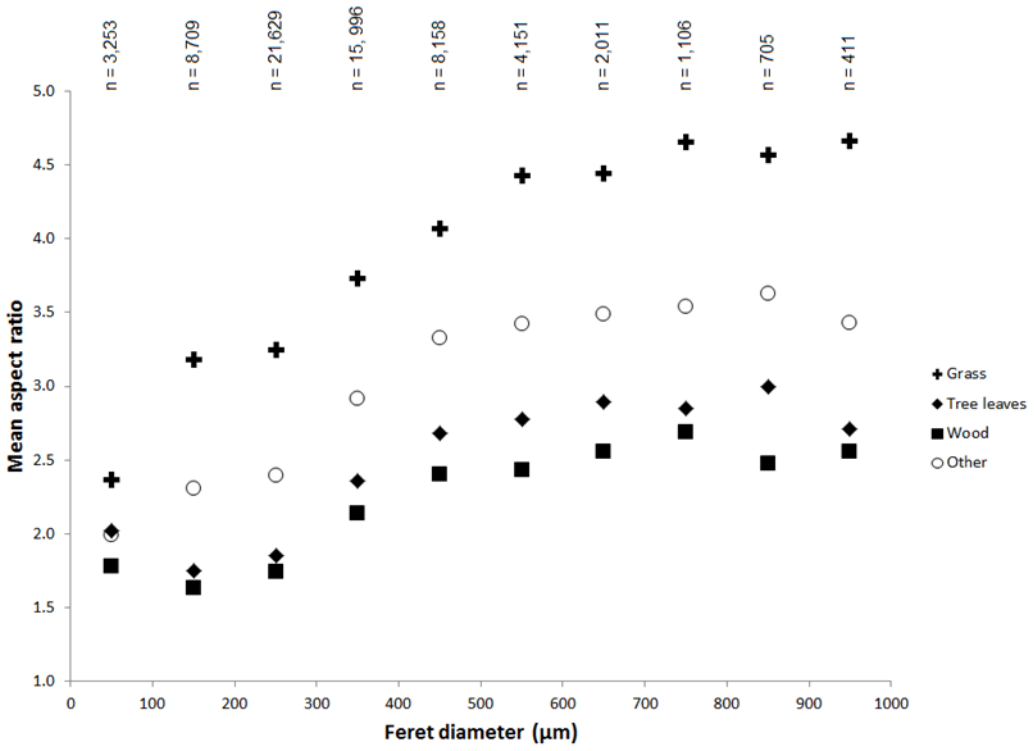

Figure 2.9: Relationship of mean aspect ratio and Feret diameter of charcoal particles (315-1,000,000 µm²), grouped into four broad material types. Feret diameters are grouped in ranges of 100 µm and plotted as the midpoint of each range.

These results suggest that differences in aspect ratio between fuel types tend to be highly significant at a range of sizes. The identification of 125-250 µm as the fraction used to separate fuel types on the basis of aspect ratio therefore seems unnecessary; grass charcoal is distinct from other materials at each size range, assuming a 95% confidence limit. This supports, in principle, Umbanhowar and McGrath's (1998) suggestion that aspect ratio can be used to identify fuel type.[9]

2.6 Conclusions

This study demonstrates a simple method for replicating the effects of fluvial transport on the morphology of mesocharcoal particles, and for applying image

[9] The current evidence in support of the method proposed by Umbanhowar & McGrath (1998) is discussed further in Chapter 6.

analysis methods to large numbers of the resultant particles in a comparatively fast manner.

The results suggest that charcoal formed from leaves displays more easily definable changes in morphological parameters than that formed from woody or rigid plant materials. Charcoal produced from leaves displays a logarithmic decrease in size (projected area) along with a logarithmic increase in circularity. Such clearly defined trends were not evident for charcoal produced from stems or woody material.

Aspect ratios of grass mesocharcoal were shown to be consistently higher than those of other vegetation types, regardless of size fraction. These data therefore appear to support the use of mean or median aspect ratio as a means of identifying the type of wildfire from which a charcoal assemblage originates.

Chapter 3: Morphologies of Holocene peatland charcoals

3.1 Introduction

The majority of studies on charcoal morphology and taphonomy have been concerned with lake sediment charcoal (see Section 1.9), with Mustaphi & Pisaric (2014) presenting a complex classification scheme of 27 charcoal morphotypes described by five levels of categorisation.

However, there is good reason to suppose that different sedimentary archives will contain different charcoal morphologies, both as a consequence of post-depositional changes and differences in morphotypes input. For example, marine deposits would be expected to contain morphologies considerably influenced by transportation, peat deposits minimally so; lithified sediments are likely to contain greater post-depositional effects than more recent lake sediments, etc. It is therefore important to sample morphologies from a variety of sedimentary environments, and of a variety of ages, if the true range of charcoal morphologies is to be gauged. Existing published studies are particularly lacking in data from peatland sources, and pre-Quaternary data. This chapter presents the results of morphometric analysis of mesocharcoal particles from a Holocene peat core, while Chapter 4 will concern charcoals from pre-Quaternary sediments.

3.2 Morphometric analysis of Holocene peatland mesocharcoal

This section constitutes the first study of charcoal morphometry from a peatland archive. As peatland charcoal will have a simpler taphonomic history, with less transportation as compared to lake sediment charcoal, there may be greater potential for preservation of morphological information relating to plant structure and fire conditions, and less effect on morphology from taphonomic processes.

This study aims to (1) assess the range of morphological variation within a typical temperate peatland core; (2) look for evidence of changes in aspect ratio

in relation to the known environmental history of the site; (3) investigate whether morphological information is persistent over time, by testing for the effect of depth or age; and (4) Compare the range of morphotypes with those reported from studies of lake sediment charcoals.

3.2.1 Materials & Methods

3.2.1.1 Location

Shovel Down is an upland area of acid grassland on eastern Dartmoor, southwest England. The area contains numerous exposed archaeological features, and has been of interest to archaeologists seeking to understand prehistoric land enclosure (Bruck et al., 2003). Exposed archaeological features, dating primarily from the Bronze Age, but with evidence of settlement since the Mesolithic, consist of extensive field systems, along with evidence of roundhouses and ceremonial areas (Fyfe et al., 2008). A small valley mire of c. 1 ha partly overlies important elements of the archaeological remains, and has been used for obtaining palaeoenvironmental information including palynology, microcharcoal and ^{14}C, indicating that the mire contains peat accumulated since c. 8.5-9 ka BP (Fyfe et al., 2008).

The palynology of the site indicates that peat initiation took place amid a local herbaceous vegetation, within a wider landscape of ericaceous heath and woodland. From c. 7 ka BP, the area was dominated by *Quercus* and *Corylus* woodland. A shift to *Calluna* heathland vegetation occurred c. 5.5 ka BP, and does not appear to have been anthropogenic or associated with burning. However, later changes in pollen ratios are attributed to distinct land-use phases. At c. 3.4 ka BP, a shift to grassland vegetation occurred, likely associated with grazing; followed by reversion to *Calluna*-dominated heath and scrub after c. 3 ka BP, with *Poaceae* increasing again from c. 1.6 ka BP. While Fyfe et al. (2008) found charcoal throughout their record, it was not obviously correlated with heathland expansion as might be expected.

The samples used for ^{14}C dating were taken at the location of the reave which crosses and is submerged by the mire. The core used in this study was taken

adjacent to the reave (< 5 m), which is visible to both sides of the mire. Figure 3.1 shows the location of the sampling point as recorded by GPS (accuracy ± 3 m).

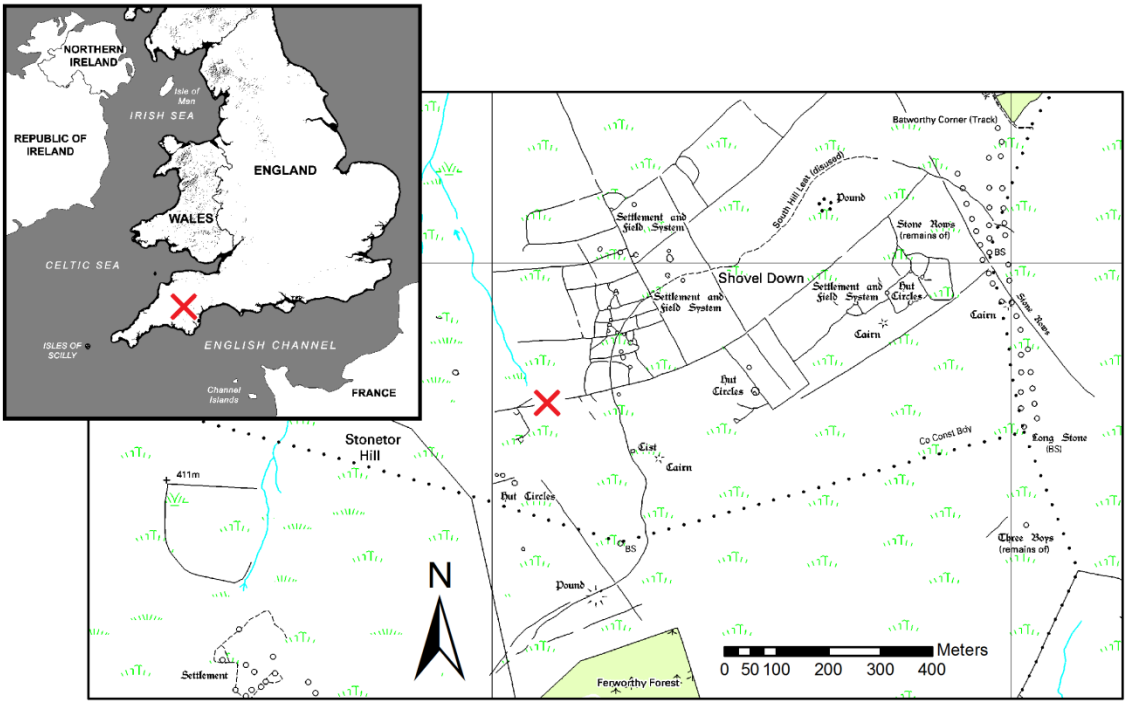

Figure 3.1: Map showing location of peat coring site in relation to exposed archaeology at Shovel Down. The coring location is marked by a red 'X'.

3.2.1.2 Charcoal extraction & analysis

A peat core was extracted from the mire at SX 65105 85730 (± 3 m) using a Russian corer. The core was extracted in three sections from two adjacent points, covering a depth of 102 cm, from 30 cm below the surface of the water. Although the corer penetrated to the base of the peat, the lowest 10 cm could not be retrieved, as this is the length of the corer's nose, while the top 30 cm could not be sampled as the material was insubstantial. Sections were transferred to plastic troughs, sealed with cling film, and refrigerated.

21 samples of approximately 2 cm^3 were removed from the core at intervals of 5 cm; each within a depth of approximately 1 cm. The samples were weighed, and volumes measured by displacement. Samples were left in sodium hypochlorite (NaOCl) solution (c. 8% Cl) for approximately 20 hours. Clumps of material that were not becoming disaggregated during this process were gently

compressed with a paintbrush and the samples given a light swirling motion. Samples were then sieved at 125 μm and the larger fraction retained for examination.

All black particles, excluding those which were clearly < 125 μm in diameter, were removed from each sample, using a stereo microscope at ×10 magnification under reflected light. These particles were then further examined at ×50 magnification. Those which were identified as charcoal were temporarily mounted (in water, beneath glass cover slips) and individually photographed. Where the number of mesocharcoal particles in a sample was very high, this process was stopped after approximately 50 images had been taken.

Images were saved in TIFF format, and analysed using ImageJ 1.47t. Images were cropped to remove extraneous detail, and in rare cases details adjacent to charcoal particles were manually masked using a graphics programme. Images were converted to 8-bit greyscale, then binarised using the Auto Threshold function and IsoData algorithm. Shape and size descriptors for the particle images were then generated. Binarised images were saved for future reference.

3.2.2 Results

Inspection of the peat prior to sampling showed it to be generally homogenous in nature throughout the core. Colour and texture varied little and no horizons were evident, with the peat being composed primarily of partially humified moss. The sediment is described for each sampling depth using the Troels-Smith classification (Aaby & Berglund, 1986) and Munsell soil colour chart (Anon., 2000) in Table 3.1.

A total of 3402 particle images were recorded from the 21 samples. These ranged in size from individual pixels (which are likely to be noise, and in any case cannot convey meaningful information on shape) to the largest with an area of 0.16 mm^2.

Depth (cm)	Colour			Physical properties				Composition		
	Hue	Value	Chroma	Nigror	Stratificatio	Elasticitas	Siccitas	*Turfa bryophytica*	*Turfa lignosa*	*Substantia humosa*
31	10YR	2	1	3	0	2	2	2	0	2
41	10YR	2	1	3	0	2	2	2	0	2
51	10YR	2	1	3	0	2	2	2	0	2
61	10YR	2	1.5	3	0	2	2	2	0	2
71	10YR	2	2	3	0	2	2	2	0	2
81	10YR	2	1	3	0	2	2	2	0	2
91	10YR	2	1.5	3	0	2	2	1.5	0.5	2
101	10YR	2	2	3	0	2	2	2	0	2
111	10YR	2	1	3	0	2	2	2	0	2
121	10YR	2	1	3	0	2	2	2	0	2
131	10YR	2	1	3	0	2	2	1	0	3

Table 3.1: Description of the peat core using Troels-Smith classification and Munsell soil colour chart. Values for composition and physical properties are on a 5-point scale (i.e. 0-4); non-integer values are mean values where two sections had different values for the same depth.

Particles of Feret diameter <100 µm were excluded from the data set. It was observed that a small number of those mounted disintegrated into very many pieces, and this is likely to account for many of these particles. As this would not constitute a reliable sampling of the particles of this size from the core, these were excluded. This left a total of 636 mesocharcoal particles.

Based on visual assessment, a wide range of morphologies were represented in the charcoal assemblage. It was evident that there were wide variations in elongation, texture, and complexity of structure, with some forms being suggestive of particular plant anatomical features, and others ambiguous or distinctly amorphous (Figure 3.5).

Aspect ratios ranged from 1.0 to 15.5, but were heavily skewed toward the lower end (Figure 3.2), with a mean of 3.4 and a median of 2.7, and values over 9.0 accounting for only 2.2% of the particles. Circularity ranged from 0.05 to 0.68 with a mean of 0.35 and an apparently normal distribution. Roundness ranged from 0.07 to 0.97, with a more irregular distribution somewhat skewed toward the lower values, and a mean value of 0.41. Solidity ranged from 0.39 to

0.96, skewed toward the higher values, with a mean of 0.80. Descriptive statistics for shape metrics are given in Table 3.2 and frequency distributions shown in Figure 3.2.

	Aspect ratio	Circularity	Roundness	Solidity
Minimum	1.030	0.054	0.065	0.388
Maximum	15.459	0.679	0.970	0.957
Mean	3.359	0.355	0.406	0.801
Median	2.709	0.344	0.369	0.822
Standard deviation	2.140	0.138	0.210	0.098

Table 3.2: Descriptive statistics for shape metrics for Holocene peatland mesocharcoal.

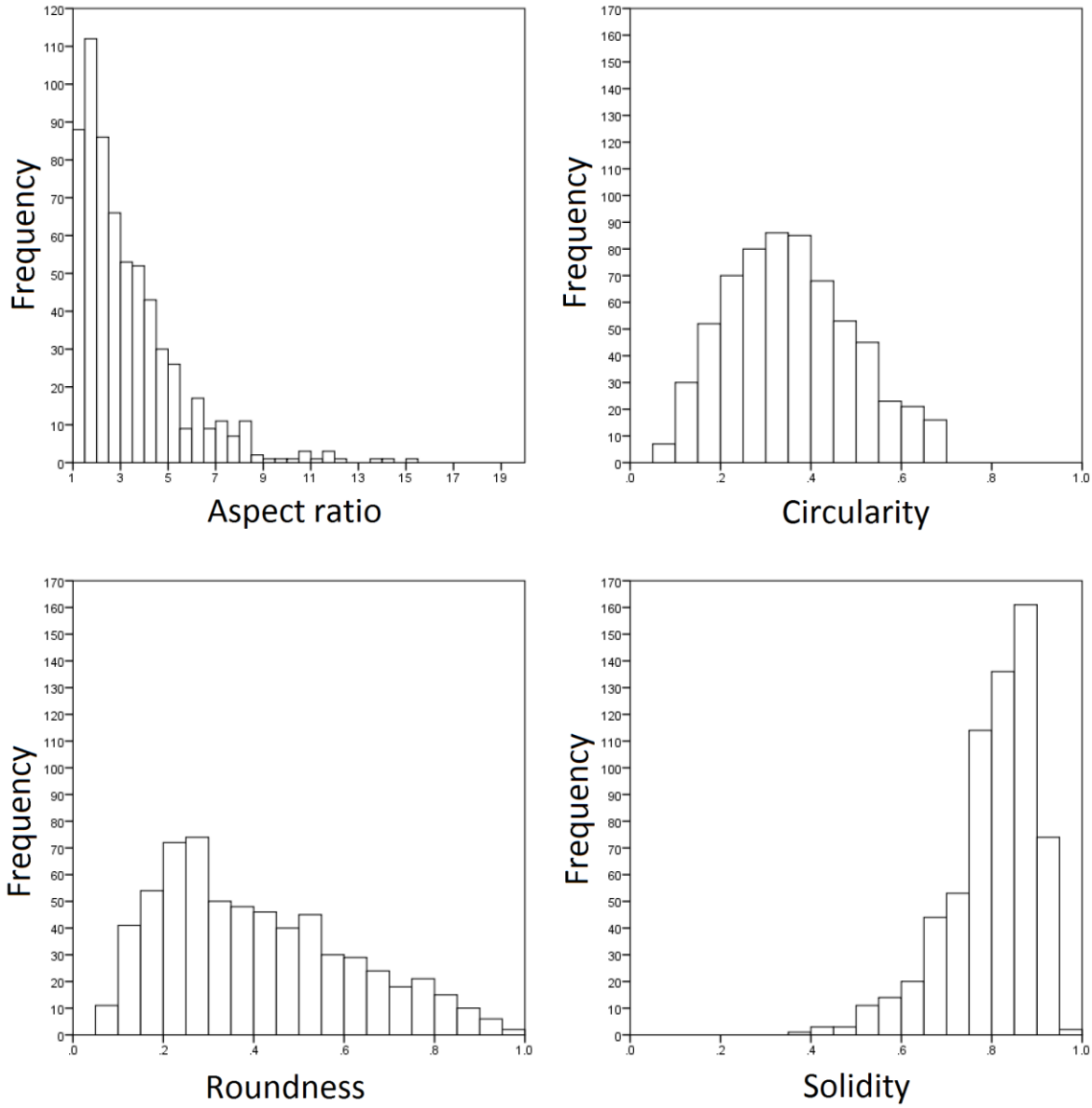

Figure 3.2: Frequency distributions of shape metrics for Holocene peatland mesocharcoal particles.

As a preliminary to statistical analysis of the data, a series of one-sample Kolmogorov-Smirnov tests was run to assess whether shape descriptors, measures of size, and age and depth values, conformed to normal distributions. The resulting P-values are given in Table 3.3. With the exception of circularity (P = 0.373), all distributions returned P-values < 0.001, indicating that the hypothesis that the distributions matched normal distributions should be rejected.

Variable	*P*
Depth	< 0.001
Age	< 0.001
Area	< 0.001
Perimeter	< 0.001
Feret diameter	< 0.001
Minimum Feret	< 0.001
Aspect ratio	< 0.001
Circularity	0.373
Roundness	< 0.001
Solidity	< 0.001

Table 3.3: P-values (two-tailed) from one-sample Kolmogorov-Smirnov tests for normality of distribution of variables

Correlations between depth and all shape descriptors were assessed using Spearman's rank-order correlation coefficient (ρ). Results are displayed in Table 3.4.

An age-depth model (Figure 3.3) was constructed using calibrated ^{14}C dates from 11 depths reported by Fyfe et al. (2008). The core used in this study was taken from within 5 m of the samples dated in that study. Median depths and ages were taken from the ranges given, and where more than one sample had been dated for one depth, the mean value was used. Depths were converted to relative depths to account for the difference in length between the two cores. This resulted in a model of $y = 0.0181 \times x^{2.8446}$ ($r^2 = 0.91$).

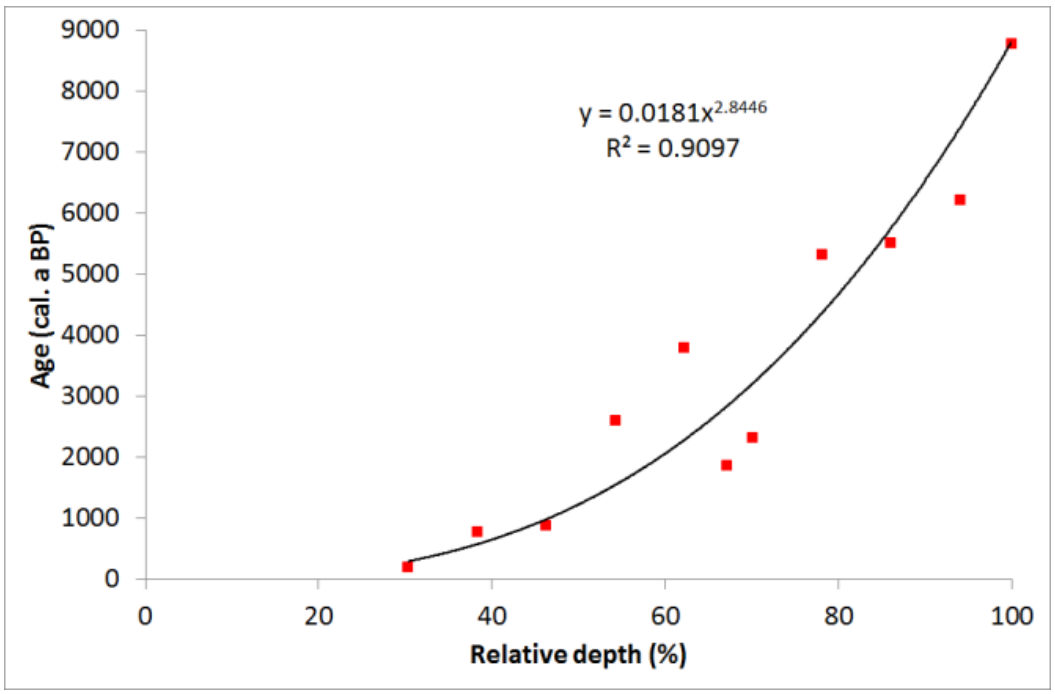

Figure 3.3: Age-depth model based on ^{14}C dates from Fyfe et al. (2008).

Correlations between estimated age and all shape descriptors were assessed using Spearman's ρ. Results are given in Table 3.4. Since the test is conducted on the ordinals, and depth and estimated age are monotonically related, each shape descriptor produces a single value for ρ whether tested for correlation with depth or age. Of the four shape descriptors, only solidity results in a sufficiently low P-value to indicate a genuine correlation with depth and age. Applying a Bonferroni correction for the fact that four tests were conducted, the P-value is adjusted to 0.072. The correlation is in any case extremely weak at 0.094.

In addition, for each shape descriptor, a Kruskal-Wallis one-way analysis of variance by ranks was run to test the hypothesis that the values did not differ (i.e. represented populations without different median values) across depth categories. The hypothesis was rejected for circularity ($P < 0.001$) and solidity ($P < 0.001$), but retained for aspect ratio ($P = 0.108$) and roundness ($P = 0.108$). Variation of mean shape descriptors with depth are shown in Figure 3.4.

		Spearman's ρ	*P*
Depth	Circularity	0.043	0.277
Age		0.043	0.277
Depth	Aspect ratio	-0.008	0.850
Age		-0.008	0.850
Depth	Roundness	0.007	0.851
Age		0.007	0.851
Depth	Solidity	0.094	0.018
Age		0.094	0.018

Table 3.4: Correlation coefficients for age / depth and shape descriptors.

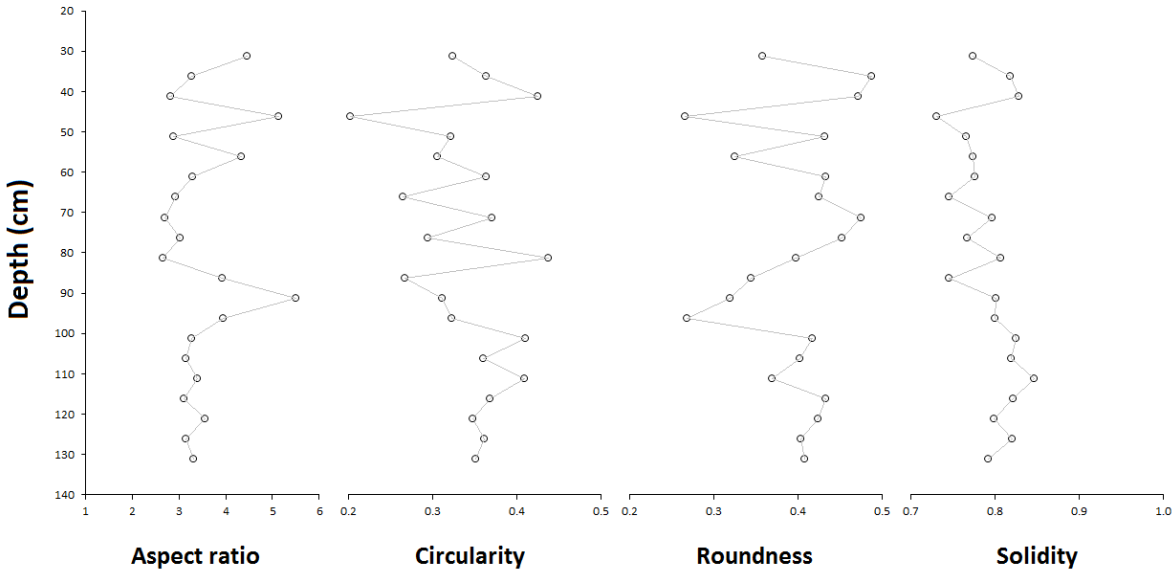

Figure 3.4: Variation of mean shape descriptors with depth for Holocene mesocharcoal particles from Shovel Down.

3.2.3 Discussion

3.2.3.1 Qualitative visual analysis and classification

The question of how peatland charcoal may differ from that preserved in lake sediments was addressed by comparison of the Shovel Down charcoal particles with previous categorisations based on lake sediment charcoal. A subset of

100 particles was randomly selected for comparison with previous morphological studies. For this, each particle was assigned a number, and 100 of these were chosen using the 'RANDBETWEEN' function in Excel 2010. Each of these particles was then categorised according to the criteria given by Mustaphi & Pisaric (2014); the most recent classification of charcoal morphotypes, and the first to comprehensively classify its own data set, and to aim to be adaptable to any other morphologies.

Of the 27 categories defined by Mustaphi & Pisaric (2014), 15 were represented. An example of each is shown in Figure 3.5 along with the illustration given by Mustaphi & Pisaric (2014). 60% of particles were in the 'irregular polygons' category (A), including 5% categorised as A4 or A5 on account of lattice-like structure. The remaining 55% displayed no such distinctive structure, and were subdivided according to the presence of variable surface texture (A1), or holes (A2), or neither (A3).

Mustaphi & Pisaric (2014) define Type A1 as deriving from wood, on the basis of the study by Enache & Cumming (2006). As it is of irregular shape but shows some structure, it can only be Type M by Enache & Cumming's (2006) criteria. Enache & Cumming (2006) cite Umbanhowar & McGrath (1998) for evidence that Type M "likely originated at high temperatures or from the burning [of] branches and leaves", but it is not clear how the findings of Umbanhowar & McGrath (1998) support this conclusion. Again citing Enache & Cumming (2006), Mustaphi & Pisaric (2014) define A3 as deriving from decomposing wood, but also observe that they could produce it by burning "a wide range of materials" including fresh wood, leaves, and other herbaceous material. Type A2 is defined as deriving from herbaceous material, citing Walsh et al. (2010), though Walsh et al. (2010) identify herbaceous charcoal by the presence of stomata, and stomata were not evident in those particles classified as A2 from the Shovel Down core.

The remaining 40% of the subset, which did not fall into the polygonal (A) category, consisted primarily of linear forms (Type D; 21% of total) and blocky or rectangular forms (Type B; 16% of total). Type D (linear) particles are divided into the highly elongate D1, which accounted for only 2%, and the flat D2 (9%) and D3 (10%). D3, which Mustaphi & Pisaric (2014) identify as

originating from *Poaceae* leaves (cf. Jensen et al., 2007), is distinguished from D2 by the presence of oval voids, while D1 and D2 may have multiple sources. Type B (rectilinear) particles are divided between five subcategories. While B1 (1%) are identified unambiguously as wood charcoal, the other four subcategories (15%) each have more than one possible source.

Mustaphi & Pisaric (2014) do not give good reason for the supposed origins of A1 and A3, and while the A2 particles may have been evidently herbaceous in their samples, those that fall into that category as they define it are not so in the Shovel Down assemblage.

These categorisations do not convey much information. All particles viewed in 2 dimensions may be regarded as 'polygonal', and the categorisation of A1, A2 or A3 results from the particles being relatively flat; and the absence of rectangularity, 'complex features' (such as branching, segmentation etc.), elongation, complexity of structure, or glassy appearance. As such, particles fall into these categories due to the absence of features more than the presence of them. This applies most of all to Types A2 and A3, whose only positive attribute is that they are flat, and which account for almost half the particles in the Shovel Down assemblage. These two types are essentially amorphous, and likely classifiable as Enache & Cumming's (2006) Type P. This is similarly a negative categorisation, based on the absence of apparent structure[10] or geometric regularity, though it is also described as having a powdery texture, which was not always evident. This morphotype was rare in the lake sediments studied by Enache & Cumming (2006), was not present at two further lakes studied by Enache & Cumming (2007), and was rare in a fourth lake studied by Moos & Cumming (2012). However, amorphous charcoal was common in the Shovel Down mesocharcoal.

As such forms are evidently rare in lake sediments, it is possible that the abundance of amorphous charcoal is related to the peatland environment itself. This might occur because the different peat is more likely to preserve forms which are inherently fragile, though since Enache & Cumming (2006, 2007) found other fragile morphotypes present, this is not likely to be the cause. It is

[10] Although lack of structure may be taken as evidence that the material is not in fact charcoal, Enache & Cumming (2006) argue that it should be included on account of its "color, opacity and black powdery track on breakage".

also possible that these morphotypes are associated with the peatland environment itself, from burning of peat. Cohen et al. (2009) have reported "lenses of fine-grained amorphous charcoal" resulting from peatland fire, while Hudspith et al. (2014) found that peatland fire produced charcoalified peat clasts composed of degraded *Sphagnum* and other plant tissues within "a matrix of undifferentiated, humified plant tissue".

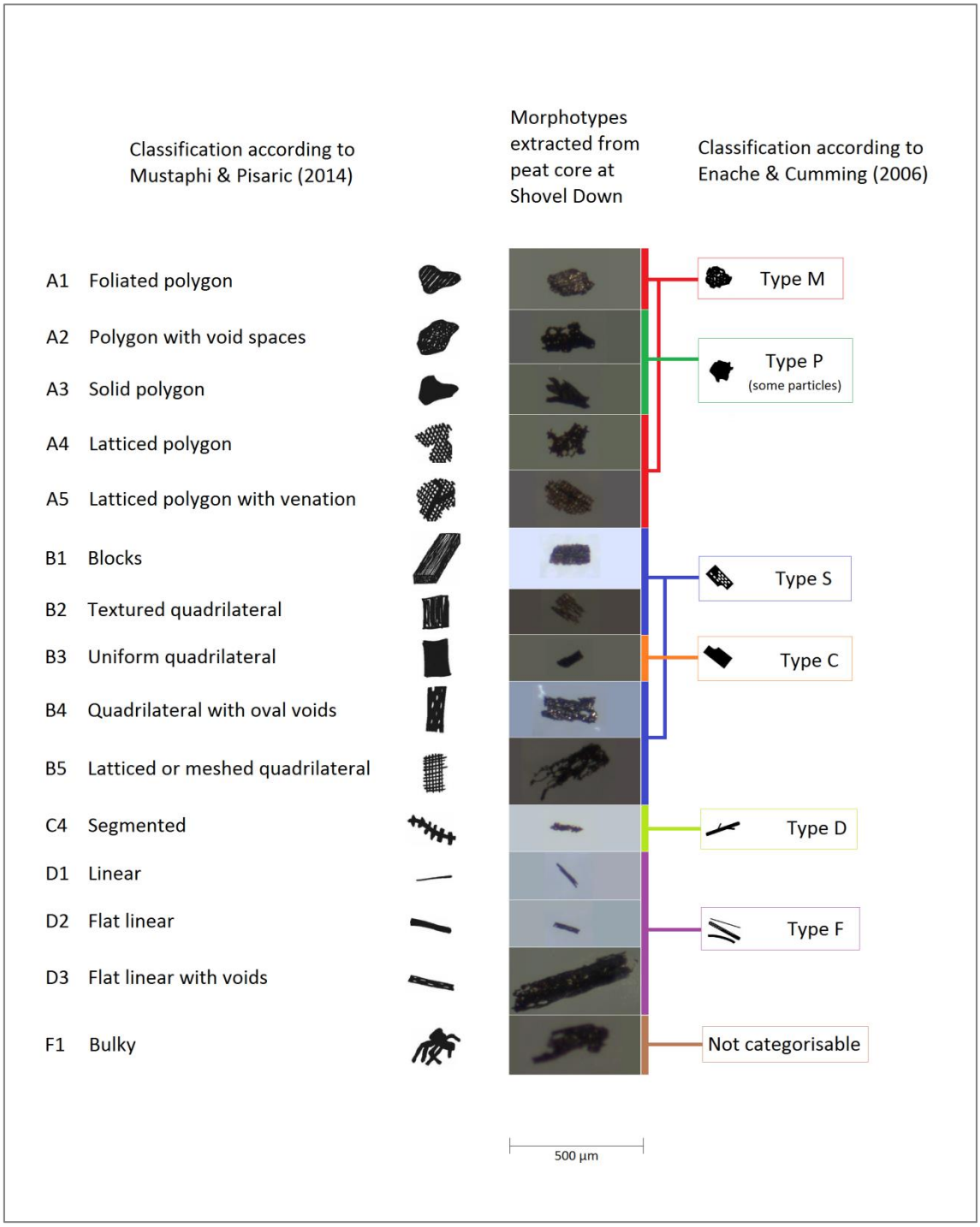

Figure 3.5: Charcoal morphotypes from the Shovel Down peat core classified according to published classification schemes.

3.2.3.2 Quantitative analysis

Previous study of the vegetation history of this site offers the opportunity to compare the quantitative measures of charcoal morphology with changes in vegetation, with the aim of assessing causative linkages between vegetation and shape. The known vegetation history of the site includes coniferous, deciduous and grassland species. Fyfe et al. (2007) established that the proportion of *Poaceae* in the pollen record from the mire fluctuates considerably, and following the findings of Umbanhowar & McGrath (1998), as well as those in Chapter 2, it might be expected that aspect ratios would reflect these changes.

The median aspect ratio of this assemblage (2.7) is fairly typical of those found for non-grassland species in earlier studies. Experiments by Umbanhowar & McGrath (1998) produced mean aspect ratios of 1.91 – 2.23 for deciduous leaf and wood charcoal, and they suggested a likely value of ~2.5 for conifer needle charcoal, while Umbanhowar et al. (2006) give 2 to 3 as the typical range expected of "deciduous leaf or wood charcoal". The results described in Chapter 2 are broadly in keeping with this, and also show that coniferous species, as well as *Equisetum*, *Pteridium* and *Rubus*, fall into the same range.

Figure 3.6 is a schematic diagram showing changes in aspect ratio with estimated age and major shifts in vegetation as described by Fyfe et al. (2008). It can be seen that mean aspect ratios > 3.6 do not occur until after the initial major shift toward grassland described by Fyfe et al. (2008), and associated with grazing. Yet the highest value occurs during the period in which grazing land was being abandoned, and heath and scrub returning. Aspect ratios fluctuate between high (> 4) and low (c. 3) values during the last 1000 years, during which time *Poaceae* pollen remains high. Notably, another very high value (5.1) occurs at 366 a BP, while Fyfe et al. (2008) place the most intensive pastural period at c. 400 a BP.

Considering the coarse sampling resolution and the approximate nature of the age-depth model, fluctuations in aspect ratio are unlikely to align precisely with known patterns of vegetation change. However, the mean aspect ratio does appear to be correlated with the prevalence of grassland, at least on a multi-millennial timescale. No high values occur prior to the establishment of a

grassland component to the landscape-scale vegetation. The subsequent fluctuations would likely require a firmer chronology to interpret effectively.

There is no evidence that any aspect of shape varies as a function of the depth within the peat, or the inferred time since deposition. The low P-values obtained for the correlation of solidity with depth or age could be subject to a variety of interpretations[11], but since the correlation coefficient is < 0.1, even a confirmed correlation would be of little interest.

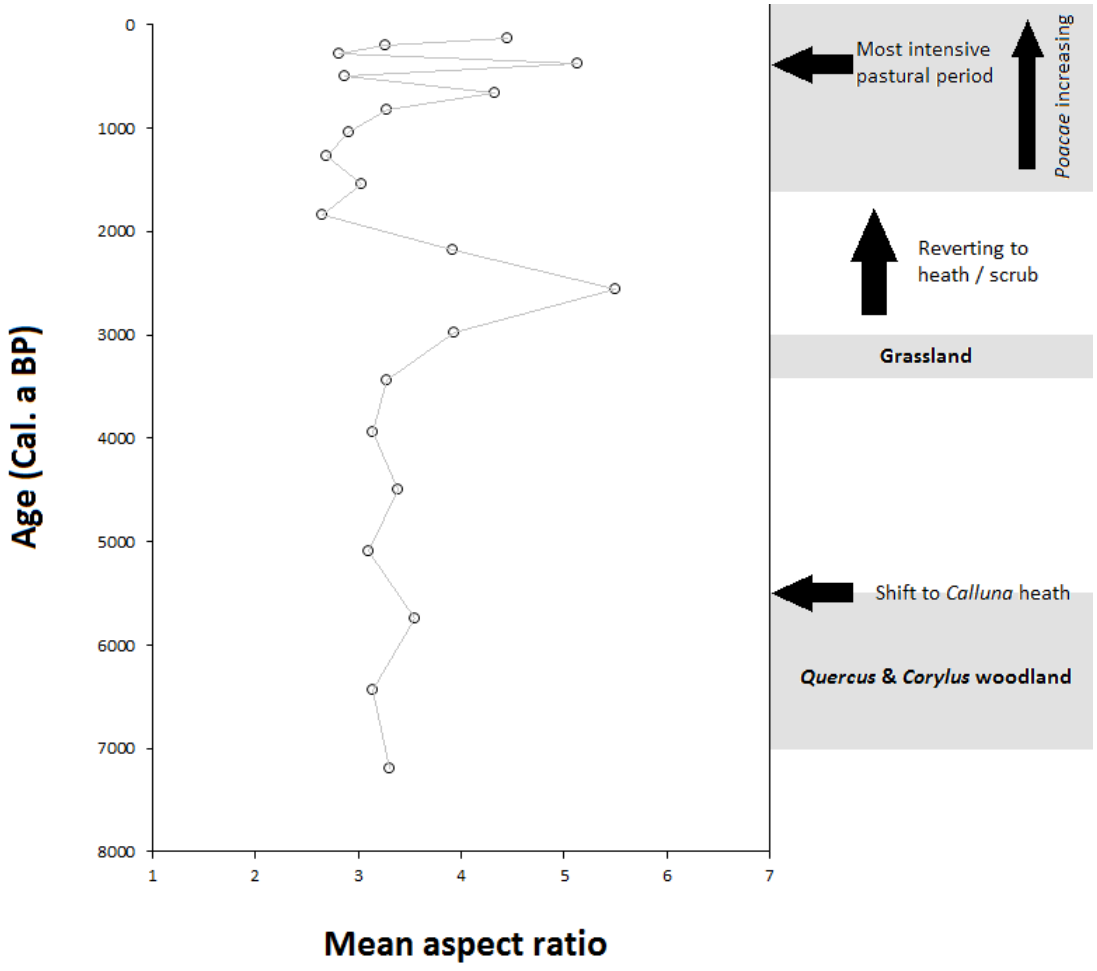

Figure 3.6: Variation of mean aspect ratio with age, showing major changes in vegetation as inferred from pollen records.

[11] E.g. a Bonferroni correction might be applied on the basis that 4 or 8 tests were conducted; and the hypothesis could be considered to be either general (does any shape descriptor have an effect) or particular.

However, two shape descriptors (circularity and solidity) are shown to vary between depths. As there is no evidence of change with time since deposition, this indicates that assemblages of differing morphometries were incorporated into the peat at different times, most likely reflecting variation in species composition, but possibly also transportation or source area.

***

The charcoal assemblage from Shovel Down shows wide variations in morphology, with a comparable diversity of geometry, structure and texture to that found in lake sediment charcoals. The notable difference compared with earlier lake sediment studies is the prevalence of amorphous charcoal particles, which lack defined external morphological features, geometric regularity, or evident internal structure. This contributes to the inability of existing classifications to meaningfully describe and interpret the morphotypes found at Shovel Down. Jensen et al. (2007) accepted that most of their particles lacked distinctive morphological features indicative of their origin, and did not seek to classify these. Mustaphi & Pisaric (2014) by contrast have produced a classification which, by virtue of containing categories based on the absence of features, can accommodate all particles. However, this categorisation attributes features of those particles which were defined only by negative attributes in their own study to those so defined in the present study, leading to unfounded inferences about the nature of the source material.

3.2.4 Summary

This first study of peatland charcoal morphometry reveals highly variable morphologies, and shows that both qualitative and quantitative descriptors of charcoal may yield a range of information. Morphologies may be identified with categories from earlier research, highlighting the fact that amorphous charcoal, lacking distinctive features, is far more common than in earlier lake sediment studies. This may be related to burning of the peat itself.

Quantitative analysis of charcoal morphology appears to yield interesting correlations with changes in land use and vegetation history. The charcoal

particles display a wide range of aspect ratios, whose averages appear to vary broadly in keeping with known changes in land use. While there is no evidence of monotonic change in morphological parameters with depth in the peat, which would indicate change in morphology with time since deposition, shape descriptors do vary with depth categories. This shows that the variation is indicative of the morphologies originally incorporated into the peat.

Chapter 4: Morphologies of pre-Quaternary Charcoals

4.1 Introduction and aims

Both quantitative morphometric analysis, and attempts to categorise morphologies based on qualitative visual criteria, have generally been restricted to Quaternary research. In this section, the morphologies of charcoal assemblages from 20 pre-Quaternary samples, obtained from 5 different sites, are assessed to determine the extent to which distinctive morphologies survive the process of lithification, and whether morphometric measurements may be of value in pre-Quaternary charcoal analysis.

4.2 Materials & Methods

4.2.1 Sites

1. Cabo Carvoeiro Formation, Peniche, Portugal – Lower Jurassic

The Cabo Carvoeiro Formation consists of hemipelagic marls and limestones, deposited c. 183 Ma BP (early Toarcian) in a submarine fan at the edge of the Tethys Ocean, and now exposed on the coast of Portugal (Hesselbo et al., 2007). The 5 samples used in this study span a section of > 17 m, corresponding to approximately 950 ka according to recent dating evidence (Huang & Hesselbo, 2014).

2. Sorthat Formation, Bornholm, Denmark – Middle Jurassic

10 samples are from the Sorthat Formation, formerly known as the Bagå Formation (McElwain et al., 2005) at Korsodde, Bornholm, Denmark. The Korsodde section consists of sandstones, silt and mudstones deposited in shoreface and lagoonal environments during the Toarcian (Hesselbo et al., 2000). Wood particles from this section, both charcoalified and unburned

(coalified), show the isotopic anomaly associated with the Toarcian OAE (Oceanic Anoxic Event) (Hesselbo et al., 2000), which occurred c. 183 Ma BP.

3. Wealden Group, Lulworth Cove, England – Lower Cretaceous

A single sample is of terrestrial siltstone/mudstone from the Wessex Formation (Wessex Sub-basin, Wealden Group) at Lulworth Cove, Dorset, UK. The Wessex Formation (formerly known as the Wealden Marls) dates from the Barremian Age (c. 129-125 Ma), and its flora consists principally of ferns and conifers (Sweetman & Insole, 2010). The exposure at Lulworth Cove represents sediments deposited in a floodplain environment (Radley & Allen, 2012).

4. Potomac Group, Maryland, USA – mid-Cretaceous

Three samples come from the mid-Cretaceous Elk Neck Beds ('Maryland Raritan') at Rocky Point on the Chesapeake Bay, Maryland, USA. These consist of terrestrial clay or silt and probably date from the earliest Cenomanian (Friis et al., 2011). The palynoflora of the Elk Neck Beds is dominated by angiosperm pollen and the macroflora by angiosperm leaves (Drinnan et al., 1991), and also contains angiosperm wood, as well as conifer wood, shoots, cones and seeds (Drinnan et al., 1991). Bulk samples were obtained from three (contiguous) depths spanning 34 cm. Drinnan et al. (1991) assign the locality to Potomac Group palynological Zone III.

5. Remington Hill, California, USA – Miocene

A single sample was obtained from Miocene (Tortonian) fluviatile deposits at Remington Hill, Sierra Nevada, California, USA (c. 9 Ma BP). Flora include both gymnosperms and angiosperms (Magnoliopsida). The 'Remington Hill flora' is described by Minnich (2007) as an oak woodland savanna.

4.2.2 Sample processing

The Wealden group and Potomac group samples were treated with concentrated hydrochloric and hydrofluoric acids to dissolve carbonate and siliceous minerals respectively, and were ‘rinsed’ with water between acid treatments to prevent formation of fluoride precipitates. Centrifugation was not required. The samples were processed according to the following protocol:

1. 5 to 10 g of the sample is weighed into a 200 ml polyethylene screw-top container. Approximately 10 ml of 10% hydrochloric acid (HCl) is added to test the strength of the reaction; then approximately 30 ml of 32% HCl is added. If the reaction is vigorous, a few drops of Industrial Methylated Spirit (IMS) are added to prevent the sample bubbling over. The sample is swirled and left overnight with the lid loosely fitted.

2. Where possible, any supernatant containing no particulate matter is decanted. The sample is then topped up with deionised water. Once the sample has settled (after several hours), so that there is no material visible in suspension, the supernatant is decanted.

3. Approximately 30 ml of 38-40% hydrofluoric acid (HF) is added, the sample swirled, and left overnight with loosely fitted lid.

4. Supernatant is decanted, the sample topped up with deionised water, and left overnight. Supernatant is decanted again once the sample has settled.

5. Another 30 ml of 32% HCl is added, the sample swirled, and left overnight with loosely fitted lid.

6. The supernatant is decanted, the sample topped up with deionised water, and left to settle. This is repeated until the sample reaches a pH of 6, as measured with pH (litmus) paper.

7. The sample is sieved at 125 µm, and both fractions are retained.

Samples from Bornholm, Peniche and Remington Hill were received in a processed form. Samples from Peniche and Bornholm were processed as

described by Baker et al. (in review). The method for the Peniche samples differed from the above only in the duration of acid maceration (48 hours in 32% HCl; 72 hours in 40% HF; 24 hours in 32% HCl), while the samples from Bornholm did not require acid treatment, and were wet sieved at 125 µm using only water. The sample from Remington Hill was processed as above, except that HF treatment lasted for 72 hours (Belcher, pers. comm.).

4.2.3 Microscopy

The > 125 µm fraction was examined with a dissecting microscope using both reflected and transmitted light. Reflected light is needed to observe anatomical structure within the particles, and the quality of the reflectance. Transmitted light reveals any translucency in the particles, which allows easy rejection of dark-coloured mineral pieces, and can reveal a reddish tinge at the edges of coalified particles which might otherwise closely resemble charcoal.

The samples, dispersed in water, were transferred to glass slides in quantities of approximately 0.1 ml, and all pieces identifiable as charcoal were removed with a fine paintbrush (5/0 grade).

Particles were identified as charcoal on the basis of meeting all the following criteria:

1. Blackness
2. Homogeneity of the material
3. Degree of reflectivity
4. Preservation of anatomy

Brittleness of the material was taken into account, but pieces were not broken for the purpose of testing this. Particles otherwise meeting these criteria were rejected on the basis of any the following:

1. Brown or reddish colouring at thin edges of otherwise apparently black material
2. Conchoidal fracturing

3. Distortion of anatomy (e.g. where preserved only on one part of the particle)

4.2.4 Image analysis

All identified charcoal particles were digitally photographed at ×50 with sufficient transmitted light to allow easy thresholding. Images were stored in TIFF format, and processed using ImageJ 1.47t.

The images were converted to 8-bit greyscale, and binarised using the IsoData algorithm (Ridler and Calvard, 1978), with the maximum threshold value manually adjusted and the minimum set to 0. Shape descriptors, as defined in Section 1.11.2, and size descriptors (area, perimeter, Feret diameter and minimum diameter) were generated using the 'Analyze Particles' function. Particles of area < 1000 μm² were subsequently excluded from the dataset.

Particles were typically photographed in groups of approximately 10; this being the most that could be positioned on the slide without being likely to overlap once under the cover glass.

Cretaceous (Wealden Group & Potomac Group) samples were counted in full. For the Jurassic (Peniche and Bornholm) and Miocene (Remington Hill) samples, further particles were photographed until at least 50 images > 1000 μm² had been obtained, except where fewer particles of this size existed in the whole sample. As numbers obtained were not known until after image analysis, the actual number of images for each of these samples is variable.

4.2.5 SEM

Particles with morphologies of particular interest were imaged with SEM. These were mounted on SEM stubs using adhesive carbon discs, and then sputter-coated with gold/palladium to a thickness of approximately 10 nm. Particles were imaged using a Hitachi S3200N SEM at c. 20 kV.

4.3 Results

4.3.1 Peniche

Numerous highly elongate particles were evident within all five samples prior to image analysis. Most charcoal particles in these samples represent one of two morphotypes: stem-like forms with vessels or tracheids clearly visible (Type A; Figure 4.1 A), and long slender forms (width c. 20-30 µm) (Type B; Figure 4.1 B). The latter were confirmed as charcoal using SEM, since their width made identification difficult. A very small number of intermediate forms (Type C; Figure 4.1 C) were also present, which appear to show the more elongate form becoming disaggregated from the stem-like form.

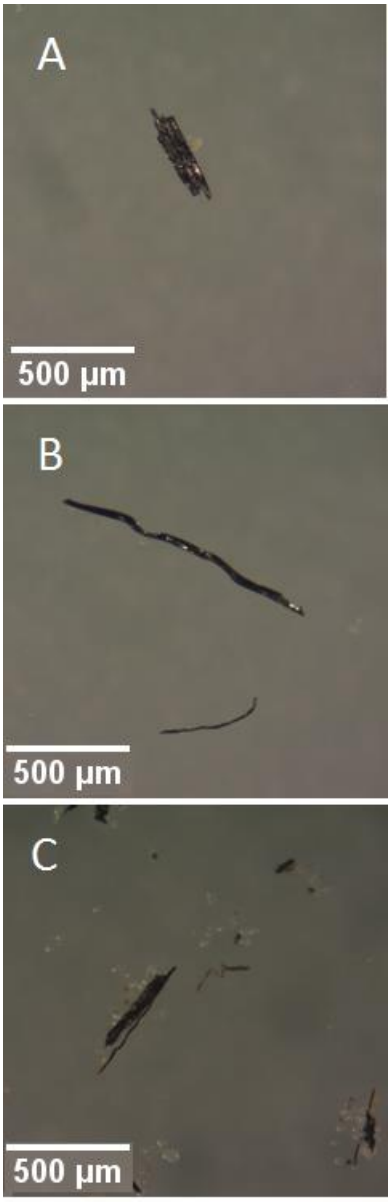

Figure 4.1: Principal morphologies evident in Jurassic mesocharcoal samples from Peniche; (A) stem-like form, (B) elongate form; and (C) rare intermediate form.

SEM images of samples 1, 6 and 11 (see Table 4.1 for sample numbers) show that elongate particles are of two types. Some (Type B1) appear to be tracheids, either individually or in small clusters (Figure 4.2, A & B). Others (Type B2) appear to be charcoalified forms of some initially elongate form, showing no evidence of having fractured from a larger particle laterally, but only at the ends (Figure 4.2, E & F). The surface texture of these particles also gives them a fibrous appearance. Some SEM images also show xylem material in which tracheids are partially separated from one another, but remain attached as a single particle, suggesting a stage between the Type A and Type B1 (Figure 4.2, C & D).

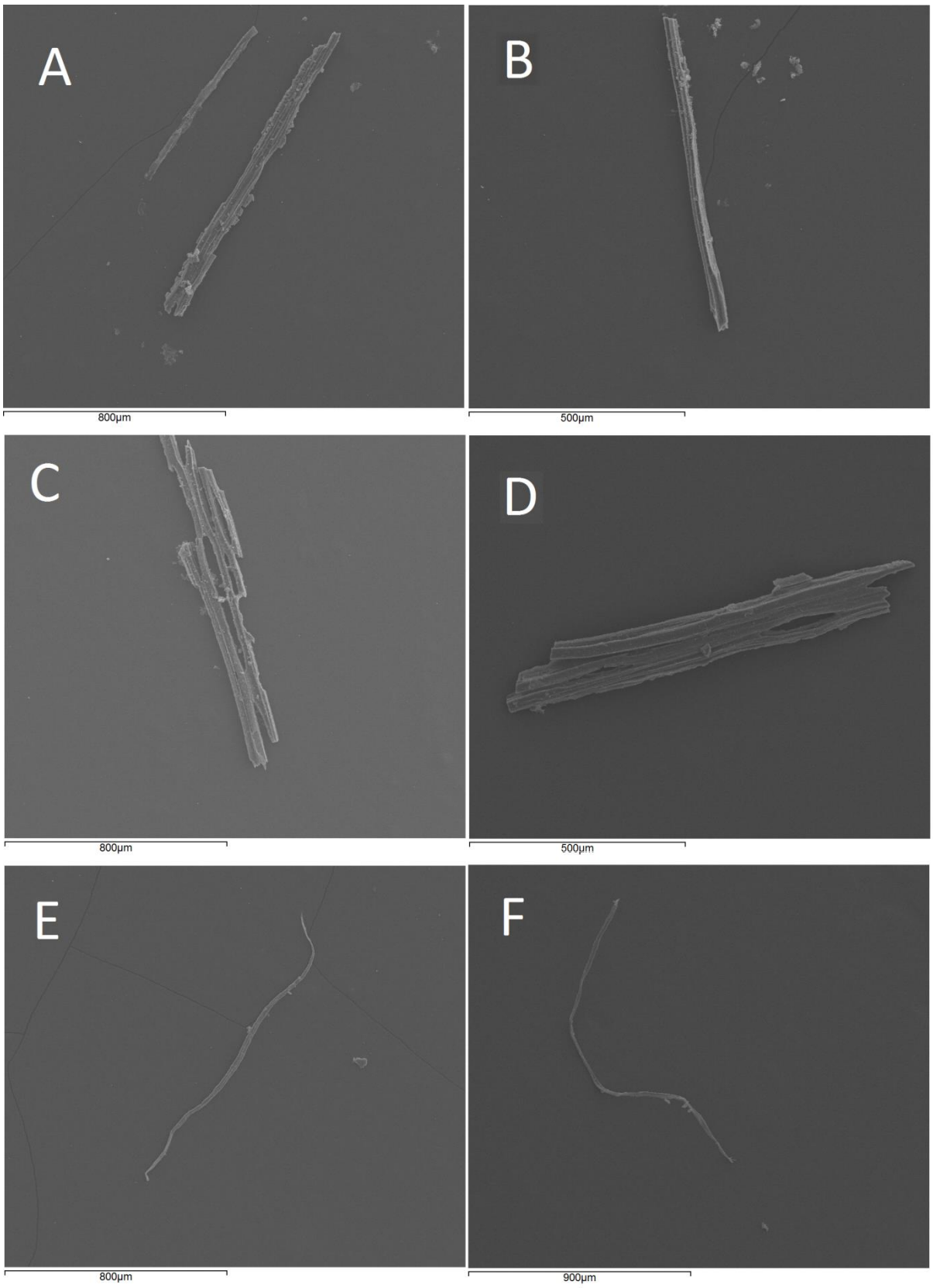

Figure 4.2: SEM micrographs of Jurassic mesocharcoal from Peniche, showing elongate forms consisting of single or small numbers of tracheids (Type B1) (A – sample 1; B – sample 11), xylem charcoal showing separation of tracheids (C – sample 11; D – sample 6), and elongate forms from another source (Type B2) (E – sample 1; F – sample 6).

4.3.2 Bornholm

Mesocharcoal appeared to consist mostly of woody or stem-like fragments. Notably, much of the charcoal in these samples displayed rounded and smoothed edges, as compared to the other four sites. A very few particles had the highly elongate appearance of Type B from Peniche, and a single particle (in sample 74) had the appearance of the intermediate Type C form with disaggregation of tracheids.

SEM images of Bornholm sample 68 show cellular structure in keeping with the assumption that the particles are mostly xylem fragments (Figure 4.3 A,B). A rare elongate particle (Figure 4.3 C) is shown to be hollow (Figure 4.3 D,E). This has the appearance of the Type B2 particles from Peniche.

4.3.3 Cretaceous and Neogene samples

The mesocharcoal in the samples from both the Wealden Group and the Potomac Group appeared to consist mostly of woody or stem-like fragments, and was lacking in highly elongate or elaborate forms.

Morphology of mesocharcoal particles from Remington Hill was highly variable in its immediate appearance, containing particles similar to Peniche Types A and B (but not C), as well as particles showing the general form associated with wood, tree leaf and grass mesocharcoal.

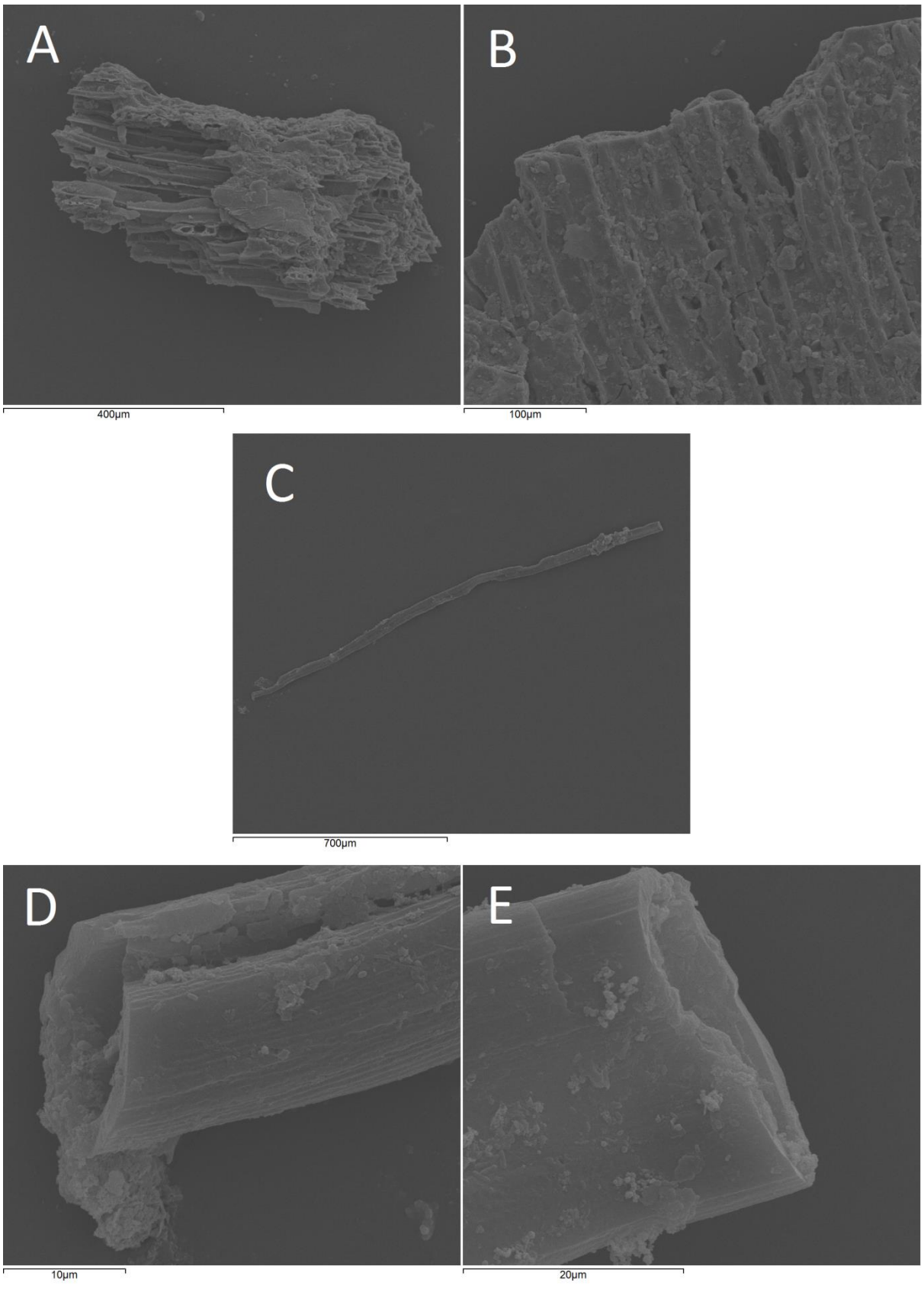

Figure 4.3: SEM micrographs of Jurassic mesocharcoal from Bornholm.

4.3.4 Morphometrics of pre-Quaternary samples

The pre-Quaternary charcoal was found to display considerable variation in aspect ratio, but in all samples distributions are heavily positively skewed, with outliers and extreme values present (Figure 4.6). Aspect ratios are especially high in all five Peniche samples (median 4.8 to 9.5). They are also high in the Remington Hill sample (median 3.52). The Bornholm samples display highly variable aspect ratios, though it is noted that this may be associated with small sample sizes, and the results for samples 67 (n = 2) and 75 (n = 2) are of little value.

Site	Depth (m)	ID	Number of particles	Mean circularity	Mean aspect ratio
Cabo Carvoeiro Formation (Peniche)	0.4	1	57	0.13	12.16
	6.3	4	58	0.23	8.47
	7.8	5	65	0.18	8.69
	9.8	6	223	0.21	9.38
	17.1	11	53	0.25	6.50
Sorthat Formation (Bornholm)	31	53	42	0.43	2.52
	30.3	56	57	0.33	3.47
	29.9	57	57	0.49	2.36
	28.7	62	35	0.51	2.16
	28.2	64	41	0.40	5.52
	27.5	67	2	0.59	1.76
	27.3	68	66	0.45	3.06
	26.5	71	44	0.55	2.02
	25.7	74	62	0.41	3.63
	25.5	75	2	0.49	1.98
Wealden Group (Lulworth Cove)	-	-	700	0.41	3.43
Potomac Group (Rocky Point)	Upper	A	306	0.40	2.76
	Middle	B	452	0.50	2.76
	Lower	C	428	0.52	2.54
Remington Hill	-	-	169	0.24	5.66

Table 4.1: Aspect ratios of mesocharcoal particles from pre-Quaternary sediments

4.4 Discussion: variation in particle morphology of pre-Quaternary charcoal

Distributions of both circularity (Figure 4.5) and aspect ratio (Figure 4.6) vary considerably across the 20 samples. Circularity appears to vary between the five sites, being consistently lower in the samples from Peniche, and consistently higher in the Potomac samples. More variability is evident among the samples from the Sorthat Formation, though this is partly explained by low numbers of particles in some samples, with samples 67 and 75 containing only two particles each within the size fraction being studied here. Aspect ratio too appears to vary by site, but in this case it is one particular site, Peniche, which is remarkably different to the others.

It is notable that the low values for circularity appear to be associated with high values for aspect ratio; particularly evident in the five samples from Peniche, and the single sample from Remington Hill. The mean values for aspect ratio and circularity are in fact highly correlated (r = -0.92) in this data set, as shown in Figure 4.4. This suggests that, given the considerable variability in aspect ratio across the 20 samples, the circularity data is largely reflecting differences in elongation.

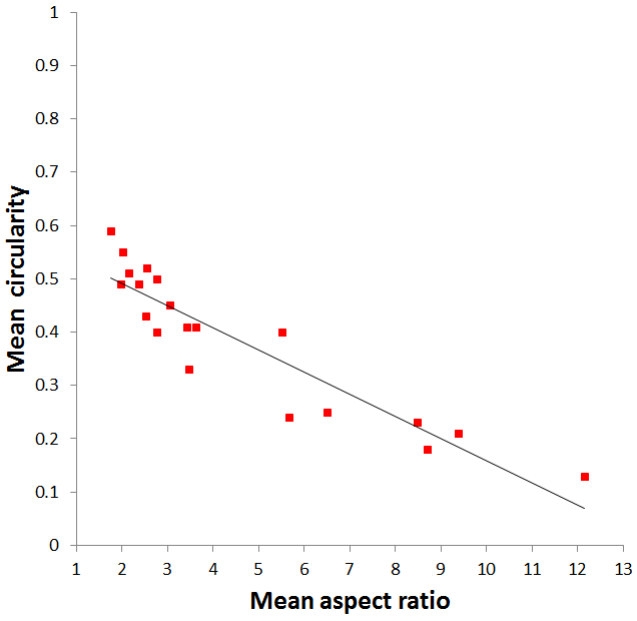

Figure 4.4: Relationship of mean circularity to mean aspect ratio for 20 pre-Quaternary mesocharcoal samples.

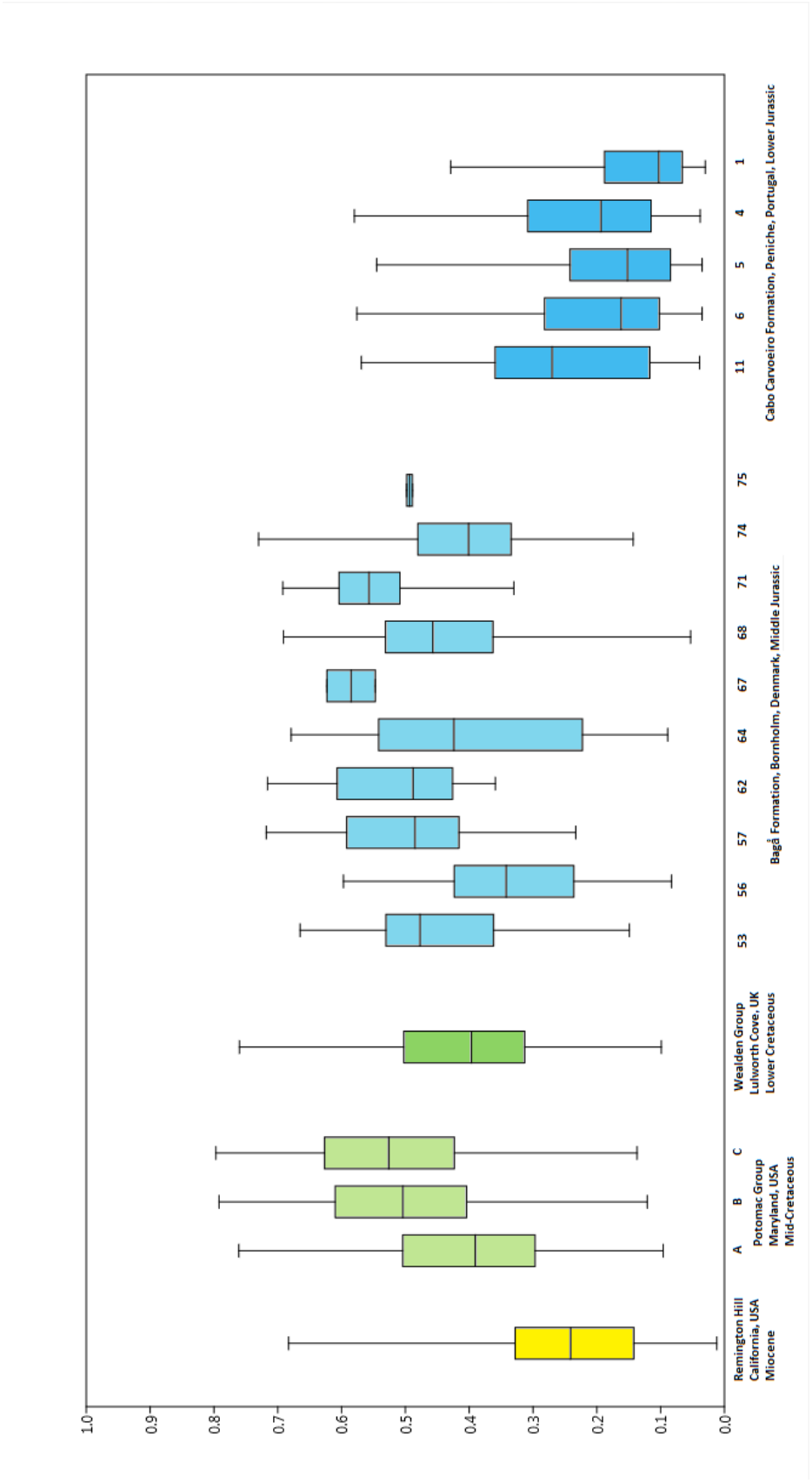

Figure 4.5: Boxplot of circularity distributions for 20 pre-Quaternary mesocharcoal samples.

The rounded and worn nature of many particles in the Sorthat samples was noted when viewed with the microscope. While such effects can be captured by measurements of circularity, this may be overwhelmed by the effect of elongation. The Potomac Group samples are similarly derived from a fluvial setting, though the rounding of the particles was not evident.

Differences in transportation may partly explain the differences between more degraded samples, which have been subject to greater transportation energies (e.g. Sorthat and Potomac, which are both fluvial sediments), and have higher circularity values; and those which retain more of their original morphological features (e.g. the Remington Hill sample, which was deposited in a lower energy mud rock). However, this is not sufficient to explain the morphology of the Peniche samples, which were deposited in a relatively deep, but near shore fault-controlled marine basin, and whose aspect ratios are remarkably high by comparison with those commonly seen, and those reported in the literature. While some of the difference in morphology may be explained by the differences in transportation, this does not have any bearing on those assemblages whose average aspect ratios exceed even those of non-transported charcoal.

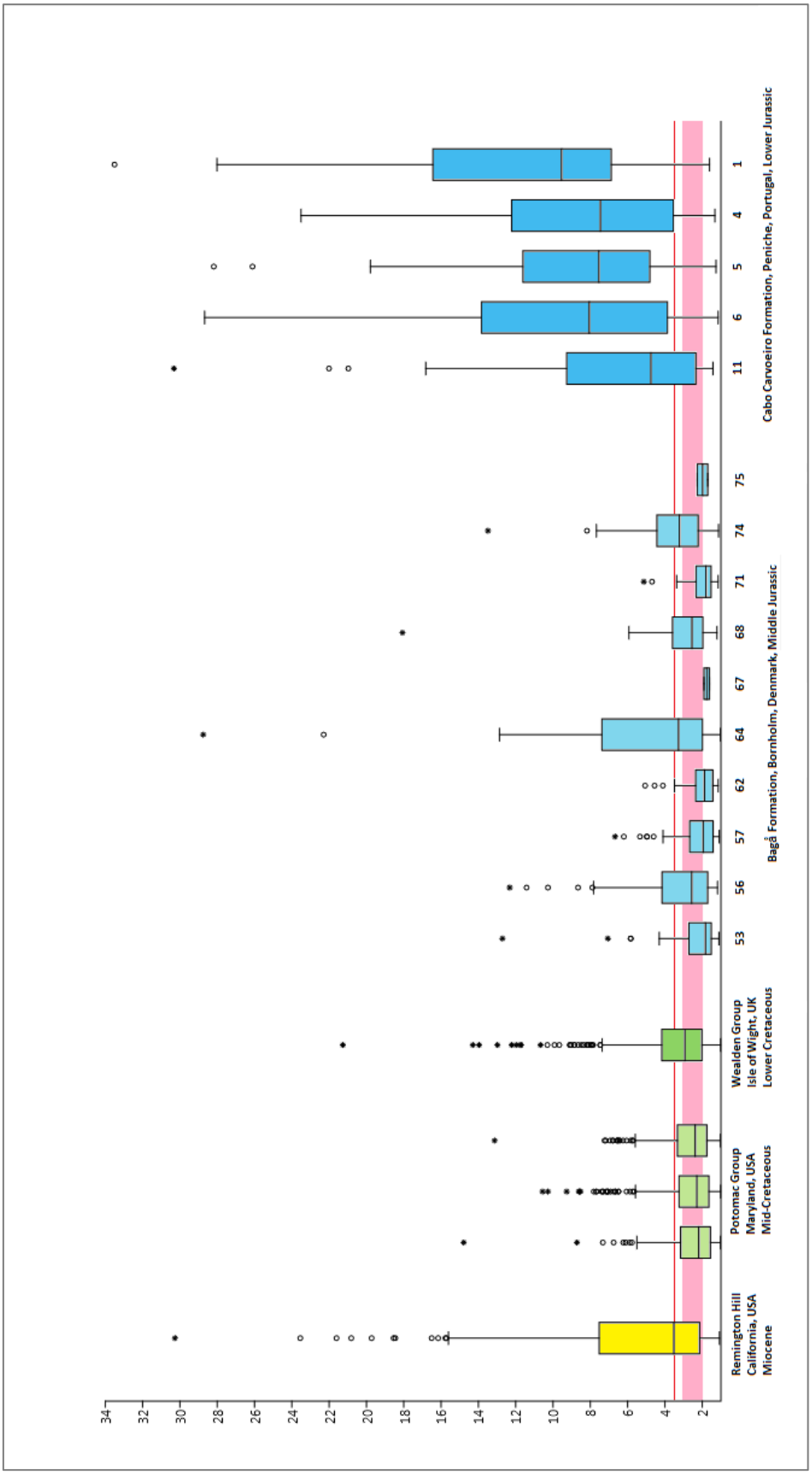

Figure 4.6: Boxplot of aspect ratio distributions for 20 pre-Quaternary mesocharcoal samples. The pink band indicates the range considered typical of woodland charcoal and the red line the lower threshold indicative of grassland charcoal (Umbanhowar et al., 2006).

Figure 4.6 contrasts the aspect ratios for these pre-Quaternary samples with the general median values given by Umbanhowar et al. (2006) as indicative of vegetation type in Holocene archives. It can be seen that most of the samples cluster within, or close to, the 2–3 range which, in Holocene sediments, is said to be indicative of woodland charcoal. The variation among the Bornholm samples may be largely explained by sample sizes insufficient to capture the true distribution of values. However all five of the Peniche samples far exceed the threshold of 3.5, above which Holocene charcoal is supposed to derive from grassland. The Remington Hill sample also marginally exceeds this threshold with a median value of 3.52.

While the high aspect ratios in the Remington Hill sample could result from the presence of grass charcoal (on account of its Miocene age), the Peniche samples show that grass is not the only source of elongate mesocharcoal. The grasses (family *Poaceae*) evolved in the latest Cretaceous or early Paleogene (Willis & McElwain, 2002), which the Peniche samples pre-date by at least 100 Ma.

The rule of thumb given by Umbanhowar et al. (2006) is based on the experiments of Umbanhowar & McGrath (1998), which concerned the forest-prairie ecotone of North America, and thus an essentially binary choice of grassland vs. woodland. The results of the simulated transport experiment described in Chapter 2 indicate that interpretation may be more difficult where other growth forms are present. Figure 4.7 shows the median aspect ratios for 26 specimens, regardless of transport time. While the four grass specimens produce higher aspect ratios than any of the 16 tree specimens, high values also occur for the pteridophytes, *Equisetum telmateia* and *Pteridium aquilinum*, and the weedy angiosperm, *Rubus fruticosus*.

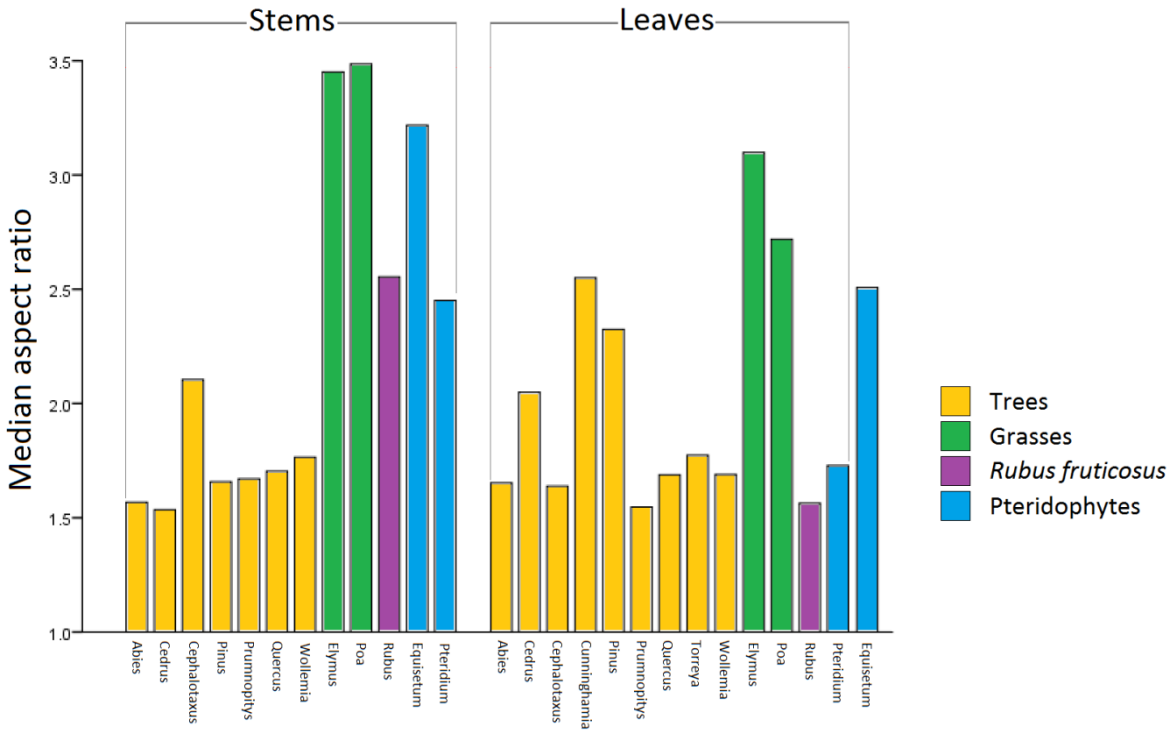

Figure 4.7: Median aspect ratios of laboratory-produced charcoal particles > 125 µm, grouped by material type and taxonomic affinity. (Data from Chapter 2.)

These results, and those of Umbanhowar & McGrath (1998), indicate no tendency for either gymnosperm or angiosperm trees to produce particularly elongate mesocharcoal. This suggests that sources of elongate mesocharcoal prior to the evolution of the grasses should be sought among non-arborescent plants, and that, at least prior to the evolution of the angiosperms, the pteridophytes may be the most likely source.

4.5 Observations and considerations of elongate particles at Peniche

Of the 20 pre-Quaternary samples studied, the 5 Jurassic samples from Peniche show the most distinctive morphologies, with the high degree of elongation evident when viewed by eye through a microscope, and in the morphometric results. The numerous highly elongate particles which cause these results are uncommon in pre-Quaternary sediments (Belcher, pers. comm.), and far outside the range of elongation values expected from

morphometric studies on more recent sedimentary charcoal, and so warranted further analysis.

The SEM images show clear evidence of xylem material separating into elongate forms (Type B1; Figure 4.2 C,D) by the lateral disaggregation of individual tracheids, or small groups of tracheids. Martill et al. (2012) present images of very similar mesocharcoal particles from the early Cretaceous of Brazil. Their images show a mixture of individual tracheids and small clusters; approximately rectangular in cross section, with similar dimensions and elongation to the Type B1 particles (Figure 4.8). Scaramuzza et al. (2016) question whether the specimens described by Martill et al. (2012) have been conclusively identified as charcoal, as the latter had not shown evidence of "homogenized cell walls or other features diagnostic of charcoal". However charcoal is routinely identified without confirmation of homogenised cell walls where SEM has not been employed.

Figure 4.8: Comparison of B1 elongate charcoal particles reported by Martill et al. (2012) (left) and those found in samples from Peniche (right). All scale bars are 100 µm.

Type B2 (Figure 4.2 E,F) are of a quite different appearance. The elongation is even greater; they are curved or twisted, with tapering towards the ends, and a different surface texture. The rounded sides show no evidence that they are detached from an adjacent particle; neither damage to the particle nor fragments remaining from an adjacent particle. In addition, their rounded nature makes it unlikely that they were previously attached laterally. They therefore appear to be elongate by nature of their growth rather than by fragmentation, with a fibrous form similar to a hair or trichome, and therefore implying a 'root' end where the cell was attached to the plant. The ends of the particles (Fig. 4.9 A) generally have the appearance of brittle fractures, indicating that they are fragmented from longer particles. The surface texture of the Type B2 particles has a scaly appearance (Figure 4.9 B), and often longitudinal striations, contributing to the fibrous appearance.

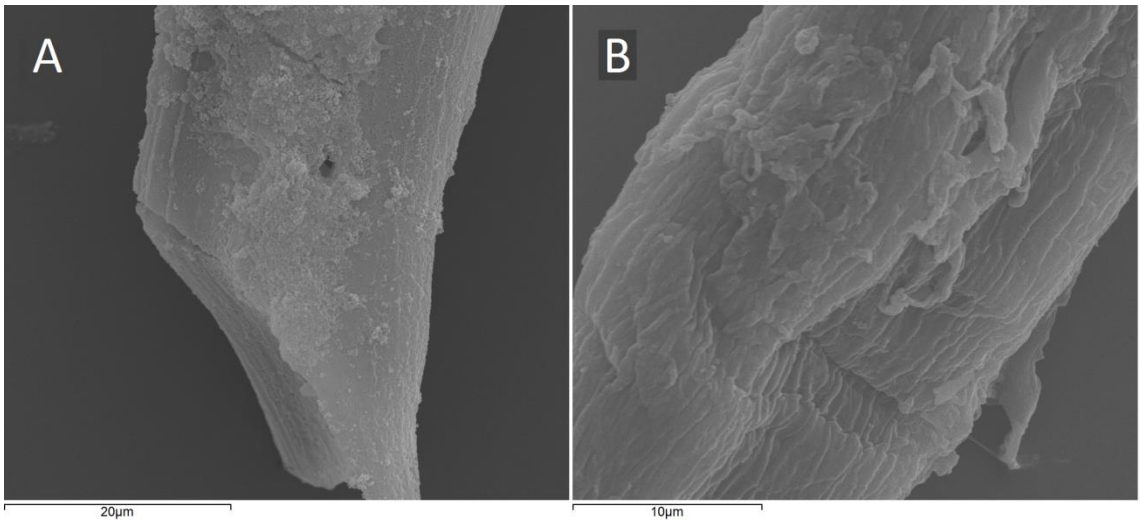

Figure 4.9: SEM images of Type B2 mesocharcoal particles from Peniche.

Many of the Type B2 particles are clearly bent or twisted, in such a manner as to suggest hollow, tubular structures (Figure 4.10). These features must have been fixed prior to charcoalification, and indicate that the particles were somewhat flexible at this time. The presence of bends or twists can be used to differentiate Type B2 from Type B1 even under low magnification light microscopy. On this basis it appears that the B1 morphotype forms the majority of elongate particles in all five of the Peniche samples.

Figure 4.10: Type B2 mesocharcoal particle from Peniche, showing twisting and apparent hollow form.

4.5.1 Possible reasons for Peniche morphotype B1

A mechanism for the formation of the Type B1 particles found in the Peniche samples is suggested by a study conducted by Jones & Chaloner (1991), who demonstrated that temperature of charcoalification can affect cell cohesion in the resulting charcoal. In their experiment, they buried blocks of *Pinus sylvestris* wood under 10 mm of fine sand, then heated them in a furnace to a range of peak temperatures, sustaining the peak temperature for 1 hour. They found that disappearance of the middle lamella occurred at 220-230 °C, indicating the point at which 'true' charcoal is formed as evidenced by the homogenisation of the cell wall; and that above 340 °C cracking occurred at the location of the middle lamella, resulting in "a characteristic fibrous texture". Cracking progressed from the edges of the block, and increased with peak temperature, until individual cells became entirely separate. Complete combustion occurred above 600 °C.

Scott & Glasspool (2013) have disputed these findings on the grounds that Jones & Chaloner (1991) did not fully exclude oxygen, and had unreliable temperature readings due to not using an internal temperature probe. The exothermic reaction which occurs above 285 °C was considered to be a particular problem, resulting in erroneously low temperature readings compared with the true internal temperature. Scott (2010), who had used temperature probes inside the samples, had found that homogenisation of cell walls occurred at the higher temperature of 300-325 °C, while Scott & Glasspool (2005) did not produce cracking of the middle lamella with temperatures of 900 °C for 24 hours, simulating the creation of volcanic charcoals. On the basis of these results, Glasspool & Scott (2013) suggest that the cracking "resulted from the ingress of oxygen". This conclusion does not automatically follow, since other factors varied between the experiments, and Glasspool & Scott (2013) do not suggest any mechanism for it. In addition, it is not clear how the presence of oxygen detracts from the findings of Jones & Chaloner (1991); the formation of charcoal indicates that oxygen levels in their experiments were low, but excluding it entirely is only relevant to the formation of volcanic charcoals, while their concern (as here) was explicitly wildfire.

Glasspool & Scott's (2013) criticism of the temperature control in the experiments by Jones & Chaloner (1991) is perfectly valid, and their conclusion that the recorded temperatures in that study would have been too low is backed up by other studies (e.g. McParland et al., 2007) which show the homogenisation of cell walls occurring at higher temperatures. However, the claim that the cracking is caused by the presence of oxygen is not proven, and if oxygen is involved this does not detract from the relevance of the finding to fossil charcoals. Nor does it follow that the cracking is not caused by high temperatures. What the experiments by Scott & Glasspool (2005) and Scott (2010) do show is that high temperatures alone are not sufficient to cause cracking of the middle lamella.

Jones & Chaloner (1991) identify two further reasons why fossil charcoal may appear "fibrous" – elongate xylem structure and 'bogen-struktur' (normally translated as 'bogen structure'). Elongate xylem structure is not sufficient to explain the morphology of the B1 particles, which are evidently disaggregated tracheids, although the original length of the tracheids will clearly be a factor.

Jones et al. (1997) define bogen structure as “a discrete mass of small fragments, where an intact fragment has been shattered *in situ* as a result of compressive forces”. Jones & Chaloner (1991) further specify fracturing “usually perpendicularly across the weakest or thinnest part of the wall and lengthwise down the cells.” While lengthwise fracturing *within* cells is evident in the Peniche samples, it is specifically fracturing between cells which appears to be the cause of the distinctive morphology.

It is therefore likely that the separation of xylem into individual tracheids, or small groups of tracheids, is related to high temperature of formation in some way; though it is evident that high temperatures alone are not sufficient to explain their formation, and the mechanism which may cause charcoal to fragment in this distinctive manner is currently unknown. The more complete that separation, the more the resulting particles will approach the aspect ratio of individual cells.

If the particles described by Martill et al. (2012) have also resulted from a process similar to that described by Jones & Chaloner (1991), it is not reasonable to expect evidence of cell wall homogenisation as evidence that the material is charcoal. The samples produced by Jones & Chaloner (1991) with cracking of the middle lamella cannot conceivably have been composed of anything other than charcoal. Therefore, regardless of the lack of understanding of the mechanisms involved, or the inability to reproduce the effect, their results are sufficient to falsify the claim that all charcoal has homogenised cell walls.

4.5.2 Possible reasons for Peniche morphotype B2

As described above, the B2 morphotype is evidently of a different origin to the B1 morphotype, being an elongate cell or structure which has been charcoalified partially intact, rather than becoming elongate by fragmentation of a larger structure.

Such forms are likely to be derived from plants with hairs or trichomes. Although many plants with hair-like forms can be found, surficial hairs or trichomes are unlikely to undergo charcoalification in any quantity. Due to their

fine form, the delay between reaching charring temperature and combustion will be extremely short. However, ferns with arboreal forms ('tree ferns') may be an exception to this. The trichomes which cover the trunks of tree ferns are unusual in that they form a dense layer, allowing a delay to occur between the advance of the heating front and oxidation front. This could potentially result in the production of large quantities of charcoalified trichomes. Such a phenomenon may explain the B2 morphotypes at Peniche.

Figure 4.11: Cross-section through a trunk of *Dicksonia antarctica*.

Figure 4.11[12] shows a cross-section of the trunk of the tree fern *Dicksonia antarctica*. The trunk consists of a woody centre, which becomes hollow with age, around which are arranged the stipes (seen here as circular cross-sections) which support the foliage; these are embedded within a dense indument of trichomes, which are in fact adventitious roots, which gives the trunk its fibrous appearance. With the indument growing to several centimetres in thickness, this form will allow the charring of those trichomes which are not close to the surface.

Present-day tree fern species are highly resistant to fire, and are among a small number of taxa defined by Clarke et al. (2013) as 'aerial apical sprouters', which survive fire by protection of the apical bud, as well as the hydraulic system. The extant tree ferns *Dicksonia antarctica* and *Cyathea australis* are both known to be fire tolerant (Ough & Murphy, 2004), while Ainsworth & Kauffman (2009) found an overall survival rate > 86% for the tree ferns *Cibotium glaucum* and *Cibotium menziesii* following lava-ignited wildfire on Hawaii. The fire-resistant nature of the tree ferns is a result of their unique structure, with the meristematic tissue being protected by a number of features. These include the green frond

[12] Specimen from Jardin Botanique Henri Gaussen; photographed by Roger Culos; downloaded from: https://commons.wikimedia.org/wiki/File:Dicksonia_antarctica_MHNT.BOT.2012.10.39.jpg. This image is reproduced under the Creative Commons Attribution-Share Alike 3.0 Unported licence: https://creativecommons.org/licenses/by-sa/3.0/deed.en.

bases around the apical bud (Clarke et al., 2013; Ainsworth & Kauffman, 2013), and in some species the thick indument or root mantle (Clarke et al., 2013) – which in *Dicksonia antarctica* also provides a means to obtain water independently of the underground root system (Hunt et al., 2002).

The tree ferns therefore represent a strongly fire-adapted growth form which produces trichomes in large quantities, and in such a form that they may reasonably be expected to become charcoalified in the event of fire.

Tree ferns of this growth form have formed a major component of tropical and subtropical biomes for much of the last 300 Ma. *Dicksonia*, *Cyathea* and similar genera were an abundant component of the tropical everwet biome from the late Cretaceous and throughout the Paleogene, while in the Oligocene tree ferns were also abundant in summerwet subtropical regions (Willis & McElwain, 2002). The Dicksoniaceae have been reported as abundant throughout southern Europe during the early Jurassic (Skog, 2001).

4.5.2.1 Attempting to recreate the B2 morphotype

To test the hypothesis that the B2 morphotype may originate as the adventitious roots of a tree fern or similar plant form, charcoal was produced from material removed from the trunk of a living *Dicksonia antarctica* at the University of Exeter. The material was wrapped in aluminium foil and buried in fine mineral sand in steel crucibles, then heated for 30 minutes at 500, 650 and 800 °C. All other aspects of the procedure were as described in Chapter 2. The resulting charcoal was examined with a stereo microscope at magnifications of 10-50×. A small amount of the material was also imaged with SEM. Areas and aspect ratios of the particles were measured from microscope images as described in Section 2.2.

Figure 4.12 shows the *Dicksonia* charcoal (heated at 500 °C for 30 minutes) under an optical microscope with reflected light. Charcoal derived from the trichomes was clearly distinguished from that derived from the stipes. The charcoalified trichomes appeared highly reflective, while material from the stipes did not. The charcoalified trichomes have the appearance of flattened, and often twisted, tubes.

Similarly, the Peniche B2 particles were highly reflective by comparison with other charcoal particles in the assemblage, and were also seen to be compressed tubular structures, though this was only visible with the SEM. Overall, the appearance of the charcoalified trichomes was remarkably similar to that of the Peniche Type B2 particles.

Figure 4.12: Optical microscope image of charcoalified *Dicksonia antarctica* stem material.

With the SEM, the *Dicksonia* trichomes are clearly seen as tubular structures, which show similarity to the Peniche charcoal in their surface texture (Figure 4.13).

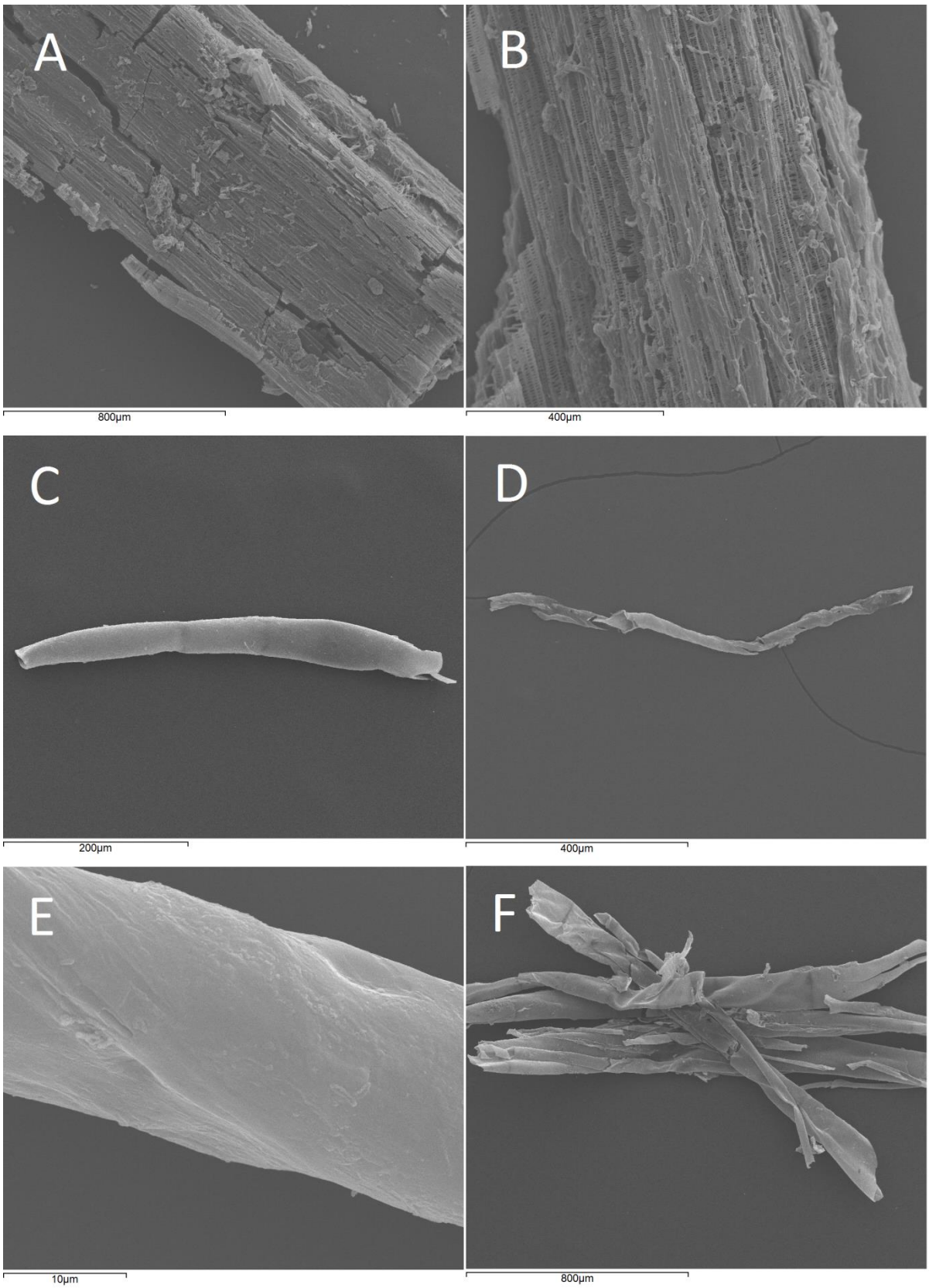

Figure 4.13: SEM micrographs of charcoal produced from *Dicksonia antarctica*: A and B – stipe; C to F – trichomes / adventitious roots.

Figure 4.14 is a plot of area against aspect ratio for mesocharcoal produced from *Dicksonia antarctica*, and the mesocharcoal from Peniche. This demonstrates that the Peniche charcoals have similar aspect ratios to the charcoalified *Dicksonia* trichomes, although it is evident that the *Dicksonia* particles tend to be larger where they are more elongate.

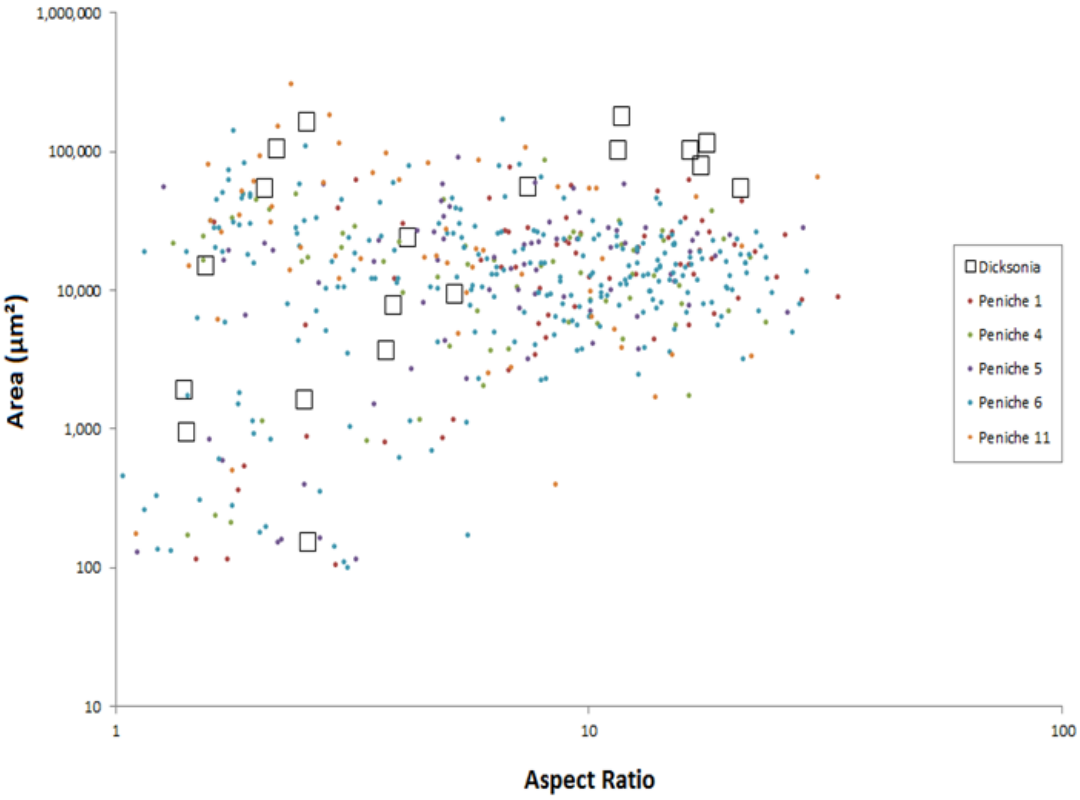

Figure 4.14: Scatterplot of area and aspect ratio of mesocharcoal particles from Peniche (Jurassic), and those created from *Dicksonia antarctica* stem material.

4.6 Summary

This selection of pre-Quaternary samples shows that wide variation in morphology persists even in lithified sediments of Mesozoic age. Of importance is that highly elongate particles can be observed in sediments that pre-date the evolution of grasses. This suggests a further complication to the use of aspect ratios to identify grassland fire, which is not the only source of elongate particles. The Jurassic samples from Peniche show highly elongate forms of

two types. One is seen to be formed by disaggregation of (gymnosperm) xylem tracheids. Based on the work of Jones & Chaloner (1991) it appears that the formation of such particles is in part a consequence of high formation temperature, but the fact that their results have not been repeated indicates that other factors are also involved. It is clear that further experimentation will be needed if we are to better understand this effect. It is possible to largely recreate the appearance of the second elongate form by charcoalifying tree fern trunk material, producing particles of the approximate size, aspect ratio, form and appearance. Together with the data presented in Figure 4.7, this suggests that pteridophytes may be another likely source of elongate charcoals in the fossil record.

Chapter 5: An Investigation of the Dimensionality of Charcoal Measurements

Parts of this chapter have been published in:

Crawford A.J. & Belcher C.M. (in press) Area-volume relationships for fossil charcoal and their relevance for fire history reconstruction. *The Holocene*, doi:10.1177/0959683615618264. [Available online 7 December 2015.]

5.1 Introduction

Many authors have quantified charcoal by means of counting the number of particles in a given volume of sediment. This has the advantage of being fast and simple, and is often conducted alongside the counting of pollens and spores in sediments sieved to around < 125 µm. Many others have favoured the measurement of the area of charcoal visible in a slide preparation or on a cross-section. This may be accomplished by estimation of particle areas using an eyepiece graticule, by a 'point-count' method in which the proportion of points on an eyepiece graticule overlaying charcoal particles are counted, or by computerised image analysis methods.

While count methods are faster, Patterson et al. (1987) wrote that areal methods were generally considered to be in principle more accurate as measures of charcoal quantity, though the difference may not be enough to outweigh the convenience of counting methods (Patterson et al., 1987). A number of studies have addressed the question of how well correlated particle counts and areal measurements are (e.g. Ali et al., 2009; Leys et al., 2013), and a high degree of linear correlation has been used to argue that, in equivalent circumstances, areal measurement is unnecessary (Tinner & Hu, 2003).

While much debate has therefore concerned the degree of correlation between counts and areal measurements, the question of how the areal measurements correlate with the actual volume of charcoal in a sample has rarely been addressed. One aspect of the problem inherent in taking an areal measurement to quantify charcoal is that fragmentation of the particles during sample preparation will increase the projected area, though the total volume

necessarily remains constant (Weng, 2005). This could lead to errors of interpretation where samples have undergone different degrees of fragmentation during processing. Differential fragmentation caused by transport processes could lead to similar errors. In addition, particles of different shapes will display different projected areas for any given volume. Weng (2005) has addressed this by deriving the general formula which relates the two types of measurement, while Belcher et al. (2013b) have applied the technique of Confocal Laser Scanning Microscopy (CLSM) to obtain volumetric measurements of individual particles and study the relationship empirically.

In this chapter, assumptions about the suitability of count and area as proxies for volume are questioned, and the relationships between metrics at three different dimensions explored. The relationship of count and area is investigated using data from the Holocene peat core from Shovel Down (Chapter 3). The nature of the relationship is established, and the results used to demonstrate errors in some prevailing assumptions in the literature. Subsequently, the less studied relationship between area and volume is addressed, extending both the theoretical approach of Weng (2005) and the empirical method of Belcher et al. (2013b). First, the volume-area relation for a range of simple morphologies is explored, and general principles derived. Second, CLSM is used to establish the relation for mesocharcoal particles (c. 100-1000 µm) extracted from the Shovel Down peat core.

5.2 Relationship between count and area in a Holocene peat core

Measured projected areas of the mesocharcoal particles from the Shovel Down peat core were used to examine the relationship of count and area. Methods for collection, processing and imaging of the samples are described in Chapter 3.

To test whether projected area could be predicted from particle counts, a linear least-squares regression of area on count was run. The relationship may be modelled either with an intercept term (Figure 5.1; Table 5.1) or with a zero intercept (Figure 5.2; Table 5.2). The regression with intercept term resulted in

a model of $y = 13{,}569\ x - 59{,}129$. With a zero-intercept, the data produce a model of $y = 12{,}396\ x$.

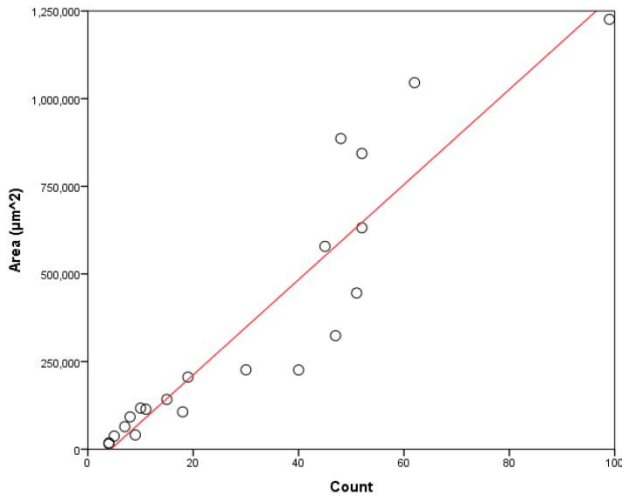

Figure 5.1: Relationship between count and area for Holocene mesocharcoal (linear regression with intercept term)

		P
r^2	0.857	-
F	113.865	< 0.001
intercept	-59,128.664	0.249
gradient	13,568.645	< 0.001

Table 5.1: Statistics for count-area model with intercept term.

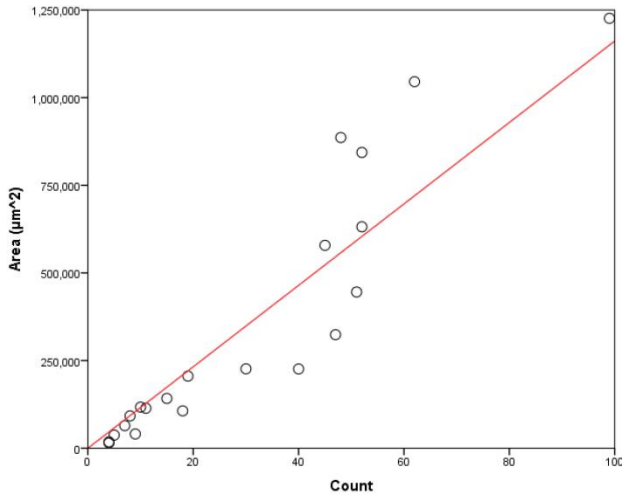

Figure 5.2: Relationship between count and area for Holocene mesocharcoal (linear regression with zero intercept)

		P
r^2	0.921	-
F	233.069	< 0.001
intercept	-	-
gradient	12,396.174	< 0.001

Table 5.2: Statistics for count-area model with zero intercept.

The true underlying relationship between count and area is by definition one with zero intercept, since a zero value for either count or area necessarily implies the same for the other. Tinner & Hu (2003) nonetheless use a model with an intercept term. Such a model is valid within the size fraction of the data from which it was derived, but if the regression line were to be extrapolated beyond the data, it could return negative values for area, thus falsifying the model. By contrast, a zero-intercept relationship could in principle represent an underlying relationship which could be extrapolated from the measured data. Ali et al. (2009) and Leys et al. (2013) use zero-intercept regressions, implying that their models are intended to represent an underlying relationship with no minimum value. So long as the regression line is not extrapolated beyond the data, neither approach is necessarily more legitimate than the other. However, zero-intercept formulae are calculated without a single standardised method (Eisenhauer, 2003), and standard measures of fit (i.e. *F* and r^2) are unsuitable for comparisons between no-intercept and intercept models (Eisenhauer, 2003). Therefore, the intercept model is best suited for comparison with the work of Tinner & Hu (2003).

The r^2 value of 0.857 for the model including an intercept term is very similar to the values of 0.82 to 0.83 from which Tinner & Hu (2003) concluded that areal measurement was unnecessary in similar cases. By the standard espoused by Tinner & Hu (2003), count and area are therefore sufficiently correlated in these samples for count to be a legitimate substitute for areal measurement.

However, despite the strength of the relationship, the residuals are very unevenly distributed. Table 5.3 shows the residuals for each sample, both as

areal values and absolute percentage errors. The mean percentage error is 47.5%, and it is clear that for some of the samples the use of count as proxy for area would lead to a serious error. It must be concluded that $r^2 > 0.8$ and $P < 0.001$ are not in themselves sufficient to justify using a particle count as a substitute for areal measurement.

The reason for this can be related to the assumptions underlying Pearson's *r* statistic, of which the coefficient of determination obtained from the regression (intercept model) is the square. The reliability of the coefficient is dependent on the extent to which the data meets the assumptions of Pearson's *r*. These include homoscedasticity, which can be seen to be violated in this case by inspection of the scatterplots in Figures 5.1 and 5.2 – the residuals are generally much smaller for low counts than for high ones.

Depth (cm)	Count	Measured area (μm²)	Predicted area (μm²)	Residual (μm²)	Absolute error (%)
31	30	226,393	347,931	-121,538	54
36	10	117,221	76,558	40,664	35
41	52	843,831	646,441	197,390	23
46	7	64,316	35,852	28,464	44
51	19	205,520	198,676	6,844	3
56	18	106,385	185,107	-78,722	74
61	52	631,753	646,441	-14,688	2
66	9	40,570	62,989	-22,419	55
71	11	114,136	90,126	24,010	21
76	4	18,222	-4,854	23,076	127
81	5	37,533	8,715	28,819	77
86	47	323,755	578,598	-254,843	79
91	8	92,335	49,420	42,915	46
96	4	15,198	-4,854	20,052	132
101	15	141,885	144,401	-2,516	2
106	40	226,143	483,617	-257,475	114
111	51	445,642	632,872	-187,230	42
116	99	1,226,458	1,284,167	-57,709	5
121	48	886,298	592,166	294,132	33
126	62	1,045,510	782,127	263,383	25
131	45	578,851	551,460	27,391	5

Table 5.3: Residuals and absolute errors for total projected areas estimated from count (linear regression model with intercept).

5.3 A theoretical approach to volumetric quantification of charcoal

Sedimentary charcoal particles are three-dimensional objects quantified by two-dimensional or zero-dimensional measurements (areal measurements and particle counts respectively). The branch of mathematics dealing with the relation of three-dimensional parameters to lower dimensional measurements is stereology. A basic principle of stereology is that, for an isotropic system, volume density is equal to area density, line density and point density (Hykšová et al., 2012).

$$V_V = S_S = L_L = P_P \quad (5.1)$$

This means that the volume density of a sample in a three-dimensional space will be equal to the area density of the sample on a sufficiently large planar section through that space, the line density on a sufficiently long line through that space, and the point density across a sufficiently large set of points within the space. (In practice, anisotropy often makes stereological measurement far more complex.)

The point-count method of charcoal quantification advocated by Clark (1982) makes use of this principle in translating point density to area density. The assumption of isotropy in this case means that the orientation of charcoal particles in the *x* and *y* dimensions is random. There is no reason to suppose that they would not be. As a consequence, a sufficiently large point set accurately quantifies area. However, on a microscope slide isotropy in the *z*-dimension is not a reasonable assumption. Gravitational settling will tend to make particles lie with their greater axes parallel to the slide, increasing area density relative to volume density. In addition, the area of charcoal measured from a microscope image is not a planar section through the particles, but their projected area. This introduces a depth of field effect, which further increases areal density (Overby & Johnson, 2005). Therefore an areal measurement is not an unbiased estimator of volume.

For these reasons, and also due to the possibility of overlapping particles, Clark's (1982) point-count method does not assume point density to be equal to

volume density; but instead takes area density as the measure of charcoal quantity. Similarly, rather than addressing the question of the relation of volume to area, most studies of sedimentary charcoal have implicitly treated area density as the fundamental object of measurement.

As charcoal particles are three-dimensional entities, the accuracy of any method which quantifies them at a lower dimension should be assessed by the correlation of its results with the three-dimensional measurements. The correlation of results from a zero-dimensional measure (particle counts) and a two-dimensional measure (charcoal area) has been used as a measure of the accuracy of the former. Yet in each of these studies, the correlation of either measure with volume is unknown. Tinner & Hu (2003) argue that a r^2 value of 0.82 or 0.83 justifies the use of particle counts in place of area measurement (in equivalent circumstances) , the former explaining 82-83% of variability in the latter. The information loss in taking a particle count in place of areal measurement is therefore only 17-18%. Yet, if the particle count is intended as a measure of how much charcoal is in the sample, this loss is additional upon the information loss in taking area as a proxy for volume, and that remains entirely unquantified.

It is therefore necessary to establish the range of relations which exist between the volumes of sedimentary charcoal particles and their projected areas, in order to understand the implicit error in taking charcoal area as a measure of quantity. If the factors controlling variation in those relations can be identified, it may also allow modification of areal measurements to better reflect volume, by developing the formula derived by Weng (2005).

5.4 Estimating volumes from areal measurements

Weng (2005) introduced a formula for translating areal measurements into closer approximations of the true volumes:

$$V_t = C \sum_{i=1}^{N} A_i^{3/2} \qquad (1.1)$$

where V_t is the volume of charcoal in the sample, C a constant, and A_i the area of a charcoal particle.

This formula can only be employed where the value of C, which is dependent on particle morphology, is known. Weng (2005) suggests that the volume of the particles must be known in order to estimate C, and that with sufficient sampling of charcoal areas produced from known volumes of any type of wood or other fuel material, a mean value for C may be taken as representative for that wood. Yet if C is not constant for each fuel type, but varies between samples, then this approach means that establishing C in any particular case would itself require volumetric measurement of the sample, making the formula redundant.

Based on areal measurements of charcoal particles produced from pine rods of known volume (n = 4), Weng (2005) suggests that C tends to approximate 1, and that applying the formula with C = 1 should still be an improvement on using raw areal measurements. However, this conclusion was based on a limited amount of data, utilising charcoal particles from a single source.

The relation of volume to projected area, and hence the value of C, is ultimately dependent on particle shape, which can be a highly variable property of charcoal particles (Mustaphi & Pisaric, 2014), being influenced by parent material, transportation and other factors. The variation in C with shape therefore needs to be investigated if the formula is to be used without error.

5.4.1 The volume-area relation for simple morphologies

The relation of volume to projected area for geometrically simple solids can be established using uncontroversial geometrical formulae. This may allow general principles to be discovered without the mathematical relations being obscured by analytical error.

Relationships between volume and surface area for three simple solids (sphere, regular tetrahedron, cube) are given in Table 5.4. Relationships between volume and projected area are more complex, since they will depend on the degree of certainty with which the object is known to lie flat on one side. Therefore projected areas are calculated on the basis of two different

assumptions. The 'flat' projection assumes that one face lies flat on a surface perpendicular to the line of vision (as on a slide under a microscope, assuming no other objects were to influence the orientation). The 'mean' projection assumes that orientation is entirely random, and is calculated by means of Cauchy's theorem that the mean projected area of randomly oriented convex particles is ¼ of their surface area (Vouk, 1948). Gravitational settling will cause the orientation of a real particle to tend toward the flat projection, though the presence of other objects on the slide will be among the factors preventing this from fully occurring. The mean projection represents a theoretical case in which gravitational settling has no effect. The orientation of a real particle will fall between these two extremes, but will almost certainly tend closer to the first case.

	Surface area	**Volume**	**Projected area (flat)**	**Projected area (mean)**	***C* (flat)**	***C* (mean)**
Sphere	$4\pi r^2$	$\frac{4}{3}\pi r^3$	$1.209v^{0.667}$	$1.209v^{0.667}$	0.752	0.752
Regular tetrahedron	$a^2\sqrt{3}$	$\frac{a^3\sqrt{2}}{12}$	$1.8014v^{0.667}$	$1.8014v^{0.667}$	0.414	0.414
Cube	$6a^2$	a^3	$v^{0.667}$	$1.5v^{0.667}$	1	0.544

Table 5.4: Formulae relating radius (*r*) and edge length (*a*) to surface area and volume for three simple solids.

By plotting projected area against volume for a range of arbitrary values of radius (*r)* or edge length (*a)*, the general relations can be found by regression. These formulae are given in Table 5.4 and plotted in Figure 5.3. In all cases, the relation of projected area to volume is defined by an equation of the form

$$a = b \times v^{0.667} \tag{5.2}$$

where *a* is projected area, *b* is a constant dependent on shape, and *v* is volume.

Having established this relationship, Weng's (2005) formula can be solved for *C* (Table 5.4). As well as demonstrating the dependence of *C* on shape, *C* is shown only to be a single value for a given shape where orientation does not affect the projected area, as is the case for the sphere and regular tetrahedron. It is therefore shown that *C* is not strictly a property of shape, but of orientation too. *C* = 1 only in the case of the cube, and then only on the assumption that the particles all lie flat.

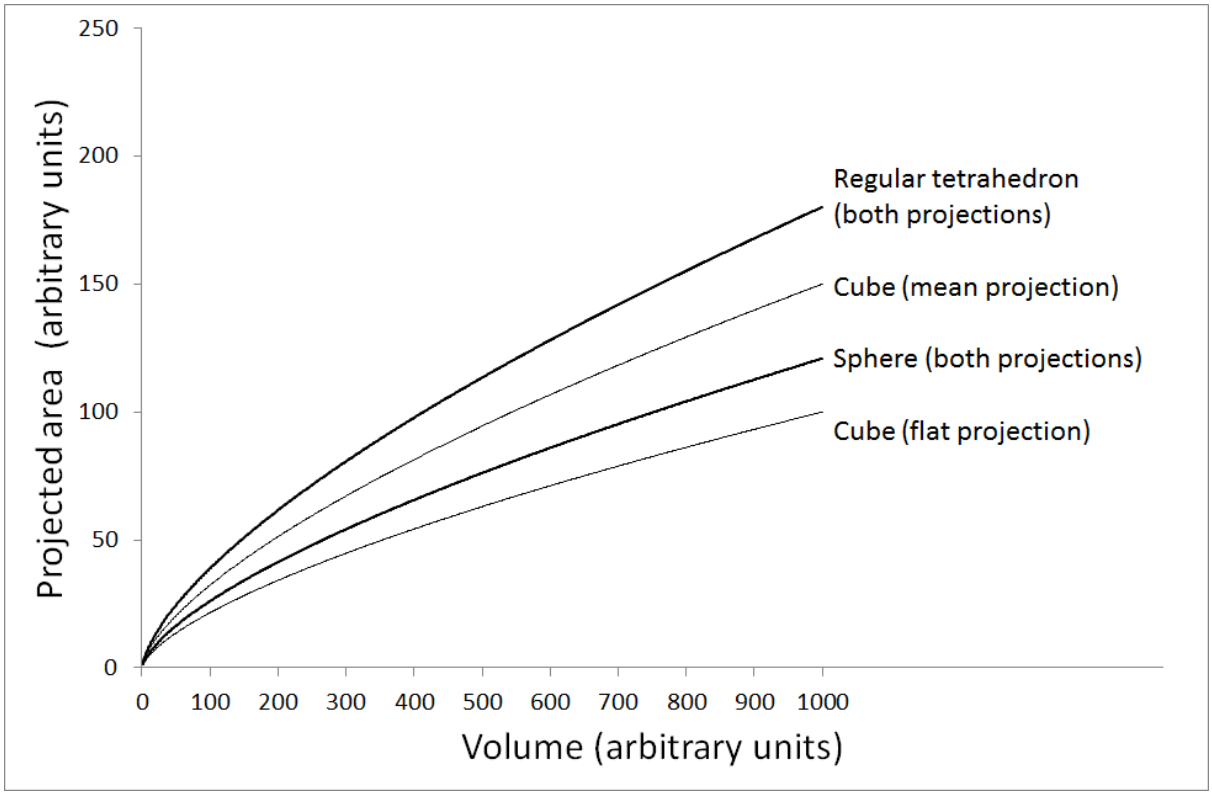

Figure 5.3: Volume-area relations for simple solids.

One potentially important feature of shape in sedimentary charcoal analysis is particle elongation or aspect ratio. To demonstrate the effect of particle elongation, volumes and projected areas were calculated for a series of cuboids of dimension 1 × 1 × *n*, for *n* = 1 to *n* = 10. Volume-area relations for both the flat and mean projections are shown in Figure 5.4 and given in Table 5.5. The value of *C* for different degrees of elongation are given in Table 5.5 and shown in Figure 5.5. It can be seen that *C* decreases with the degree of elongation, with the flat projection described by the function:

$$C = n^{-0.5} \tag{5.3}$$

The mean projection results in lower values of *C* than the flat projection. However, as the particles become more elongate, the larger sides account for a greater proportion of the surface area, and so the values for the flat and mean projections converge.

Dimensions	Projected area (flat)	Projected area (mean)	*C* (flat projection)	*C* (mean projection)
1 × 1 × 1	$v^{0.667}$	$1.5v^{0.667}$	1.000	0.544
1 × 1 × 2	$1.2599v^{0.667}$	$1.5749v^{0.667}$	0.707	0.506
1 × 1 × 3	$1.4422v^{0.667}$	$1.6826v^{0.667}$	0.577	0.458
1 × 1 × 4	$1.5874v^{0.667}$	$1.7858v^{0.667}$	0.500	0.419
1 × 1 × 5	$1.71v^{0.667}$	$1.881v^{0.667}$	0.447	0.388
1 × 1 × 6	$1.8171v^{0.667}$	$1.9685v^{0.667}$	0.408	0.362
1 × 1 × 7	$1.9129v^{0.667}$	$2.0496v^{0.667}$	0.378	0.341
1 × 1 × 8	$2v^{0.667}$	$2.125v^{0.667}$	0.354	0.323
1 × 1 × 9	$2.0801v^{0.667}$	$2.1956v^{0.667}$	0.333	0.307
1 × 1 × 10	$2.1544v^{0.667}$	$2.2622v^{0.667}$	0.316	0.294

Table 5.5: Relations of volume (*v*) to projected area for cuboids of varying elongation.

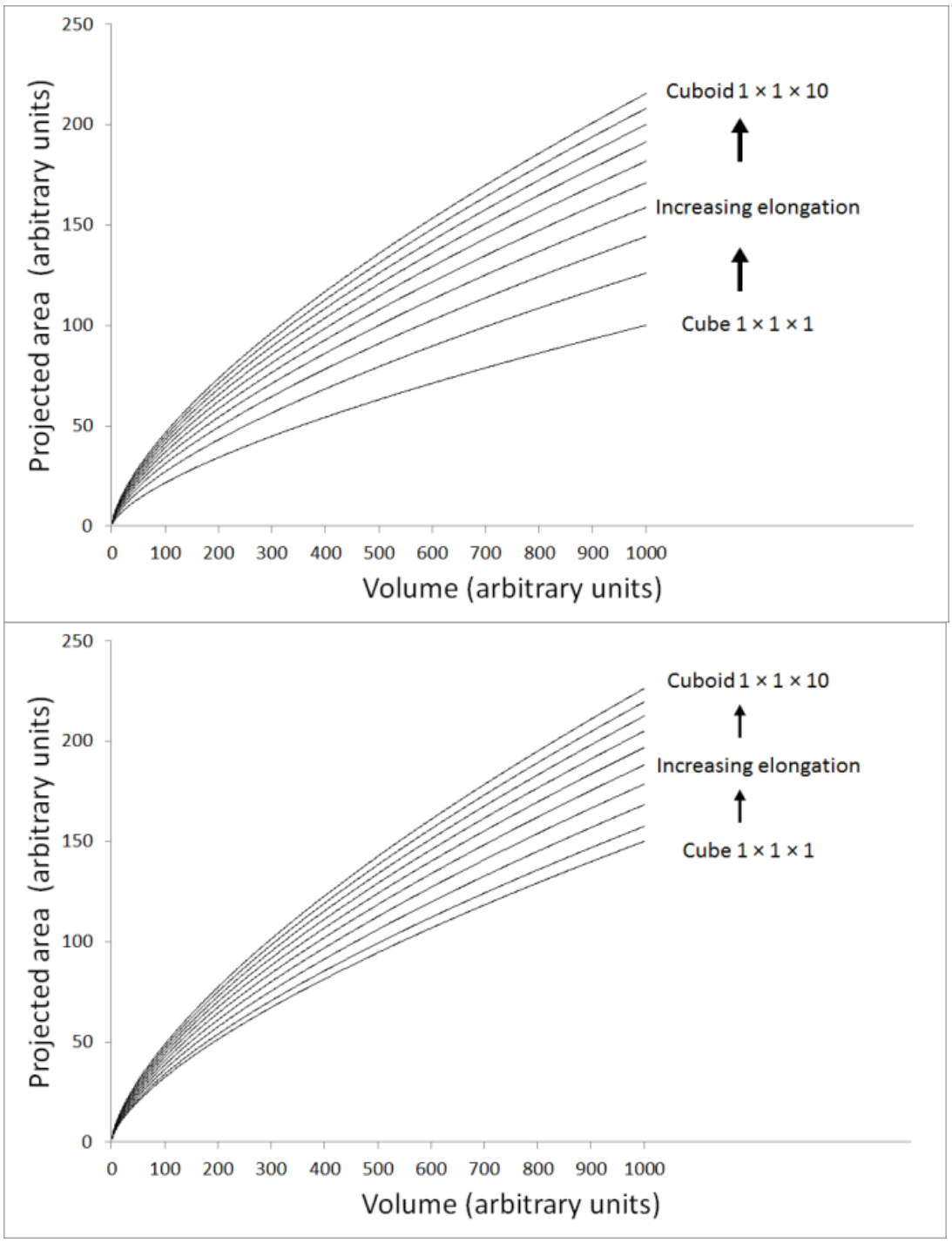

Figure 5.4: Volume-area relations for cuboids of differing degrees of elongation, calculated as a flat projection (left), and mean projection (right).

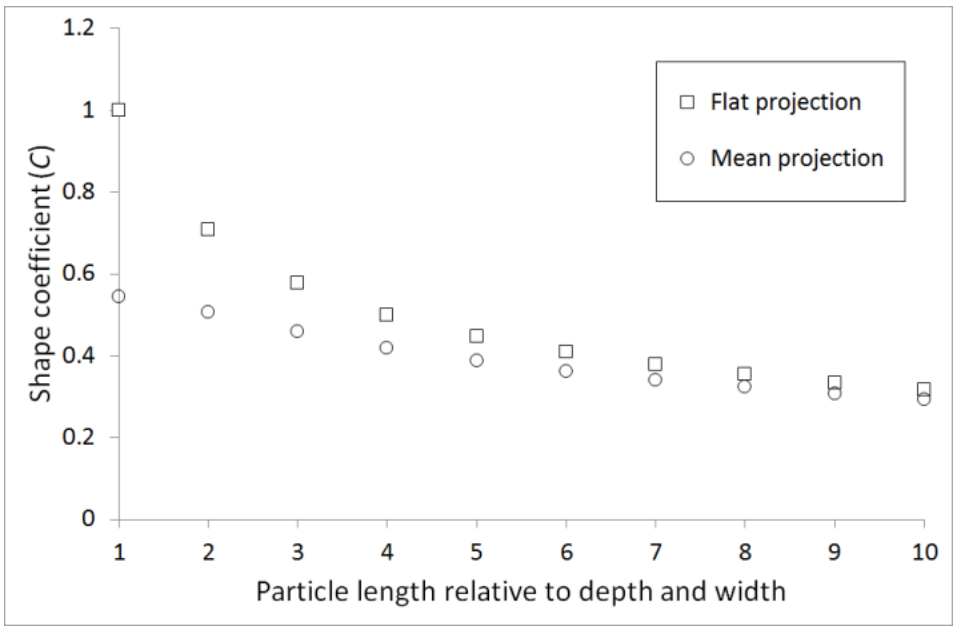

Figure 5.5: Variation of the constant C with degree of elongation of a cuboid measuring 1 × 1 × n arbitrary units.

5.4.2 Variation in the value of *C*

The value of *C* is seen to vary with both general shape and elongation of the charcoal particles, as well as with their orientation with respect to the viewing angle. Weng's (2005) original suggestion that *C* may approximate to 1 was based on a small amount of data using charcoal from a single source. As it is known that the shape of charcoal particles is highly variable (Mustaphi & Pisaric, 2014), and affected by both parent material (Umbanhowar & McGrath, 1998) and transportation (Crawford & Belcher, 2014), *C* cannot be assumed to approximate a singular value.

It is likely that 1 is in practice a maximum value for *C*. This can be demonstrated by considering how its value responds to deviations from the flat cube. *C* = 1 for the flat cube because its volume is the cube of the square root of its area; that is to say that it is the area to the power 3/2, and therefore *C* = 1. To generalise this to cuboids, *C* will remain 1 if the height of the cuboid remains equal to the geometric mean of length and width. If the height exceeds this value, *C* would exceed 1; but gravitational settling will tend to prevent this for any one particle, and certainly prevent it in aggregate. Therefore, elongation will realistically occur on the *x*-*y* plane, with a resultant decrease in the value of

C, in accordance with the results for the cuboid particles. Furthermore, the reason that *C* = 1 for a flat cube derives from the fact that a flat cuboid has a constant cross-sectional area on the *x-y* plane for any value of *z*. If at any point on the *z*-axis the cross-sectional area on the *x-y* plane is lower than the projected area, the volume relative to area, and therefore *C*, is decreased. However, the inverse is not true, since any larger cross-section on the *x-y* plane would itself become the projected area. Therefore variation in this parameter can also only decrease the value of *C*. Finally, the results show that *C* is not strictly a property of shape, but of orientation too, and indicate that deviation from the flat projection will also decrease the value of *C*.

The variation in *C* with elongation is of practical importance to the quantification of sedimentary charcoal, whose elongation is highly variable. As shown in Figure 5.5, the constant *C* for cuboid particles is equal to 1 only for perfect cubes that lie flat on one side. Since mesocharcoal sourced from grassland fires typically has median aspect ratios of 3.5 or greater (Umbanhowar et al., 2006), the value of *C* for such particles would be expected to be < 0.6. If Weng's (2005) formula were used to estimate the volume of such particles based on an assumption that *C* = 1, the resultant error would be proportional to this; i.e. where *C* = 0.6, the formula would overestimate volume by approximately 67%. If it were used on (cuboid) particles of equivalent elongation to the highest median aspect ratio found in the Jurassic mesocharcoal samples described in Chapter 4 (9.5) *C* would be c. 0.4, resulting in a volume overestimate of 150%.

Therefore, if Weng's formula is to be used, aspect ratio should be considered, and if necessary *C* can then be adjusted to account for elongate particles based on simple morphometric measurements of a representative number of particles. This is especially important to avoid bias where aspect ratio varies as a function of time; but even where aspect ratios significantly different to 1 remain constant over time, accounting for their elongation will give more truthful measures of volume.

5.5 An empirical approach to volumetric quantification of charcoal

Belcher et al. (2013b) used CLSM to obtain precise volumetric measurements of charcoal particles from three sources, and related these to projected area by linear regression. Cretaceous mesocharcoal, and micro and meso fractions of modern wildfire charcoal (primarily *Pterocarpus angolensis*) were imaged. All three showed a linear correlation > 0.9 between volume and projected area. Belcher et al. (2013b) suggested that taking volume to be 13 × projected area may give a good approximation for mesocharcoal. However, they noted that much more extensive sampling is needed, to take account of the range of ages, size fractions, plant taxa and organs which may affect the relationship. Here, this approach is extended by using CLSM to measure the volumes of mesocharcoal particles from the Holocene peat core from Shovel Down.

5.5.1 Methods

Details of the extraction of the core and processing of the peat samples are given in Chapter 3. Samples from depths of 101–131 cm were used in this study, corresponding to ages of c. 3425–7178 cal. a BP.

Particles were mounted in silicone oil on a cover glass of 22 × 50 mm (No. 1), and covered with a 18 × 18 mm cover glass (No. 0) sealed with nail polish, to enable CLSM imaging from both sides. Three-dimensional images were obtained with a Zeiss LSM510 Meta confocal laser scanning microscope, operating in reflection mode. Settings are given in Table 5.6.

Image stacks (Figure 5.6) were edited in the Zeiss LSM Image Browser (Version 4.2.0.121). Image stacks were imported as .lsm files, and the closed polyline tool used to define an area around the maximum extent of the particle in the *x*-*y* plane. The ‘extract region’ function was then used to create a new image stack with less extraneous image space around the particle. The ‘subset’ function was then used to remove half of the images (in the *z*-dimension) so that the two stacks representing each particle were non-overlapping, and image stacks were saved as new .lsm files.

Setting	Value
Scan mode	Stack
Scaling X	0.44 µm; 0.28 µm
Scaling Y	0.44 µm; 0.28 µm
Scaling Z	1.68 µm; 2.10 µm
Scan Zoom	1.0; 1.6
Objective	Plan-Apochromat 20×/0.8 M27
Average	Line 2
Pinhole	130 µm; 126 µm
Filters	LP 560
Beam Splitters	MBS: NT 80/30 DBS1: Mirror DBS2: NFT 545 FW1: None
Wavelength	633 nm, 4.1 % (Helium-Neon)

Table 5.6: CLSM settings.

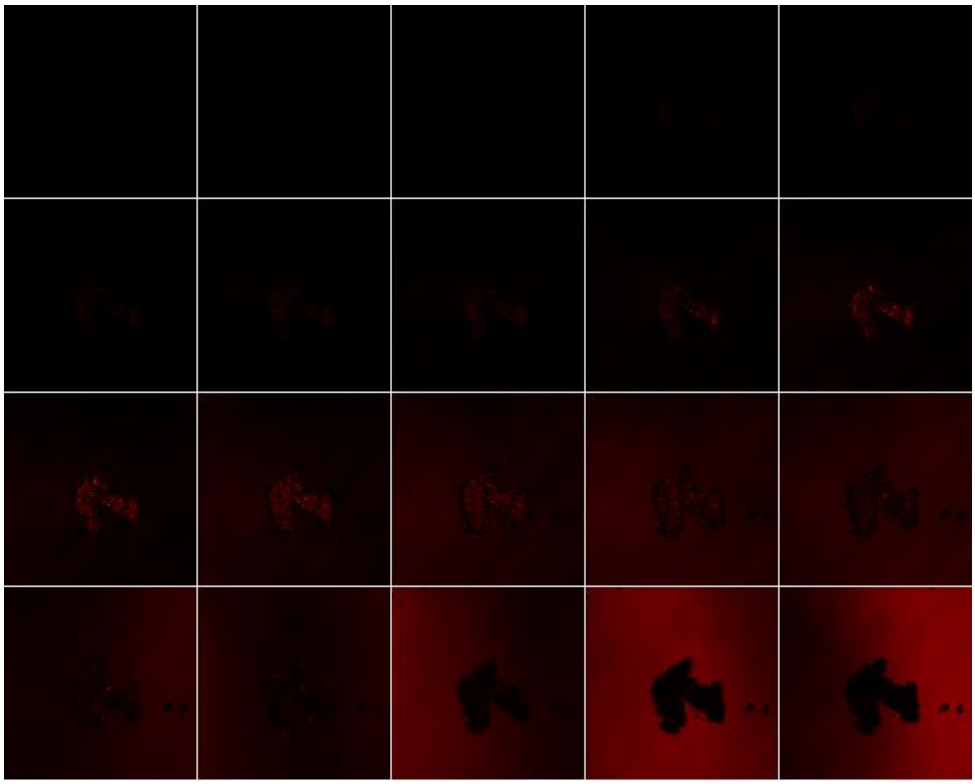

Figure 5.6: Image stack of a mesocharcoal particle imaged with CLSM.

All subsequent image processing was done in FIJI (Schindelin et al., 2012). Images were binarised with the 'Auto Threshold' function, using the IsoData algorithm (Ridler & Calvard, 1978). In a small number of cases this function was replaced with the 'Moments' algorithm (Tsai, 1985) based on visual assessment of the results. Contiguity of the image in each *z*-layer was enhanced by applying the 'close' function, using between 1 and 10 iterations. This factor was adjusted for each stack to obtain the optimum balance between contiguity of the image and accuracy. Particles were then rendered in 3D (Figure 5.7) and measured using the 'Particle Analyser' function of the BoneJ plugin (Doube et al., 2010), with the surface resampling factor set to 6.

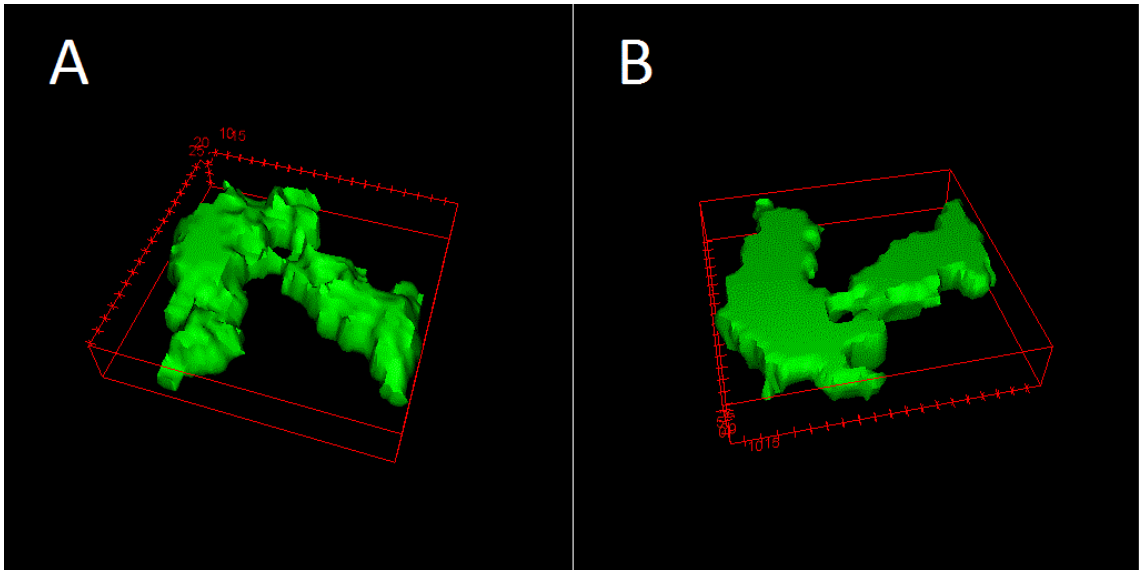

Figure 5.7: 3D rendering of one half of a mesocharcoal particle, showing surface topography on one side (A) and the flat surface adjoining the other half of the particle (B).

In a number of cases the section of the particle represented in a stack was rendered as more than one particle, though this is an expected consequence of dividing the particle into to image stacks about the midpoint of its extension on the *z*-axis. The volume of each particle was calculated as the sum of all particles measured in both stacks derived from that particle.

The projected area of each particle was measured from an optical image. Particles were photographed at × 50 magnification using a stereomicroscope

with transmitted and reflected illumination, and saved in TIFF format. Images were thresholded in ImageJ (Version 1.46r) (Rasband, 2012) using the default algorithm, and area measurements generated using the 'Analyze particles' function, with the 'Include holes' option unchecked so as to accurately measure those particles which showed holes in the 2D view.

All statistical analysis was done in SPSS Statistics 21 (IBM Corp., 2012).

5.5.2 Results (Empirically derived relationships between volume and projected area)

Volumes, projected areas and aspect ratios for all particles are shown in Table 5.7 along with age and depth data.

A series of one-sample Kolmogorov-Smirnov tests was used to determine whether size and shape descriptors were normally distributed. Particle volume and projected area were normally distributed at $P = 0.093$ and $P = 0.133$ respectively. Aspect ratio was not normally distributed ($P = 0.010$).

For each of these descriptors, an independent-samples Kruskal-Wallis test was run to determine whether it varied across categories of depth. Volume and area did vary across categories of depth; aspect ratio did not. The same hypothesis was tested by one-way ANOVA, with the same results at a significance level of 0.05. P-values for both tests are given in Table 5.8.

Metric	P-value (ANOVA)	P-value (Kruskal-Wallis)
Particle volume	0.008	0.021
Projected area	0.008	0.006
Aspect Ratio	0.822	0.631

Table 5.8: P-values for the hypothesis that size and shape descriptors are the same across categories of depth.

NEXT PAGE: Table 5.7: Measured volumes, projected areas and aspect ratios for 45 Holocene peatland mesocharcoal particles.

Depth (cm)	Age (cal. a BP)	Volume (μm³)	Area (μm²)	Aspect ratio
101	3,425	30,296	4,523	1.616
101	3,425	106,773	3,821	1.690
101	3,425	98,274	3,644	1.372
101	3,425	58,493	5,566	6.649
106	3,930	197,623	14,371	1.553
106	3,930	52,716	5,385	2.322
106	3,930	28,179	2,892	1.600
111	4,481	53,947	7,077	3.523
111	4,481	56,246	6,264	1.758
111	4,481	268,389	14,599	2.889
111	4,481	82,996	8,970	3.826
111	4,481	162,447	16,941	1.124
111	4,481	247,734	14,866	1.432
111	4,481	51,115	7,478	4.558
111	4,481	139,765	6,382	2.287
116	5,079	568,558	41,104	2.060
116	5,079	597,774	49,192	2.020
116	5,079	233,925	12,574	1.303
116	5,079	211,386	13,626	1.925
116	5,079	73,131	14,382	2.142
116	5,079	127,831	11,533	1.134
116	5,079	285,769	18,665	1.928
116	5,079	291,969	11,075	4.603
116	5,079	310,849	23,652	1.408
121	5,727	36,076	13,070	1.935
121	5,727	91,924	8,617	4.670
121	5,727	34,601	3,076	2.618
126	6,426	505,314	31,302	3.391
126	6,426	351,414	19,485	1.647
126	6,426	46,007	3,190	1.782
126	6,426	19,647	6,439	1.643
126	6,426	338,028	21,638	1.670
126	6,426	415,252	38,065	5.094
126	6,426	146,424	20,006	1.846
126	6,426	124,105	11,604	1.854
126	6,426	97,555	6,904	2.019
131	7,178	174,439	10,728	1.969
131	7,178	83,320	8,033	1.397
131	7,178	231,231	15,598	2.381
131	7,178	90,993	7,944	1.809
131	7,178	4,147	2,981	2.789
131	7,178	39,501	3,383	4.216
131	7,178	96,691	6,109	1.907
131	7,178	48,831	3,870	5.421
131	7,178	75,697	8,258	1.757

A linear regression was carried out to determine if particle volume could be predicted from projected area. Weng's (2005) theory specifies that the linear relation will be not between volume and area (A), but between volume and $A^{1.5}$. A second linear regression was therefore carried out to determine if volume could be predicted from $A^{1.5}$. Volume was related to projected area by a linear no-intercept model of $y = 13.036x$ ($r^2 = 0.933$; $F = 616$). Volume was related to $A^{1.5}$ by the linear no-intercept model $y = 0.072x$ ($r^2 = 0.865$; $F = 281$). Plots of linear models are shown in Figure 5.8.

To obtain a measure of the linearity of the relationship which could be assessed for its robustness, Pearson's product moment correlation coefficients (r) were calculated, along with 95% confidence intervals, which were calculated using Fisher's z' transformation, as described by Cohen et al. (2003). Pearson's r was 0.92 (95% confidence interval 0.86-0.96) for area and volume, and 0.90 (95% confidence interval 0.82-0.94) for $A^{1.5}$ and volume. The robustness of the gradient coefficients was also addressed, by calculating 95% confidence limits for both regression models, as shown in Figure 5.8.

To test whether volume prediction could be improved by incorporating aspect ratio as a predictor variable, hierarchical multiple linear regressions were run, with area (A) or $A^{1.5}$ as primary independent variable, and aspect ratio as secondary independent variable, and intercept terms of 0. For the prediction of volume from area, the addition of the aspect ratio variable failed to increase the adjusted R^2. F decreased from 616 to 301 ($P < 0.001$). For the prediction of volume from $A^{1.5}$, the additional variable increased the adjusted R^2 from 0.861 to 0.889. F decreased from 281 to 182, and this was significant ($P < 0.001$). Statistics and formulae for all four models are given in Table 5.9.

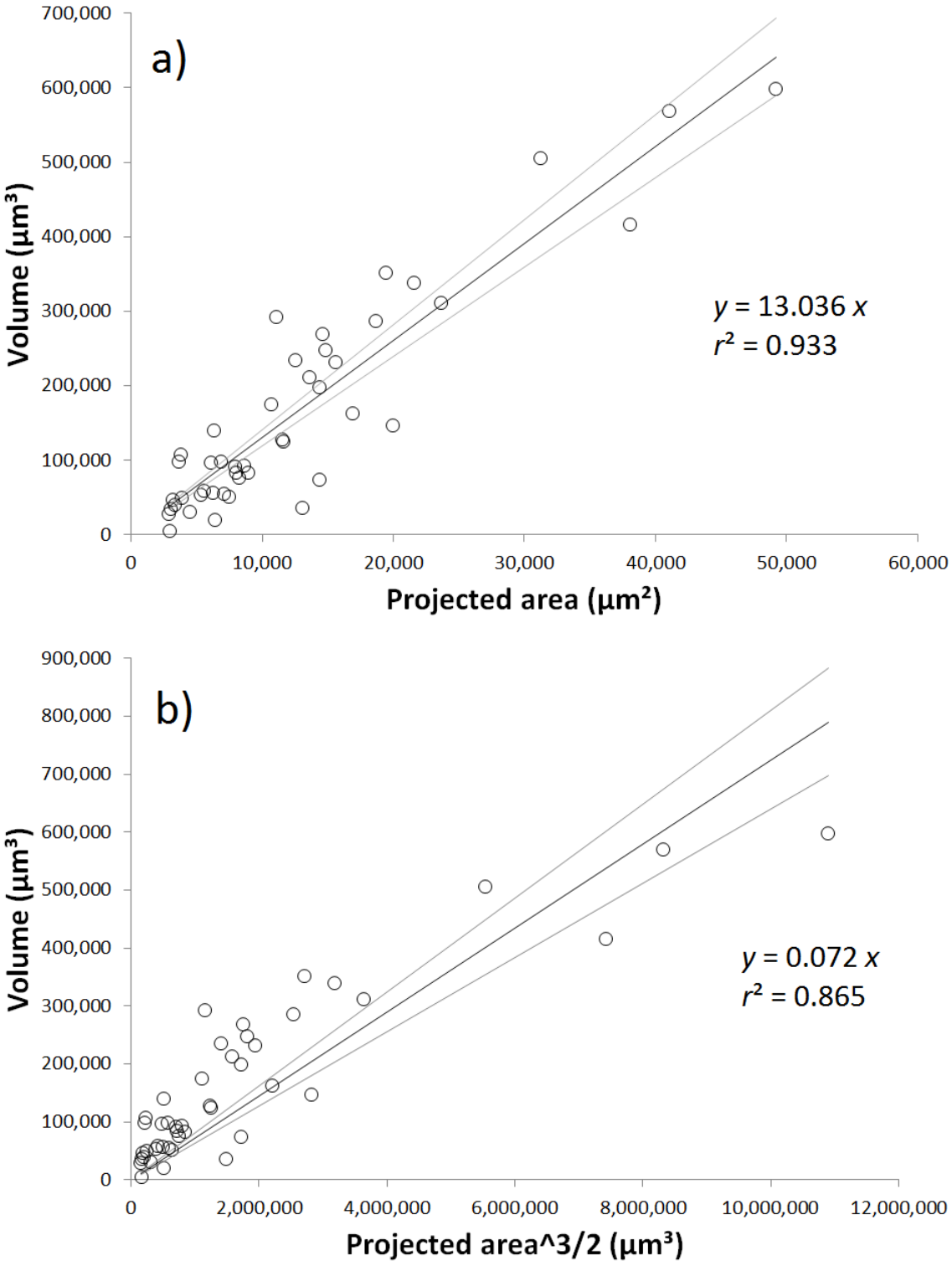

Figure 5.8: Linear models relating projected area (*A*) to volume (*V*) (a), and $A^{1.5}$ to *V* (b), for Holocene mesocharcoal particles. Grey lines indicate 95% confidence intervals for the gradient coefficients.

1st predictor variable	2nd predictor variable	Formula	R^2	Adjusted R^2	F	P
Projected area (A)	-	$Volume = 13.036 \times A$	0.933	0.932	615.729	< 0.001
	Aspect ratio (B)	$Volume = (13.127 \times A) - (787.27 \times B)$	0.933	0.930	301.126	< 0.001
$A^{1.5}$	-	$Volume = 0.072 \times A^{1.5}$	0.865	0.861	280.893	< 0.001
	Aspect ratio (B)	$Volume = (0.064 \times A^{1.5}) + (16291 \times B)$	0.894	0.889	182.079	< 0.001

Table 5.9: Statistics and formulae for regression models for the prediction of particle volume. P-values refer to the significance of the F-ratio.

5.5.3 Discussion of regression model results

Since Weng's (2005) formula is valid for all values of *n*, it specifies a linear relation between volume and $A^{1.5}$ with gradient *C*. Yet contrary to theoretical considerations, our data show a higher degree of linear correlation between volume and projected area than between volume and $A^{1.5}$. Both the coefficient of determination (r^2) and *F* ratio are higher for the linear regression of volume on projected area than for volume on $A^{1.5}$.

However, it can be proven from established principles that a linear relation cannot exist between areas and volumes of particles of the same shape. Galileo's square-cube law states that, for a solid of any given shape, a cross-sectional area will increase as the 2nd power of length, and the volume as the 3rd power. More generally, 2-dimensional and 3-dimensional metrics vary as the 2nd and 3rd powers of 1-dimensional metrics. For this reason, for regular polygons and polyhedra, the relation of 1D to a 2D parameter always contains a term to the power 2, a 1D to a 3D parameter a term to the power 3, a 2D to a 3D parameter a term to the power 1.5, and so on. (For irregular shapes, powers of singular metrics are replaced by powers of geometric means.) More generally, the relation of an *n*-dimensional metric to an *n'*-dimensional metric

must contain a term to the power n'/n. Because of this principle, Weng's (2005) formula raises the projected area (A) of each particle to the power 3/2.

For any geometric form, linearity between metrics of differing dimensions (over a range of sizes) is not possible. The fact that the linear model provides a better fit than the power model is therefore surprising. While the power model assumes a constant value for C, determined by the shape and orientation of the particles, the linear model assumes particles of constant mean thickness (in the z-dimension) regardless of their size. The better fit for the linear model is therefore likely to be a consequence of the degree to which C varies within the data, and the degree to which thickness is constant in the data. Since the power model is itself highly accurate, the greater accuracy of the linear model will be better explained by the degree to which the particles are of constant thickness. This could be a consequence of the particular morphologies of the Shovel Down particles, in which case highly accurate linear models would not be expected from other assemblages. This issue is further discussed in Section 5.5.4 by comparison with the data of Belcher et al. (2013b).

Ignoring the theoretical requirement to account for the change of dimension, the apparent linearity shows that projected area is a highly effective predictor of volume within this data set, with each metric accounting for > 93% of the variability in the other. A high value is to be expected, since larger volumes will obviously tend to project larger areas.

An r^2 value of 0.93 is close to the values of 0.96 and 0.92 found by Belcher et al. (2013b) for Cretaceous and modern mesocharcoal respectively; and would be considered sufficient to allow one metric to act as proxy for the other according to prevailing standards in the field, by which Tinner & Hu (2003) accept r^2 values c. 0.83 for the prediction of area from count. Similarly, the gradient coefficient 13.036 ($P < 0.001$) supports the suggestion of Belcher et al. (2013b) that mesocharcoal volume approximates to 13 × area.

This does not imply that the relation could be applied to a different mesocharcoal data set with the expectation of this level of accuracy. As a predictive measure, the approximate relation of $y = 13x$ derived here and in two cases by Belcher et al. (2013b) should be demonstrated to pertain across the range of relevant variables (size fraction, depositional environment, age etc.)

within which it would be used. As such, the evidence for its utility presently constitutes a sample of 3.

If further studies find similarly strong linear relations, albeit of different gradient, it would be advantageous, since while demonstrating linearity alone does not allow prediction of volume in other cases, it makes the measurement of volume redundant for the purposes of revealing fire history. If volume and area obey a linear relation, the shape of a charcoal abundance curve produced from them will be identical. While the relationship cannot be strictly linear, if it were sufficiently close it would allow area to be used as a measure of charcoal abundance without concern for an unquantified bias which is under standard methodologies inherent.

***

The fact that shape determines the relationship between volume and projected area (Section 5.4.1) indicates that measures of shape should have value as predictors of volume, in conjunction with areal measurements. Though there is sound theoretical evidence that elongation can be an important determinant of the area-volume relation (Section 5.4.2), the results of the multiple regression (Table 5.9) show no clear evidence that aspect ratio is of value in refining volume estimations in this case. For the linear model, the change in adjusted R^2 is negligible (down from 0.932 to 0.930) on adding the second variable, but for the more theoretically plausible power model it increases from 0.865 to 0.889. However, in both cases the *F*-ratio decreases upon the addition of the second variable.

It is likely that the low level of variability in aspect ratio within this particular data set is the reason for this. In a data set with highly variable degrees of elongation, it is to be expected that using aspect ratio as a second predictor variable would improve the regression model, compared with using area alone.

5.5.4 Comparison with data from Belcher et al. (2013b)

The data presented above represent the fourth charcoal assemblage to be volumetrically measured. In the following section they are considered alongside the three assemblages measured by Belcher et al. (2013b).

The CLSM-measured volumes from both studies may be used to demonstrate the inaccuracy of the simple version of Weng's formula with $C = 1$. Figure 5.9 shows the actual volume-area relationships for all four charcoal samples, as well as that derived from Weng's formula for different values of C. Volume and area values are given in the Appendix, along with calculated values of C for each particle. Applying the formula with $C = 1$, the volumes calculated overestimate the measured volumes by a factor of between 2.2 and 103.5. Calculating C for each particle results in a range from approximately 0.01 to 0.45.

The data set from Belcher et al. (2013b) can also be used to further test whether raising area measurements to the power 1.5 improves their value in predicting volume. Linear, 0-intercept regressions were carried out to determine if particle volume could be predicted from projected area, with or without first raising the area by the power 1.5. The results are given in Table 5.10.

Sample	Predictor variable	gradient	r^2	F	P (significance of F)
Modern microcharcoal	A	3.587	0.970	3156	> 0.001
	$A^{1.5}$	0.014	0.928	1237	> 0.001
Modern mesocharcoal	A	14.171	0.970	2855	> 0.001
	$A^{1.5}$	0.014	0.951	1713	> 0.001
Cretaceous mesocharcoal	A	10.578	0.988	8334	> 0.001
	$A^{1.5}$	0.016	0.957	2205	> 0.001

Table 5.10: Results of linear zero-intercept regressions to determine whether volume could be predicted from area (A) in the charcoal assemblages measured by Belcher et al. (2013b).

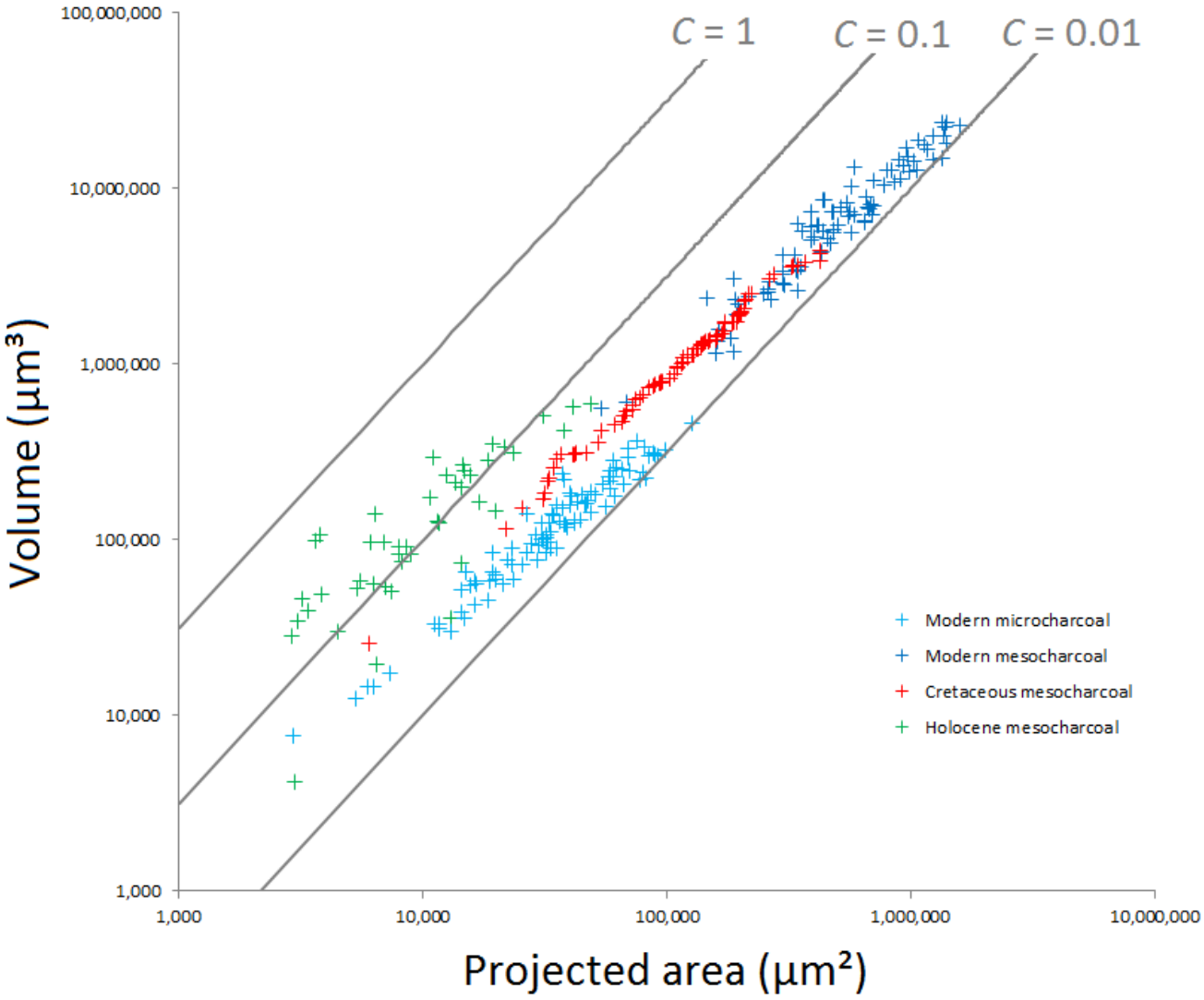

Figure 5.9: Volume and projected area values for charcoal particles measured in this study and by Belcher et al. (2013b). Grey lines indicate area-volume relations for different values of the shape factor *C*, as proposed by Weng (2005).

As with the data presented in this chapter, both r^2 values and *F*-ratios indicate that the raw areal measurements are better predictors of particle volume than the same values raised to the power 1.5. It therefore appears that the result from the Holocene data is not merely a chance deviation from the theory outlined in Section 5.5.3. Although it is shown from Galileo's square-cube law that linearity between metrics of differing dimensions (over a range of sizes) is not possible, the linear models provides a better fit to the data than the power

models. As the same applies to all four assemblages, it is likely there is an underlying cause, which should be sought in the morphology of the particles.

As discussed in Section 5.5.3, both the power model and the linear model assume a certain constancy of shape. The power relation assumes a constant value for Weng's constant *C*, which is determined by particle shape and orientation but not by size; the linear relation assumes constant mean thickness of the particles, regardless of their size, or their shape as projected on the *x*-*y* plane. Therefore, the reason for this unexpected result could be sought in the degree to which *C* is variable, and the degree to which particle thickness is constant, within each data set. However, as both types of model show consistently very high accuracy, the pertinent question is not the variability in *C*, but the apparent constancy of particle thickness in the *z*-dimension.

Taking the Shovel Down assemblage by itself, it was plausible that the particular morphology of the particles may have been responsible. However, similar results from four different assemblages suggest otherwise. The accuracy of the linear models may be an artefact of the procedure used for 3D rendering of the CLSM images. The CLSM images are obtained by reflection of a beam which scans the specimen across the *x*-*y* plane; the location of the specimen in the *z*-dimension being determined by the return time of the beam. Data is collected as a *z*-stack, consisting of a series of layers separated within the *z*-dimension, on which intensity of signal across the *x*-*y* plane is recorded. As such, the *z*-dimension is subject to a different level of error than the *x* or *y* dimensions. Resolution in the *z*-dimension is far lower. This could result in a tendency to produce 3D renderings which underemphasise *z*-dimension variability, thus increasing the accuracy of the linear models.

However, if linearity could be assumed, this would go a considerable way to defining the overall relation between volume and projected area. Since the intercept term must by definition be zero, the only other component of the relationship would then be gradient.

For each of the four samples for which both volume and area measurements are available, there is a single gradient obtainable by least-squares regression with 0 intercept. These are given in Table 5.11.

Sample	Gradient	r^2
Modern microcharcoal (Belcher et al., 2013b)	3.5875	0.970
Modern mesocharcoal (Belcher et al., 2013b)	14.171	0.970
Cretaceous mesocharcoal (Belcher et al., 2013b)	10.578	0.988
Holocene mesocharcoal (this study)	13.036	0.933

Table 5.11: Gradients and coefficients of determination for linear volume-area models for four charcoal assemblages.

In each case the gradient results from the combination of morphologies of the individual particles. In addition each particle can be considered to have its own gradient, determined by its morphology and its orientation within the slide. This value is the increase in volume for the projected area; or the volume / projected area for that particle as mounted. Just as combinations of morphology and orientation determine the area-volume relation regardless of number or size of particles (Section 5.4), these values represent the gradient which would be obtained by regression of volume on area for an assemblage of equally shaped and oriented particles, regardless of number or size.

The distributions of these values for the four samples are shown in Figure 5.10. In each sample, gradient was normally distributed at 95% confidence (One-sample Kolmogorov-Smirnov test; P-values are given in Table 5.12.)

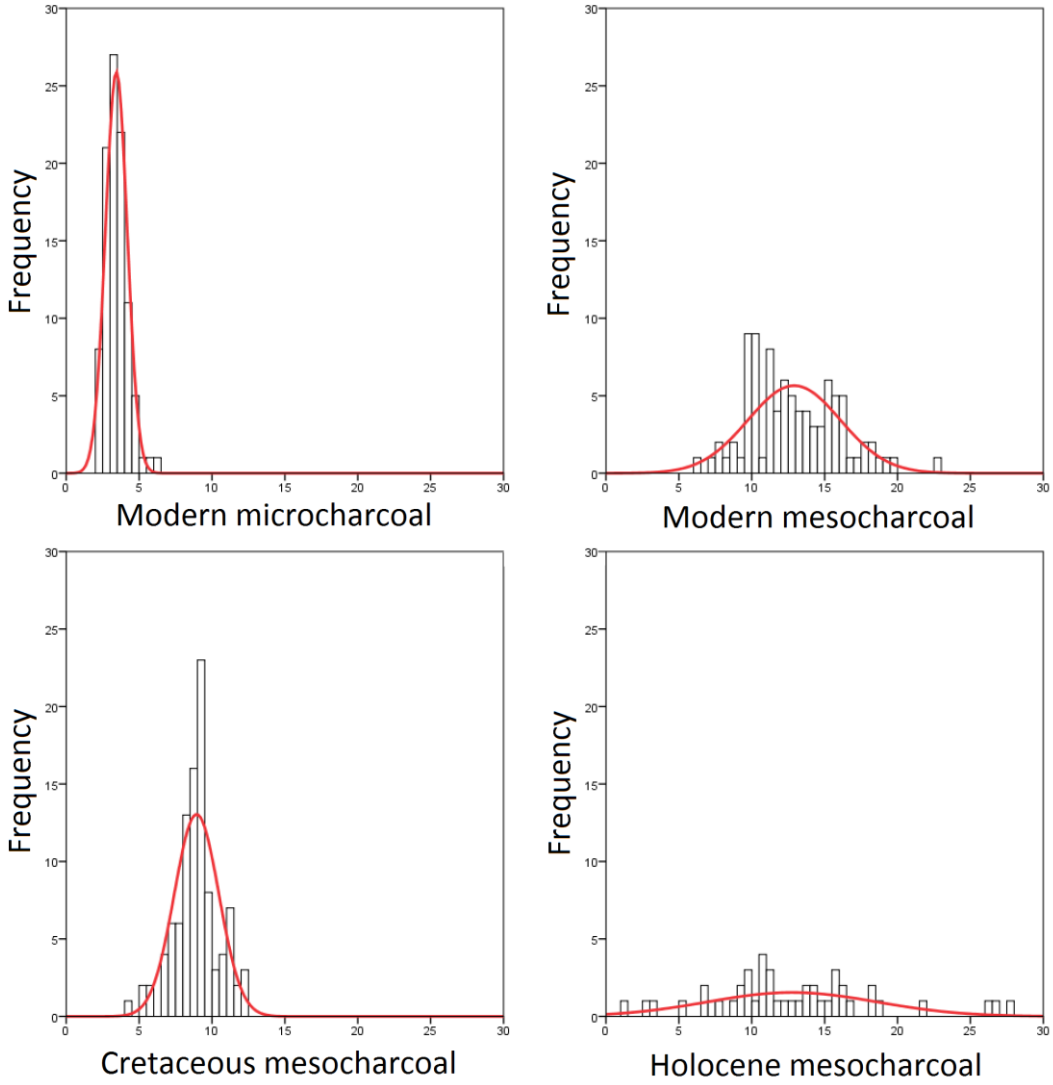

Figure 5.10: Distributions of gradient values for individual particles in four charcoal assemblages.

Sample	P-value
Modern microcharcoal	0.438
Modern mesocharcoal	0.601
Cretaceous mesocharcoal	0.171
Holocene mesocharcoal	0.804

Table 5.12: Results from one-sample Kolmogorov-Smirnov test, testing H_0 that the distribution is normal.

A one-way independent samples ANOVA was carried out to test the hypothesis that at least two of the four samples represented distributions with different

mean values. This hypothesis was retained at $P < 0.001$. A Bonferroni post-hoc test (Table 5.13) revealed that differences were highly significant for all pairings ($P < 0.001$) except that of Modern mesocharcoal with Holocene mesocharcoal ($P > 0.999$). The results of the ANOVA (Table 5.13) therefore indicate that the difference in gradient between the modern and Holocene mesocharcoal samples was not significant, but highly significant differences between gradients were evident for all other pairings.

Comparison	*P*-value
Modern microcharcoal – Modern mesocharcoal	< 0.001
Modern microcharcoal – Cretaceous mesocharcoal	< 0.001
Modern microcharcoal – Holocene mesocharcoal	< 0.001
Modern mesocharcoal – Cretaceous mesocharcoal	< 0.001
Modern mesocharcoal – Holocene mesocharcoal	> 0.999
Cretaceous mesocharcoal – Holocene mesocharcoal	< 0.001

Table 5.13: Results from one-way independent samples ANOVA multiple comparisons, for the hypothesis that pairs of samples represent populations with different means.

5.5.5 Discussion of gradient values

The fact that the ratios conform to normal distributions within each sample indicates that sample sizes are sufficient to be representative of the underlying population.

The apparent difference between the distributions of volume-area ratios for Cretaceous and modern mesocharcoal undermines the argument that $y = 13x$ may be a useful approximation, indicating that not only does gradient differ

between the two samples, but that the difference results from an underlying difference in the distributions of volume-area ratios, and would therefore be expected to persist if further sampling were to increase the dataset, rather than decreasing as might have been supposed. In the light of this, it is very likely that the gradient for the Holocene data (13.036) being so close to that suggested by Belcher et al. (2013b) is coincidental.

However, it might be expected that morphology of mesocharcoal in Holocene peat would conform better to that of fresh mesocharcoal than Cretaceous mesocharcoal would, having been subject to much less compaction and damage. The post hoc results from the ANOVA suggest that the Holocene and modern mesocharcoal ratios come from distributions with equivalent means, though Figure 5.10 shows clearly that the distributions themselves differ substantially, and while the mean values for the two are very close, the actual gradients for the whole samples (13.0 and 14.2) are less so.

The result of the ANOVA suggests that the similarity of the gradients for modern and Holocene mesocharcoal may be the result of the underlying volume-area ratios being sampled from similar distributions. But whether these values are indeed representative of mesocharcoal in general cannot be answered without further sampling. What is clearer is that the different morphology of the Cretaceous mesocharcoal particles results in an entirely different ratio distribution and resultant gradient. These data therefore do not indicate a singular value for the gradient across the mesocharcoal samples.

5.6 At what dimension should charcoal be quantified?

Taking a particle count from an image constitutes a loss of information which must be balanced against the time saved. A high coefficient of determination for a regression of area on count may imply little loss of information in taking count as a proxy for area (e.g. the r^2 = 0.83 found by Tinner et al. (1998) could be taken to imply a loss of 17%). However, the example from Shovel Down demonstrates that this may be misleading if underlying assumptions are not met. This example demonstrates that a strong and highly significant relationship

between count and area does not mean that count can be used to predict area with accuracy.

In addition the areal measurements are already serving as a lower-dimension proxy for volumetric measurements. The information loss already inherent in this substitution is unquantified and is additional to that of the subsequent decrease in dimension. Furthermore, if counts are transformed to areas post hoc for the purpose of comparability with other studies, as suggested by Tinner & Hu (2003), an additional error will be introduced.

Yet particle counts have been successfully used for the reconstruction of fire histories – success being judged by the ability to discover correlations between fire activity and causative factors such as astronomical forcing (Daniau et al., 2013) or anthropogenic influences (Colombaroli et al., 2014). The supposition that areal measurements produce more accurate fire histories (Patterson et al., 1987) is based on their being closer in dimension to the particles themselves. Areal measurements may reveal a correlation in a case where particle counts were not sufficient to do so. Similarly, volumetric measurement may reveal a correlation where areal measurement was not sufficient.

Since particle counts are fastest, and volumetric measurement highly complex and time consuming, it is clearly not the case that quantification at a higher dimension is always desirable. In many cases, particle counts may be preferable, based on the need to strike a balance between time and accuracy. Where counting is not sufficient, areal measurement may be so. However, these measures should always be used with an explicit understanding of their suppositions. The use of count as a proxy for volume implicitly assumes that all particles have equal volume; the use of area assumes that equal projections have equal volume. Neither is plausible, but if the results of either measure can be demonstrated to correlate with another variable of interest, then they are for practical purposes usable. However, the possibility of a genuine correlation going undiscovered will be increased by the loss of information.

If time and cost could be discounted, volumetric measurements would be used. Although they are impractical, other measures should always be considered in relation to volume.

5.7 Conclusions

The decision of which dimension to quantify sedimentary charcoal at is a matter of balancing accuracy, which favours higher dimensions, against practicality, which favours lower dimensions.

Two important points have been overlooked in the debate over whether particle counts are as suitable as areal measurements. Firstly, a high degree of correlation does not necessarily mean that large errors will not be introduced by relying on particle counts. This is demonstrated by the data from Shovel Down, and may be linked to the assumptions underlying the correlation coefficients used. Secondly, the error introduced by substituting particle counts for areal measurements is in addition to the unquantified error inherent in using areal measurements as a measure of volume.

Although the relation between projected area and volume cannot be truly linear, the data from this chapter supports that previously published by Belcher et al. (2013b) in showing the approximation to linearity to be high. However, comparison of the distributions of volume-area ratios of individual particles within both data sets indicates that they do not tend toward a single linear model.

The formula introduced by Weng (2005) can help to address the error inherent in using areal measurements of charcoal quantity. However, the shape coefficient (C) needed to transform areal measurements to volumes can be expected to vary with parent material, burning conditions and taphonomic processes, and the aspect ratio in particular may affect its value substantially. The assumption that $C \approx 1$ is therefore not well founded. It is shown both theoretically and empirically that the use of Weng's formula with $C = 1$ can lead to very large errors. The very limited volumetric data obtained so far suggests that C tends closer to 0.1 or even 0.01. The implication of this is that assuming a value of 1 would overestimate charcoal content by one or even two orders of magnitude. Further study is needed to establish the variation in C both between and within vegetation types, sedimentary settings, and size fractions. A first step toward accounting for variation in C would be to adjust its value to account for changes in aspect ratio, where elongate particles are evident.

Constancy of morphology is an inherent assumption of any comparison of sedimentary charcoal contents. As vegetation type is known to affect morphology (Chapter 2), this may be problematic where changes in fire regime are either a response to, or driver of, changes in vegetation.

Chapter 6: Summary Discussion

This thesis contributes to the existing literature on sedimentary charcoal morphology in three distinct areas. Chapter 2 describes the first known attempt to recreate the natural morphologies of charcoal particles by a laboratory simulation of the breakdown processes acting in the natural environment. Chapters 3 and 4 constitute the first known studies of charcoal morphometry outside of a lake sediment environment. Chapter 5 shows that morphology is a vital element overlooked in arguments about the correct quantification of sedimentary charcoal. The present chapter summarises the key findings of this thesis in the context of its contribution to existing knowledge and the potential for future research, and answers the three central questions posed in Chapter 1.

6.1 Can mesocharcoal particle elongation be used as an indicator of fuel type?

6.1.1 Analysis of prior research

The use of morphometric measurements in fossil charcoal analysis has been limited, with the use of aspect ratio as an indicator of changes between grassland and forest being the only established method.[13] This was first based on Umbanhowar & McGrath's (1998) demonstration that mean aspect ratios differed significantly between grass charcoal and wood or tree leaf charcoal. Their research was undertaken using eight grass species and eight angiosperm tree species from the prairie-deciduous forest ecotone of North America, obtained in the vicinity of Northfield, Minnesota, USA; the significance of the differences being demonstrated by means of an ANOVA. The method was subsequently employed by Umbanhowar (2004), Umbanhowar et al. (2006), and only recently used more extensively (Aleman et al., 2013; Daniau et al., 2013; Lim et al., 2014; Colombaroli et al., 2014).

[13] Thevenon & Anselmetti (2007) used circularity measurements to identify spherical carbonaceous particles, indicative of fossil fuel combustion, but the utility of the method was not evaluated; nor was it taken up subsequently.

Three problems can be identified in using the original study to justify the use of mesocharcoal aspect ratios as an indicator of fuel type in other situations. The first is that demonstrating in any particular case that there is a relationship between aspect ratio and fuel type does not automatically allow this to be assumed in other cases. The ANOVA conducted by Umbanhowar & McGrath (1998) did not constitute a demonstration of a significant difference between the aspect ratios of grassland charcoal and forest charcoal in general, since this would require that the vegetation samples had been randomly selected from the entire categories of 'all grasses' and 'all trees'. Therefore these results do not in themselves justify extending the technique to other environments with different species. Strictly speaking, the results do not constitute evidence that aspect ratios differ significantly between grasses and trees even within the environment studied, since the specimens were sampled from a subset of the species present. However, there is reason to believe that extending the results in this more limited sense is justified. Firstly, the species used are common, and likely to form a substantial component of total biomass, in the ecosystem studied (cf. Smeins & Olsen, 1970; Grimm, 1984). Secondly, the study was the result of unpublished prior observations that charcoal from grassland environments tended to be more elongate.

However, when applied to very different environments (Daniau et al., 2013; Lim et al., 2014; Colombaroli et al., 2014), the use of elongation to indicate differences between woodland and grassland charcoal relies on the assumption that the grassland species studied by Umbanhowar & McGrath (1998) produced more elongate mesocharcoal than the forest species because grassland and forest species produce distinctive aspect ratios generally.

Aleman et al. (2013) sought to establish the use of the method in tropical ecosystems, referring to the relationship between fuel type and elongation as a hypothesis to be evaluated, and studying data from three lake sites in the Central African Republic; one surrounded by forest, one savanna, and one having undergone deforestation. They concluded that width-to-length ratio is "a good proxy for changes in fuel type" and suggest that aspect ratios > 2 indicate grassland, and < 2 indicate forest. These conclusions are based on "average" aspect ratios being > 2 throughout the record at the savanna lake, and an increase in aspect ratio coincident with deforestation at the deforested lake

catchment. However, the forest lake also has average aspect ratios > 2 in all but one sample. This fact is discounted due to small sample size, but there is no demonstration of this supposed lack of significance. There is also no formal test of the difference in aspect ratios before and after deforestation. While the findings of Aleman et al. (2013) offer some support for the application of Umbanhowar & McGrath's finding to tropical environments, they are not unambiguous.

A second problem in interpreting and utilising the findings of Umbanhowar & McGrath (1998) is the influence of the laboratory method on particle morphology. In particular, the use of crushing and sieving to produce particles of the correct size is very unlike the natural processes by which larger charcoal pieces are broken down, and could tend to suppress or enhance differences in morphology between fuel types.

A third problem is entailed in placing a value on the aspect ratio at which elongation is taken to be indicative of grassland charcoal. Umbanhowar & McGrath (1998) found a mean value of 3.62 for grass charcoal, and 1.91 and 2.93 for tree leaf and wood charcoal respectively. Umbanhowar et al. (2006) give a rule of thumb: grasses typically have median aspect ratios ≥ 3.5, and values of 2-3 "are indicative of deciduous leaf or wood charcoal." Suggesting absolute values such as these is problematic, since transportation will be expected to decrease aspect ratios, and so the degree of transport will also be a factor. Daniau et al. (2013) use Umbanhowar & McGrath's (1998) findings to infer that changes between mean aspect ratios of 1.65 and 1.82 indicate changes in proportion of grassland charcoal, though both values are below those suggested by Umbanhowar et al. (2006). Aleman et al. (2013) and Lim et al. (2014) take an aspect ratio of 2.00 as the dividing line between "mainly wood" and grass, and do not include any intermediate range within which aspect ratios may be considered ambiguous. This implies that rather than distinctly high or low aspect ratios being interpretable as deriving from a particular fuel type, any charcoal particle may be assigned to one of the two fuel categories on account of its morphology. This goes far beyond any previous claims made for the utility of this method.

6.1.2 Contribution made by this thesis

The results presented in Chapter 2, and published in Crawford & Belcher (2014), improve understanding of this use of aspect ratio measurements in several ways. Most importantly, the key finding of Umbanhowar & McGrath (1998) – that grass mesocharcoal is more elongate – is replicated with an entirely different set of species. This gives some support to the assumption that the differences in aspect ratio found by Umbanhowar & McGrath (1998) were the result of an underlying difference between grasses and trees in general. It is also important that the tree species used in this study were predominantly coniferous, as it may have been supposed that the different leaf morphologies of coniferous species could result in more elongate mesocharcoal particles.

The fact that the method by which the particles were broken down was entirely different to that used by Umbanhowar & McGrath (1998) is similarly important. Although the method presented in Chapter 2 is designed to simulate fluvial transport using simple equipment, it is not easy to quantify the extent to which it does so. While it could be argued that it is itself either unrealistic, or pertinent only to a very specific transport regime which may not apply to any specific real charcoal assemblage, the important fact is that the processes in the two studies are distinct. While either one might be suspected of tending to exaggerate the difference between fuel types, it is far less plausible that both would do so to such a similar degree.

A further finding of potential importance is that the significant differences between fuel types are evident across the full size range studied (315-1,000,000 μm^2), since Umbanhowar & McGrath (1998) specifically identified the mean aspect ratio of the 125-250 µm fraction as indicative of fuel type. The study also demonstrates a simple and replicable method for a more realistic breakdown of charcoal pieces, as well as a comparatively rapid means of obtaining morphometric measurements of large numbers of particles.

Added to the findings of Aleman et al. (2013) and Daniau et al. (2013), which suggest that the original finding was not biased by exclusion of tropical taxa, the results presented in this thesis contribute to growing evidence that the greater elongation of mesocharcoal particles from grasses is a generally applicable rule. In particular, these results provide strong evidence that the essential

finding of Umbanhowar & McGrath (1998) was not dependent on bias in terms of taxa studied, laboratory method used for charcoal breakdown, or specific size fraction of mesocharcoal studied.

However, a strict proof of the hypothesis that ‘grassland fires produce more elongate particles than woodland fires’, if intended to be globally applicable, would require randomised sampling of both categories; i.e. grass species and tree species. As this is clearly impractical, it should be remembered that the assumption of a general rule applying to all ecosystems remains a supposition, and the method of using aspect ratio measurements to infer fuel type should be applied with consideration of the differences between the taxa and ecosystems in which it is to be used, and those for which its utility has been demonstrated. Further testing of the hypothesis with additional taxa would be valuable. Consideration should also be given to the underlying structural or anatomical reasons why grasses should tend to produce elongate particles.

It is not reasonable to seek to divide charcoal assemblages into categories of ‘grassland’ and ‘woodland’ based on which side of some particular value of aspect ratio they fall. Different studies obtain different aspect ratio values within each category; and make different recommendations for their guidelines. These differing values are compared in Figure 6.1, showing that the idea that the average aspect ratio of a charcoal sample can be directly translated into a categorisation of fuel type is untenable. For example, by the rule of thumb given by Umbanhowar et al. (2006), all of the charcoal samples of Daniau et al. (2013) would be classified as forest. By the rule given by Aleman et al. (2013), all charcoal assemblages must be classified as grassland or forest, though they could be neither, and in any case real charcoal assemblages may rarely contain particles from only one source. It is also evident that many of the Mesozoic samples studied in Chapter 4 display mean aspect ratios high enough to indicate grass according to the ranges given by Umbanhowar et al. (2006) or Aleman et al. (2014), despite these samples predating the evolution of grasses. Therefore, elongation should only be used as a relative indicator, in cases where aspect ratio changes while other relevant variables can be assumed to remain constant; for example within a single core of generally homogeneous sediment.

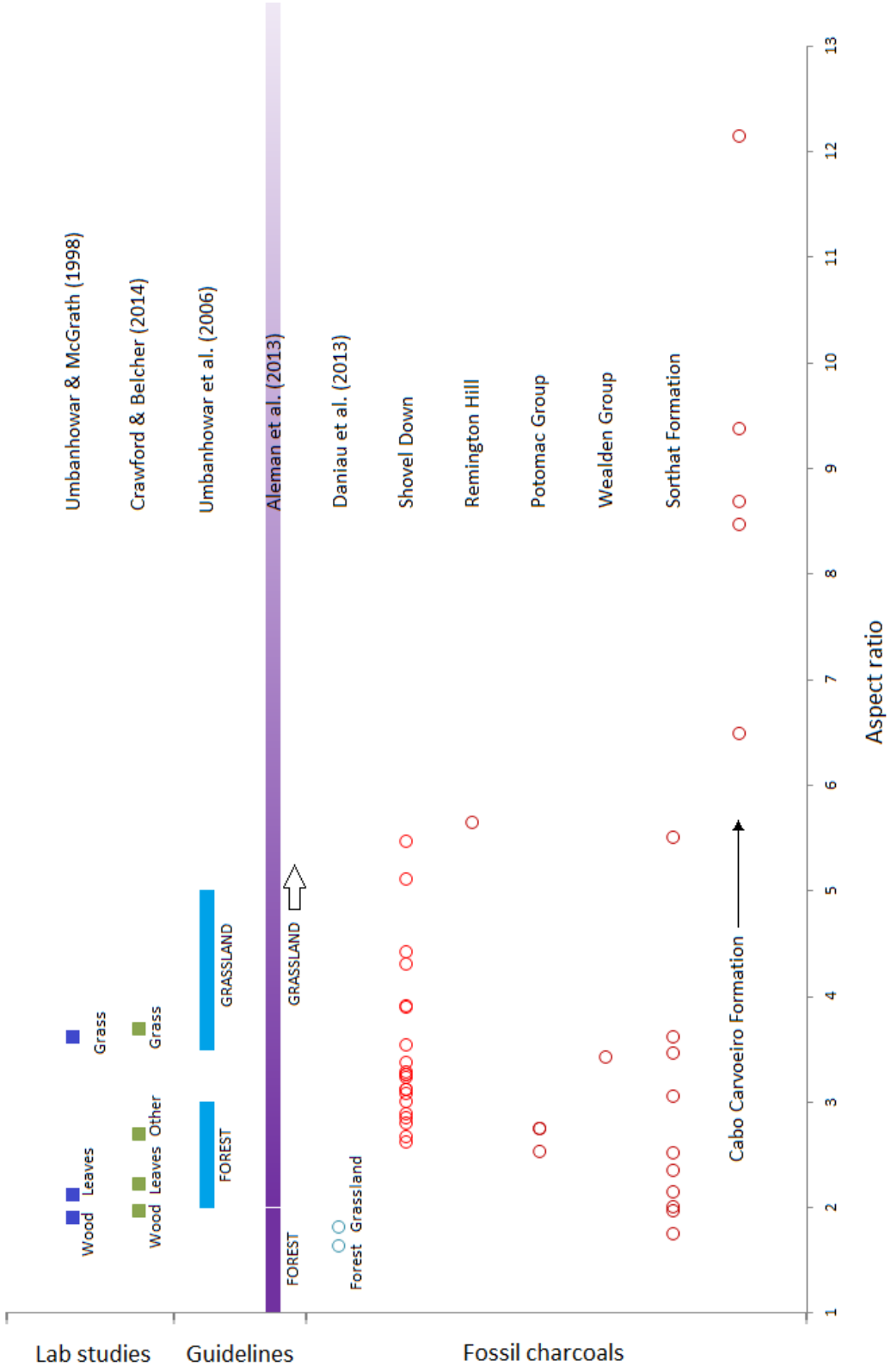

Figure 6.1: Comparison of published mesocharcoal aspect ratios. Showing mean values for different fuel types in laboratory studies, ranges of average values suggested as indicative of grassland or forest, and actual mean values as interpreted by Daniau et al. (2013), and as found in this thesis. Relevant studies not included are Lim et al. (2014) who follow the rule given by Aleman et al. (2013), and Colombaroli et al. (2014) who do not provide values measured or used.

Changes in aspect ratio that can be shown to correlate with other evidence for changes in vegetation will clearly be more convincing than aspect ratio changes alone. This need not necessarily mean direct correlation with palynological or macrofossil evidence of plant types; for example Daniau et al. (2013) find that changes in aspect ratio are correlated with the Milankovitch cycles which they propose drive the shifts in vegetation and fire regime.

Further research should also be aimed at establishing the range of aspect ratios of mesocharcoal produced from neither grasses nor trees. While the results in this thesis corroborate the idea that grasses and trees produce mesocharcoal of distinctly different average aspect ratios, the inclusion of species which fall into neither group demonstrates that such a clear separation is not to be expected in the palaeoenvironmental record. The three further species included in the simulated transport experiment – two pteridophytes and the weedy angiosperm *Rubus fruticosus* – each produced highly elongate mesocharcoal particles from its stem, and *Equisetum telmateia* produced highly elongate particles from its branches too (Figure 4.7).

In addition, the extremely elongate morphotypes presented in Chapter 4, which are apparent in the Jurassic sediments of the Cabo Carvoeiro Formation (Peniche), suggest both that the nature of the fire can lead to fragmentation in favour of high aspect ratios, and that fuel type is critical, as indicated by the charcoalified trichomes present. Further research is therefore required, both into the influence of fire properties and into the aspect ratios of charcoal from ferns and from non-arborescent species other than grasses. This is necessary to ensure the correct interpretation of charcoal aspect ratios in future.

6.2 Do different sedimentary archives preserve different charcoal morphologies?

6.2.1 A first morphometric study of peatland charcoal

The study of mesocharcoal in the Holocene core from Shovel Down (Chapter 3) is believed to constitute the first morphometric study of peatland charcoal of any kind. The samples demonstrate a similar level of morphological diversity to that

seen in morphometric studies of lake sediment charcoal. The study highlights a deficiency in the classification scheme proposed by Mustaphi & Pisaric (2014), within which it is shown that the majority of particles from the Shovel Down core lack the distinctive morphological features needed to assign them to a category based on positive criteria. This gives further evidence of the morphological diversity of charcoal particles, and suggests that a qualitative categorisation designed on the basis of lake sediment charcoal may not be applicable to all depositional systems. Consistent with the findings of some modern day studies (e.g. Hudspith et al., 2014), it appears that amorphous charcoal may be a particular feature of peatland assemblages, related to charring of the peat itself in addition to the surface vegetation.

As well as differences in initial morphotypes, peatland charcoal may have different, and possibly greater, potential for the preservation of morphology. The simpler taphonomic history expected of peatland charcoal, without high energy transportation, suggests that morphology could potentially be better preserved upon its incorporation into the peat than in lake sediments. At the Shovel Down site, it is shown that no relationship between shape and depth or age can be found, suggesting that morphological information is retained after burial, and could therefore be a useful source of palaeoenvironmental information. The apparent variation in aspect ratio with changes in land use and dominant vegetation is likely to be the first use of Umbanhowar & McGrath's (1998) aspect ratio theory in a peatland archive, suggesting that this may be a viable extension of the method. Importantly, however, it is not applied here on the basis of relating the aspect ratios to any specific cut-off point.

6.2.2 A first morphometric study of pre-Quaternary charcoal

The morphometric study of pre-Quaternary mesocharcoal (Chapter 4) is also believed to be the first of its kind. The samples studied represent a somewhat arbitrary collection, and are not intended to be a representative sample, but an open-ended inquiry into the variability of morphology.

The most interesting finding is the presence of the highly elongate particles which are abundant throughout the c. 950 ka Toarcian sequence at Peniche,

Portugal. The presence of these forms in such abundance has not previously been noted or commented on, and has important implications for both the identification and quantification of charcoal. It is shown that many of these elongate particles are formed by longitudinal disaggregation of tracheids (Section 4.5.1), though it remains unknown what conditions are necessary to produce this unusual type of tracheid separation. Further highly elongate particles in these samples cannot be explained by such a process, but appear to originate in the charcoalification of some initially elongate plant structure, which is hypothesised to be the result of charcoalification of the indument of adventitious roots which covers the trunk of many tree ferns (Section 4.5.2).

The implications of these forms for the identification of fossil charcoal are important. They may be missed if identification is based on sources which discount the existence of such forms. This is connected with the widely stated idea that true charcoal will always show homogenised cell walls under SEM. The study by Jones & Chaloner (1991) provides strong evidence against this belief, and while subsequent studies have shown that high temperature alone is not itself sufficient to produce the separation of tracheids seen, it demonstrates the existence of the effect.

It is clear that such elongate mesocharcoal forms can persist on timescales of hundreds of millions of years, and since a small number of similarly elongate forms were present in the samples from Bornholm and Remington Hill, it seems unlikely that they are a particularly rare phenomenon. This makes the effect of particle elongation on both identification and quantification of charcoal of real, rather than merely theoretical, importance.

6.2.3 Variation in fossil charcoal morphology

These two studies, extending the use of morphometrics beyond the Quaternary lake sediment environments in which they have previously been deployed, affirm that wide variation in mesocharcoal morphotypes is not limited by depositional environment or by the age of the deposits. This implies that morphology ought to be a consideration wherever sedimentary charcoal is found.

It is evident that morphotypes in all of these sedimentary environments are influenced by vegetation types, transportation history, and aspects of the fire that produced them. The effect of vegetation is demonstrated by the highly elongate particles which dominate the Jurassic assemblages from Peniche, and are shown to originate in elongate features of the plant material (both tracheids and trichomes). The wide range of morphotypes from the Shovel Down assemblage, which we can conclude is essentially homogeneous in terms of transport and depositional processes, further attests to the range of variation deriving from the initial source vegetation. Comparison with the known land use history indicates that presence of grass species is among the vegetation features contributing to variation in aspect ratio at this site, while the tumbler experiments described in Chapter 2 indicate that ferns may also be a likely source of elongate mesocharcoal at others. All of this suggests that elongate particles may come from a variety of fuel sources.

Distinctive morphologies, such as those found at Peniche, would not be preserved if subjected to high energy transport prior to sedimentation. By contrast to the Peniche samples, the rounded and smoothed nature of the particles in the Jurassic samples from Bornholm attests to a significant degree of fluvial transport, which is unlikely to leave elongate particles present in the assemblage if they were present beforehand. The effects of variations in the conditions of the fire that forms the charcoal are less clear (and have not been a focus of study in this thesis), but the presence of such effects can be inferred. Those particles in the Peniche assemblages that are formed from disaggregated tracheids appear to owe their unusual morphology to a high intensity fire (cf. Jones and Chaloner, 1991), in conjunction with other unknown factors. The conditions under which fires may produce such charcoal forms remain unclear, and require further research. Detailed studies of charcoals from experimental, prescribed or wildland fires where measurements of fire behaviour have been taken may help to resolve this question.

It is clear that the interpretation of charcoal morphotypes should take account of the potential effects of vegetation as a fuel source, fire dynamics and transport regime, if the maximum possible information is to be obtained from a charcoal assemblage. Further research on modern charcoal production and the resulting

morphologies will be required in order to realise the potential of this field of study.

6.3 How does charcoal's morphology affect the accuracy of its quantification?

It is shown in Chapter 5 that the effects of morphology on the quantification of sedimentary charcoal are closely linked with the question of the dimensionality of the measurements, and that morphology largely determines the potential error associated with the use of two-dimensional measurements.

As a three-dimensional quantity, the volume of charcoal in a sediment sample can in principle be measured in four ways; the resultant measurements being either of the volume itself, or else measures of area, length, or number which may stand as proxies. These proxies entail certain assumptions. A measurement of projected area will be an unbiased estimator of volume only if the particles are randomly oriented with respect to the viewing angle (Weibel, 1979), which is not a reasonable assumption due to the effect of gravitational settling. A particle count is an unbiased estimator of area only if the mean area of particles within each sample is constant, which is also not a reasonable assumption, but becomes more so the narrower the size fraction studied.

Volumetric measurement is clearly impractical for routine use, and no method to obtain volumetric methods would have been available when the first attempts to quantify sedimentary charcoal were made. Early studies using charcoal quantification were primarily for the purposes of understanding vegetation dynamics (Marlon et al., 2015), and for this purpose it is natural that the quantification should be thought of in two-dimensional terms, when it was an adjunct to quantification of pollens and spores viewed through a microscope. It is also natural that researchers should count the number of particles, rather than measure extent in any dimension, when this is adequate for the quantification of pollen grains. Now that researchers seek to establish fire histories for multiple purposes, including understanding quantitatively the effects of fire on the carbon cycle (e.g. Santín et al., 2015), it is necessary to address the inherent bias in this approach.

While the accurate measurement of volume is complex, expensive and time-consuming, particle counts and areal measurements are much less so. It is therefore comparatively straightforward to assess the correlation between count and area. A major problem in addressing the bias introduced to charcoal records by the use of lower-dimension proxies has been the fact that the relationship between volume and area has been overlooked, and measures of projected area have been treated as though they are themselves the variable of interest, when they are in fact a biased proxy for it.

6.3.1 Count as a proxy for area

The question of whether a particle count can be used as a proxy for charcoal area, without a meaningful loss of information, is well rehearsed in the literature (Section 1.7). A high degree of linear correlation has been accepted by many authors as evidence that particle counts are a suitable proxy for area (e.g. Conedera et al., 2009). However, the Holocene mesocharcoal data from Shovel Down (Section 5.2) demonstrate that a correlation with a high Pearson's correlation coefficient ($r^2 > 0.8$)) and low P-value ($P < 0.001$) does not in itself justify the use of a count method. In this case, $r^2 = 0.86$ ($P < 0.001$) still results in a mean error of 47.5% in the prediction of area. This highlights the fact that the assumptions underlying the use of Pearson's r must be considered before r^2 is used as justification for the use of a particle count. These assumptions include random selection of subjects from the population they represent, bivariate normal distribution of the variables, and homoscedasticity (Sheskin, 2004). These assumptions should be explicitly checked if the strength of a correlation is to be used to justify a particular methodology.

Where these assumptions are met, a high degree of correlation does indicate that count is an effective predictor of area in that particular case. However, as area will already have been measured, the utility of this depends on demonstrating that the finding can be applied to new cases where only a particle count will be used, and this requires that correlations are shown to be consistently high within some set of which the samples to be counted are a constituent. A rigorous application of this rule would mean that a random

sample of sediment cores should be taken from a pre-defined set (e.g. 'boreal lakes'), and the consistently high correlation be established before relying on particle counts from other sites within that set. Although this may exceed what can realistically be accomplished, it should draw attention to the potential error that extrapolation of results from a few sites implies. If the supposed justification for particle counts cannot be grounded in sampling theory in this way, the extrapolation must be suspect. Indeed some studies (Ali et al., 2009; Leys et al., 2013) have found correlations between count and area to be weak.

Even with all the necessary assumptions met, there will still be a loss of information involved in taking a particle count as a proxy for area. The stronger the correlation, the less information will be lost, but the loss will only be 0 where $r = 1$. A value of 1 for r implies that all the particles in the data set have equal projected area, which is clearly implausible for any real charcoal assemblage. The degree of linearity observed in a processed sample will depend on how narrow a size fraction is studied: the narrower the size fraction, the closer to linearity the count-area relationship will be. Therefore, an approximately linear relationship is likely to be a consequence of sieving procedures. If the presence of strong linearity is used to justify the use of particle counts over areal measurements, it will be found that counting is sufficient where narrow enough size fractions are involved. Conversely, narrow size fractions may be favoured in order to simplify the measurement procedure.

Most importantly, it must be appreciated that even a perfect correlation ($r = 1$) between count and area conveys no information on the relationship between count and volume in the absence of information on the relation between area and volume. To demonstrate that a particle count is a reliable measure of the amount of charcoal in a sample, the correlation between area and volume must also be demonstrated.

6.3.2 Area as a proxy for volume

The essential reason for believing that projected area is a biased estimator of volume is simply that gravitational settling will increase the areal projection on the x-y plane relative to the mean. The degree to which it will do so will depend

on the shape of the particle; for a perfect sphere there can be no bias, but for a very flat particle it could be very great. Properly accounting for this bias is therefore a further application of charcoal morphometry, albeit one for which three-dimensional data must be employed.

6.3.2.1 Developing the theory of volume estimation from area

Weng (2005) had identified the essential error in relying on areal measurements, and outlined an approach to dealing with it which had not been developed subsequently. Weng's formula essentially does two things in estimating volume from area, one to account for the size and one to account for the shape of the particles:

1. It accounts for the fact that a given area, projected by particles of a given shape, will represent different volumes if the number (i.e. the individual size) of the particles varies. It does this by raising the area of each particle to a power equivalent to the change in dimension (i.e. 3/2), prior to summing the areas. This process alone would result in the correct calculation of volume if all particles were cubic, lay flat, and did not touch one another.

2. It accounts for the fact that a given area, projected by a given number of particles, will represent different volumes if the shape of the particles varies. It does this through the inclusion of the constant *C*.

However, Weng (2005) did not explore the causes of variation in *C*. This thesis, and the resulting paper by Crawford & Belcher (2016) contain the first attempts, both theoretical and empirical, to investigate the range of values of *C*.

In Section 5.4.1, it is shown from a sound theoretical basis that *C* will vary greatly among differently shaped particles, including with different degrees of particle elongation. As aspect ratio is shown to be highly variable in certain cases, this has important implications for the use of Weng's formula (Section 5.4.2). It is also shown that *C* is a function of orientation as well as shape – a

fact that was not recognised in Weng's (2005) original presentation of the formula. While Weng (2005) suggested that *C* may approximate to 1, its value was found to be considerably lower for many of the combinations of shape and orientation investigated, and, as explained in Section 5.4.2, 1 is in practice the maximum value that *C* could obtain in any realistic situation. Using the formula with the assumption that *C* = 1 (e.g. McMichael et al., 2012a, 2012b; Leys et al., 2013) will therefore lead to overestimation of charcoal volume.

Empirical evidence for the range of values of *C* is extremely limited. Belcher et al. (2013b) took the first volumetric measurements of microcharcoal and mesocharcoal, but did not relate this data to Weng's theory. Their data is in fact very revealing in this respect, as it allows the calculation of the first substantial data set of *C* values (see Appendix). The CLSM study of Holocene mesocharcoal particles presented in Chapter 5 extends the data set of Belcher et al. (2013b), and provides further empirical evidence of the level of error that areal measurement may entail (see Figure 6.2). Taking all four volumetrically measured samples, it is seen that *C* is likely closer to 0.1 or 0.01 than the assumed value of 1 (Figure 5.9), suggesting a very serious bias in the absolute volume estimates produced by researchers using the simple version of Weng's formula. The study described in Section 5.5.1 also demonstrates a more rigorous method for CLSM imaging of mesocharcoal, by imaging the particle from two sides, as well as a method for 3D rendering which relies solely on freeware. These developments may enable easier extension of this data set in the future.

6.3.2.2 Two models for the volume-area relation

As described above, volume should be better predicted from $A^{1.5}$ than from *A*, since the power term accounts for variations in particle size, assuming a given particle shape. However in the four cases for which there is both area and volume data, the power change did not improve prediction of volume, but apparently had the opposite effect. This may imply a problem with the methodology.

As discussed in Section 5.5.4, the power model assumes a constant value of *C*, and the linear model assumes constant mean thickness. Therefore variability in *C* and constancy in particle thickness could both be explanatory factors – the former explaining low fit for the power model, and the latter explaining high fit for the linear model. However as both models are in fact highly accurate, it is more relevant to ask why the linear model fits so well. The method by which CLSM images are acquired means that resolution in the *z*-dimension is subject to a different level of error to that in the *x* or *y* dimensions. Lower resolution could lead to variability in the *z*-dimension being under-represented in the 3D rendering, which would have the effect of artificially inflating the accuracy of the linear models. This suggests that the accuracy of the linear models could be an artefact of the procedure used for 3D rendering of the CLSM images. Substantially improving resolution in the *z*-dimension would require an equally substantial increase in imaging time. There may therefore be potential in seeking another method for the volumetric measurement of charcoal particles. However the problem of increasing imaging time, cost, and file size with increasing resolution will remain an issue regardless of the method employed.

Where the volume-area relation is modelled in a linear fashion, the gradient is vital. If no minimum particle size is assumed, and a zero-intercept model therefore used, the gradient itself fully specifies the relationship. The analysis of all three mesocharcoal data sets (Section 5.5.4) leads to the rejection of the proposal by Belcher et al. (2013b) that the formula y = 13x may usefully predict mesocharcoal volume from area. By identifying that each particle can be considered to have its own gradient value, determined by its shape and orientation, it is possible to formally test the significance of the differences between the four populations of gradient values. Analysis of these individual particle values indicates that there is no single gradient for the linear volume-area relation.

6.3.3 Quantifying the error introduced by lower dimension proxy measurements

To allow a direct comparison of the results of measurements of different dimensionalities, different measurements of charcoal quantity from the Shovel Down peat core (count, area, volume estimate with constant *C*, and volume estimate with *C* adjusted for aspect ratio) are transformed to standard scores (of mean 0 and standard deviation units). These values are plotted against depth in Figure 6.2.

This provides a real example of the differences between count, area, and estimated volume, both with and without adjustment for aspect ratio. While this transformation removes information on the absolute magnitude of the different measures, it makes clear that the differences between the series matter for the interpretation of relative charcoal curves. The charcoal quantity curve assumes a different shape dependent on the dimension of the measurements. As an example of the impact of this, peak charcoal abundance would be assumed at 126 cm depth according to volume estimates, but at 116 cm depth according to a particle count. This equates to approximate ages of either 6426 a BP or 5079 a BP; a difference of approximately 1347 years. If trying to understand peak fire activity in terms of other environmental parameters, this could change interpretations dramatically.

For the series with variable *C*, the value of *C* in each sample is determined by raising the aspect ratio to the power -0.5, which will return the correct value of *C* for cuboid particles (Section 5.4.1). This differentiates the series from that with a uniform value *C*, though only marginally in this particular data set.

Although plotting the series as standardised scores, with standard deviation units, is necessary to compare series of different dimensions, this results in the same curve being produced for any constant value of *C*, even though this value is of considerable importance to the determination of absolute volume. In Figure 6.3, the absolute magnitudes of charcoal volume estimates are plotted for the same data set, with different values of *C*, showing that the magnitude varies considerably dependent on what assumptions are made about *C*.

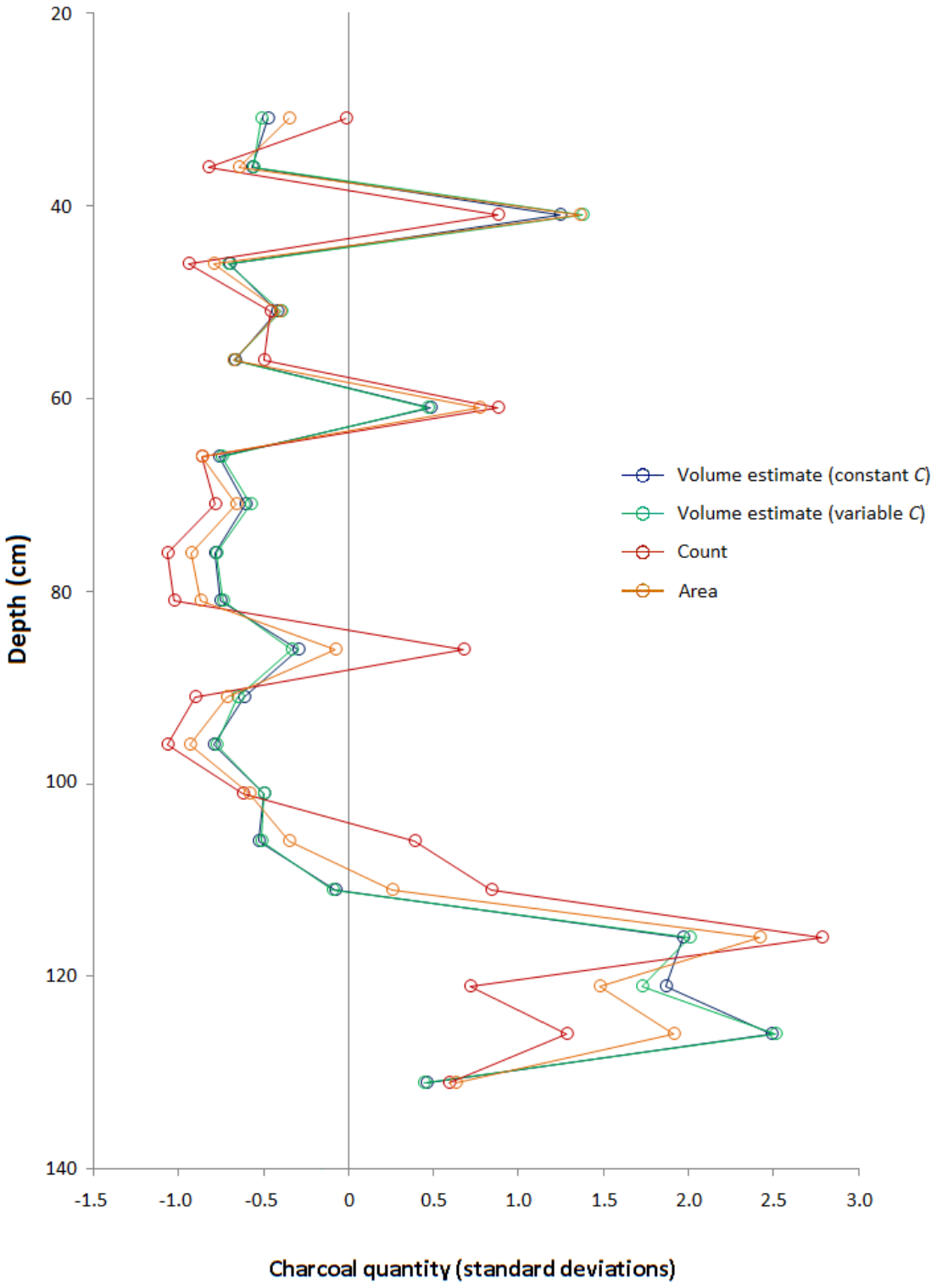

Figure 6.2: Charcoal quantities derived from measurements of different dimension for samples from the Holocene peat core from Shovel Down, shown as standardised scores.

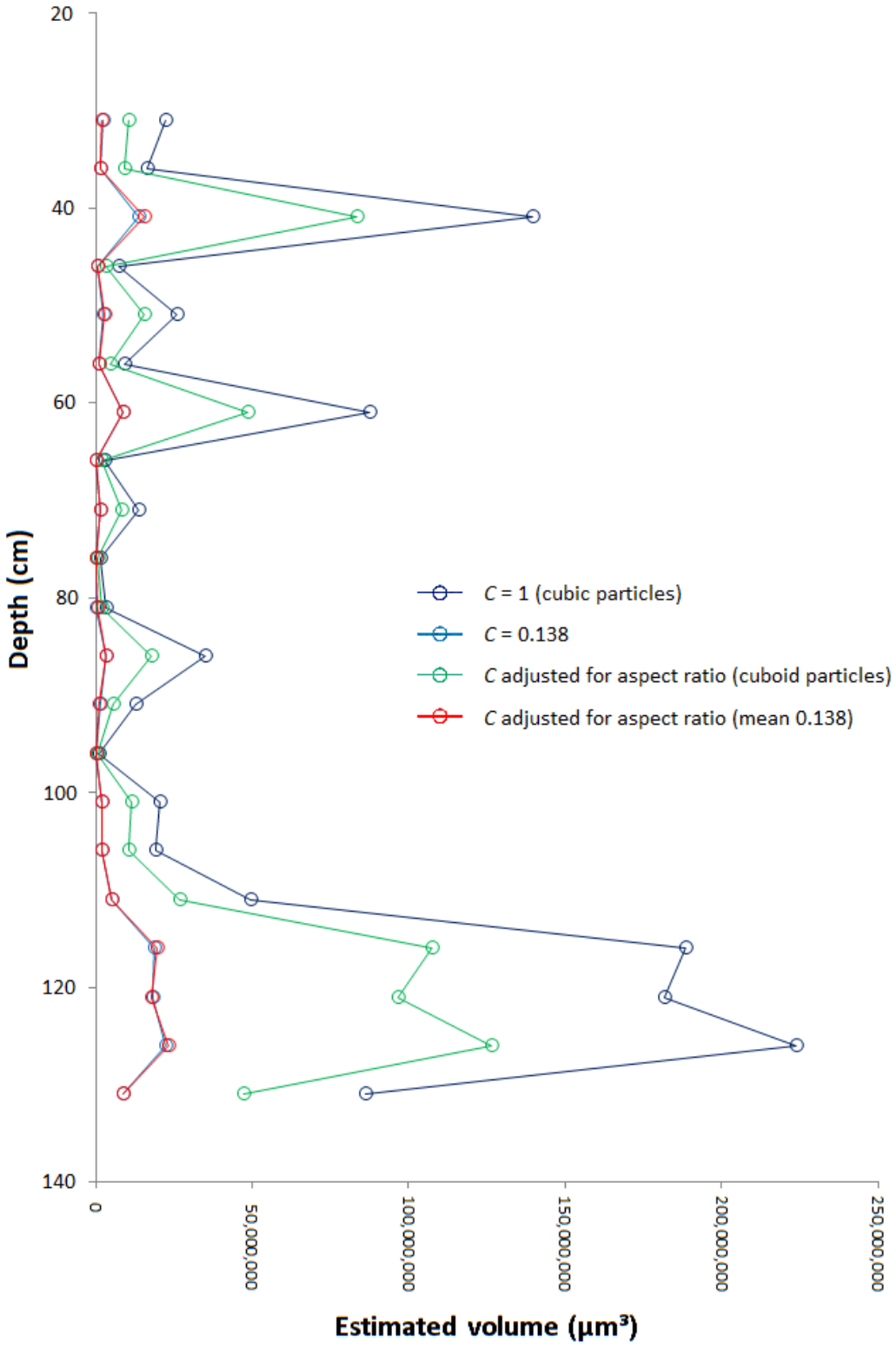

Figure 6.3: Estimated total charcoal volumes for samples from the Holocene peat core from Shovel Down, shown as absolute magnitudes based on varying assumptions about the value of *C*.

The largest volumes are obtained by using $C = 1$. These are substantially reduced by adjusting C according to the mean aspect ratio of the particles in each sample, which is the simplest method of accounting for shape. Values are much further reduced by taking C to be 0.138; the mean C value obtained from the CLSM measurements of a subset ($n = 45$) of the particles. Finally, the most accurate estimates obtainable with the present data are calculated using values of C based on the aspect ratio model, but adjusted to average 0.138 across the samples. It can be seen that the effect of accounting for aspect ratio once the mean value of C is known is far less than the effect where particles are assumed to be cuboid.

In this data set, the effect of accounting for aspect ratio appears negligible by comparison with the effect of different dimensionality, or the replacement of the cubic assumption value for C with that obtained from volumetric measurement. This does not mean that it should be discounted, since in this data set the variation in aspect ratio happens to be low. As described in Section 5.4.2, the effect of elongation on estimated volume can be considerable, and so adjusting volume estimates for aspect ratio should significantly improve the estimates where the variance in aspect ratio is high.

6.3.4 The importance of absolute charcoal quantification

Where the aim of a study is to establish fluctuations in fire activity over time at a particular site, establishing the actual volume of charcoal in a given volume of sediment may seem unnecessary, as long as it can be assumed that changes in charcoal area represent proportional changes in fire activity. But this will only be the case if two conditions apply: that the shape and the size of particles both remain constant. If either of these varies, the relation between volume and area will change, according to Weng's formula, and thus the change in area measured will not be proportional to the change in the amount of charcoal in the samples.

Variation in shape and size should in fact be minimised, though not excluded, by conscientious application of the existing principles of charcoal analysis. Changes in transportation regime imply changes in source area, and therefore

should be screened against by looking for evidence of changes in sedimentation before a charcoal record is interpreted. Also, different fuel materials cannot be expected to produce equal volumes of charcoal under the same fire conditions (Antal & Grønli, 2003), and so changes in charcoal quantity do not necessarily indicate proportional changes in fire activity unless vegetation composition remains constant. Ensuring that vegetation composition and transportation regime have remained fairly stable for the duration of the record is therefore a prerequisite to reliable interpretation of a charcoal record, even under existing methodologies. Doing this will ensure that the two clearest sources of morphological variation, and thus of bias in the record, are largely removed. More generally, a record indicative of an environment relatively stable over time would indicate that the size and shape of the charcoal particles would likely remain similarly constant. Yet variations in particle size and shape cannot be entirely excluded, and it is in any case implausible that fire activity should vary while other environmental parameters remain constant. In particular, vegetation composition and fire regime are inextricably linked, each influencing the other.

It therefore seems preferable to seek to use two-dimensional measurements of charcoal quantity for the purpose of estimating volume, with an explicit recognition of the errors involved in doing so, than to seek out circumstances under which raw areal measurements should be legitimate.

6.3.4.1 Charcoal quantification for carbon dynamics

Absolute quantification of charcoal content is vital when it comes to quantifying the relationship between fire and carbon dynamics. By rendering biomass into a relatively inert form, charcoalification may have a significant impact on the carbon cycle; yet the role of pyrogenic carbon in the carbon cycle is not well understood (Zimmerman, 2010; Santín et al., 2015), and it is not normally included in global carbon cycle and climate models (Santín et al., 2015). Since minor changes in carbon dynamics can have “large effects in global climate change scenarios” this is a deficiency which should be addressed (Santín et al., 2015).

Santín et al. (2015) note that quantitative studies of the pyrogenic carbon sequestered in soils and sediments are not currently reliable, since both chemical and visual methods of quantification focus only on certain size fractions, and so underestimate the total. To this it can be added that visual methods cannot in any case give true quantitative information unless they are transformed to volume estimates using information on number and shape of the particles in addition to total area.

Previous studies (e.g. McMichael et al., 2012a, 2012b; Leys et al., 2013) have purported to give volumetric estimates of charcoal quantity in sedimentary environments on the basis of the simple version of Weng's formula, with $C = 1$. C values obtained from CLSM show this assumption to be seriously flawed. However the approach itself is not invalidated by previous false assumptions regarding the value of the shape factor. If it can be shown that C tends to be distributed around some particular value (indicated by Figure 5.9 to be of the order of 0.1), within certain confidence limits, then the formula may be used to give volumetric estimates of charcoal content with a quantifiable degree of accuracy. This could provide a valuable tool to refine estimates of the carbon fluxes associated with fire activity, at the size fractions typically quantified from soil and sedimentary systems.

6.3.5 Conclusions on dimensionality of measurement

Measurement at different dimensions should be thought of as a hierarchy in which accuracy of measurement increases monotonically with dimension. The greatest accuracy is to be had by taking volumetric measurements, while areal measurements are preferable to particle counts[14].

Though it is clearly impractical for charcoal to be quantified on a volumetric basis in ordinary palaeoenvironmental studies, it is important to recognise that where a spatial quantity is measured at a lower dimension than its own, a loss of information occurs with each dimension. Taking an area measurement means losing information on the particle's extension in the z-dimension. Taking

[14] Linear measurements could in principle be used, but have not been employed in this field since there is no practical advantage over taking areal measurements.

a particle count instead of an area measurement means losing the information on its extension in the *x*- and *y*-dimensions. Furthermore, measures of correlation based on Pearson's *r* are problematic as indicators of the amount of information lost. Pearson's *r* provides a reliable measure of effect size only where its assumptions are attended to, and extrapolating a finding of a high correlation to other data sets should be done in the context of an explicit sampling theory if the outcome is not to be doubted.

Areal measurement assumes that all particles have equal depth, while a particle count assumes that all particles have the same volume. Neither assumption is plausible, and so it must be assumed that neither measure accurately records volume. However Weng's (2005) formula provides the prospect of a method to take areal measurements, but then account for their morphology to give an accurate estimate of volume. The evidence presented in this thesis for the variation in the value of *C* helps advance toward this goal. It is proposed that as a first step toward properly accounting for differences in shape, the value of *C* could be adjusted where elongate particles are evident, replacing the cubic assumption of $C = 1$ with a cuboid assumption with variable *C*. This would immediately improve volume estimates from Weng's formula. However, empirical evidence of the true range of *C* values will also be needed to fully realise the potential of this approach. If further volumetric studies of sedimentary charcoal particles are able to constrain the value of *C* within a sufficiently narrow range, Weng's formula may subsequently be used to estimate charcoal volume from areal data with a reasonable and quantifiable degree of error.

6.4 Thesis Conclusions

This thesis extends the use of charcoal morphology beyond the existing territory of Quaternary lake sediment studies, in which morphology was a potentially important addition to charcoal quantification, and proposes that it is an essential aspect of the study of charcoal from any sedimentary archive, whose understanding is integral to accurate charcoal quantification.

The studies of charcoal from a peatland environment, and various pre-Quaternary sites, shows that charcoal morphometry has applications beyond the Holocene lake sediment environment in which it has previously been deployed. Morphological variation is considerable in both cases, highlighting the importance of recognising the diversity of morphology, in order that the identification or quantification of charcoal should not be biased by narrow notions of its morphological characteristics.

The experiment in simulated transport of charcoal provides strong support for the idea that the morphological difference identified by Umbanhowar & McGrath (1998) between grass and forest mesocharcoal is a general characteristic of the two vegetation types, rather than a consequence of species selection or laboratory method. This assumption, previously untested, has underlain the extension of their method into other biomes. This now appears to be justified, but it is necessary to abandon the idea that a specific value can be given to divide grass and forest charcoal, and to investigate the influence of the many other growth forms (e.g. ferns) which may contribute to the charcoal record.

Previous research has assumed that charcoal quantification and charcoal morphology are separate issues. By approaching quantification as a problem of stereology, in which measurement at dimensions lower than the objects of interest are understood as proxy measurements, whose reliability is dependent on the shape and orientation of the objects, it has been shown here that morphology is in fact vital to charcoal quantification.

A number of problems are identified which undermine claims to show that particle counts are a suitable measure of charcoal content, but the most fundamental of these is that they are based on the assumption that area is the correct measure of charcoal content.

The true relationship between area and volume had been approached from two distinct perspectives. Weng (2005) had outlined a sound theoretical approach for the estimation of charcoal volume from image data, which could not however be reliably utilised without empirical morphological data; while Belcher et al. (2013b) had described a method for obtaining such data, though not related it to Weng's approach. By extending Weng's theory both conceptually, and through applying the empirical approach of Belcher et al. (2013b), this partial theory of

volumetric quantification is developed. In contradiction to the original presentation of the formula, the shape factor *C* is shown to be highly variable, a function of orientation as well as shape. Far from approximating to a value of 1, it cannot in fact exceed that value, and may be lower by one or two orders of magnitude. With further study on the values of *C*, it could be possible to use two-dimensional visual measurements for the accurate quantification of charcoal, rather than as a relative measure of fire activity. This could extend the use of charcoal measurements to contribute to quantitative understanding of the effects of fire on carbon cycling, with the potential to improve our understanding of the linkages between climate, vegetation and fire, and of the co-evolution of plants and fire regimes throughout Earth's history. The errors introduced by using the wrong value of *C*, or by taking proxy measurements in a lower dimension, have been shown to be substantial. It is proposed that instead of treating areal measurements of charcoal as proxies for fire activity in themselves, measurements from charcoal images should instead be used to make estimates of the actual volume, with an explicit recognition of the degree of error involved in doing so.

The research presented in this thesis suggests that a new approach is needed in the study of palaeofire, which currently relies heavily on long-established methods of charcoal measurement, and a simplistic approach to charcoal morphology. It is clear that charcoal morphologies are controlled by source vegetation, fire dynamics and transportation prior to their incorporation in sediments. Information on each of these may be inferred from charcoal morphologies, and critically all three will ultimately affect charcoal quantification. If charcoal assemblages are to help us decipher the role of fire in the Earth system, all these stages in their formation need to be better understood, and the inseparability of morphometry and quantification must be recognised.

Appendix: Values of *C* for volumetrically measured charcoal particles

The following tables contain CLSM measurements of particle volume and projected area for the three charcoal samples studied by Belcher et al. (2013b), and for the Holocene mesocharcoal studied in this thesis. The correct value of *C* is calculated for each particle, together with the volume overestimate which would result from the assumption that *C* = 1.

Modern microcharcoal (measurements from Belcher et al., 2013b)				
Projected area (µm²)	**Volume (µm³)**	**Volume estimate where *C* = 1**	**Overestimate (where correct volume = 1)**	**Correct value of *C***
69,610	292,013	18,365,714	62.89	0.016
21,419	56,358	3,134,754	55.62	0.018
26,733	139,762	4,370,843	31.27	0.032
6,308	14,618	501,056	34.28	0.029
33,849	140,265	6,227,654	44.40	0.023
2,943	7,691	159,654	20.76	0.048
30,685	101,525	5,375,256	52.95	0.019
16,449	58,777	2,109,659	35.89	0.028
27,945	95,572	4,671,375	48.88	0.020
39,915	182,672	7,974,400	43.65	0.023
38,801	117,968	7,643,045	64.79	0.015
34,634	137,838	6,445,511	46.76	0.021
58,661	246,930	14,207,721	57.54	0.017
32,096	102,332	5,750,027	56.19	0.018
38,352	121,339	7,510,626	61.90	0.016
54,406	205,903	12,690,200	61.63	0.016
37,692	239,844	7,317,592	30.51	0.033
60,552	228,627	14,900,366	65.17	0.015
14,407	52,078	1,729,253	33.21	0.030
35,225	158,901	6,611,104	41.61	0.024
19,863	63,441	2,799,330	44.12	0.023
5,331	12,396	389,198	31.40	0.032
39,894	157,686	7,968,271	50.53	0.020
70,283	247,218	18,632,532	75.37	0.013
69,253	333,697	18,224,604	54.61	0.018
48,949	186,201	10,829,635	58.16	0.017
31,003	101,058	5,458,980	54.02	0.019

50,750	180,318	11,432,944	63.40	0.016
19,960	59,644	2,819,889	47.28	0.021
98,951	326,574	31,126,571	95.31	0.010
79,863	244,171	22,569,474	92.43	0.011
37,713	220,228	7,323,788	33.26	0.030
81,867	225,057	23,424,014	104.08	0.010
37,516	152,786	7,266,537	47.56	0.021
19,427	65,737	2,707,725	41.19	0.024
14,940	65,380	1,826,086	27.93	0.036
29,241	107,402	5,000,324	46.56	0.021
26,827	83,695	4,393,951	52.50	0.019
57,469	226,516	13,776,993	60.82	0.016
41,877	125,579	8,569,665	68.24	0.015
14,913	35,671	1,821,189	51.06	0.020
81,169	336,246	23,125,163	68.77	0.015
45,168	181,094	9,599,533	53.01	0.019
62,288	258,859	15,545,718	60.05	0.017
18,844	58,018	2,586,842	44.59	0.022
32,842	125,921	5,951,822	47.27	0.021
84,896	302,644	24,735,860	81.73	0.012
14,324	38,529	1,714,304	44.49	0.022
30,604	125,408	5,353,774	42.69	0.023
60,417	280,565	14,850,443	52.93	0.019
75,958	365,417	20,934,189	57.29	0.017
11,121	33,359	1,172,714	35.15	0.028
65,422	250,661	16,733,420	66.76	0.015
16,620	55,557	2,142,591	38.57	0.026
44,507	130,406	9,389,605	72.00	0.014
47,641	167,347	10,398,523	62.14	0.016
58,653	194,295	14,204,987	73.11	0.014
23,195	89,701	3,532,481	39.38	0.025
58,824	213,949	14,266,974	66.68	0.015
19,230	85,073	2,666,709	31.35	0.032
5,944	14,726	458,292	31.12	0.032
32,049	107,596	5,737,375	53.32	0.019
23,273	72,298	3,550,433	49.11	0.020
41,008	177,701	8,304,158	46.73	0.021
33,623	89,101	6,165,310	69.19	0.014
42,115	130,876	8,642,853	66.04	0.015
30,115	93,357	5,226,000	55.98	0.018
25,451	71,647	4,060,369	56.67	0.018
30,927	100,261	5,438,932	54.25	0.018
90,038	308,658	27,017,179	87.53	0.011
18,606	45,258	2,537,934	56.08	0.018

48,632	141,976	10,724,631	75.54	0.013
36,546	128,098	6,986,365	54.54	0.018
11,722	32,792	1,269,096	38.70	0.026
56,316	154,700	13,364,248	86.39	0.012
37,940	123,551	7,390,035	59.81	0.017
22,285	76,329	3,326,671	43.58	0.023
43,337	165,472	9,021,727	54.52	0.018
92,502	300,091	28,133,470	93.75	0.011
15,604	54,824	1,949,134	35.55	0.028
23,690	59,124	3,646,327	61.67	0.016
33,578	110,487	6,152,862	55.69	0.018
66,578	205,589	17,178,769	83.56	0.012
32,263	84,005	5,794,919	68.98	0.014
61,039	176,736	15,080,322	85.33	0.012
12,979	30,312	1,478,668	48.78	0.020
16,318	42,917	2,084,580	48.57	0.021
7,325	17,538	626,894	35.75	0.028
32,550	96,693	5,872,637	60.74	0.016
46,279	159,559	9,955,694	62.40	0.016
88,407	310,315	26,286,154	84.71	0.012
35,350	88,846	6,646,224	74.81	0.013
29,629	76,856	5,099,997	66.36	0.015
126,843	457,438	45,175,400	98.76	0.010
77,218	221,754	21,457,244	96.76	0.010
11,630	31,343	1,254,286	40.02	0.025
46,766	161,827	10,113,201	62.49	0.016

Modern mesocharcoal (measurements from Belcher et al., 2013b)				
Projected area (µm²)	**Volume (µm³)**	**Volume estimate where *C* = 1**	**Overestimate (where correct volume = 1)**	**Correct value of *C***
258,696	2,674,759	131,578,057	49.19	0.020
1,067,202	18,652,768	1,102,477,841	59.11	0.017
505,726	6,171,831	359,644,444	58.27	0.017
666,251	7,766,319	543,821,666	70.02	0.014
1,394,332	23,565,312	1,646,453,490	69.87	0.014
707,741	7,896,958	595,403,390	75.40	0.013
691,326	7,021,503	574,809,950	81.86	0.012
1,032,036	14,345,037	1,048,436,262	73.09	0.014
68,811	600,651	18,050,405	30.05	0.033
429,293	4,329,977	281,274,757	64.96	0.015
53,715	557,042	12,449,137	22.35	0.045

1,346,920	14,952,293	1,563,193,527	104.55	0.010
1,375,589	22,242,852	1,613,366,964	72.53	0.014
800,774	12,638,414	716,580,266	56.70	0.018
335,714	4,206,717	194,515,892	46.24	0.022
643,248	6,362,490	515,902,917	81.09	0.012
392,221	7,400,491	245,638,784	33.19	0.030
553,586	6,950,260	411,886,446	59.26	0.017
262,261	2,946,200	134,307,762	45.59	0.022
187,081	3,086,142	80,917,571	26.22	0.038
479,817	7,352,866	332,364,049	45.20	0.022
476,703	7,380,828	329,133,335	44.59	0.022
420,051	6,189,282	272,240,750	43.99	0.023
193,293	1,908,403	84,981,450	44.53	0.022
1,399,237	17,904,686	1,655,147,446	92.44	0.011
300,403	3,240,509	164,647,899	50.81	0.020
355,258	3,602,017	211,746,677	58.79	0.017
390,531	6,098,952	244,052,564	40.02	0.025
215,381	2,434,509	99,956,173	41.06	0.024
300,906	3,372,690	165,061,812	48.94	0.020
250,653	2,494,248	125,490,363	50.31	0.020
1,059,386	12,818,259	1,090,388,126	85.07	0.012
399,730	5,276,444	252,726,201	47.90	0.021
563,516	7,341,300	423,018,657	57.62	0.017
986,690	12,438,057	980,101,117	78.80	0.013
545,474	8,296,033	402,866,570	48.56	0.021
482,578	5,806,658	335,236,193	57.73	0.017
773,094	10,451,101	679,748,364	65.04	0.015
359,117	5,713,380	215,205,423	37.67	0.027
935,604	13,494,900	904,977,629	67.06	0.015
197,559	2,194,948	87,810,232	40.01	0.025
702,615	11,155,193	588,947,195	52.80	0.019
297,926	2,874,453	162,615,828	56.57	0.018
389,327	5,074,971	242,924,586	47.87	0.021
158,606	1,142,649	63,165,275	55.28	0.018
342,082	3,380,596	200,075,936	59.18	0.017
300,539	4,178,811	164,759,414	39.43	0.025
434,897	8,664,166	286,799,909	33.10	0.030
345,695	6,264,198	203,254,449	32.45	0.031
520,945	7,847,691	375,999,700	47.91	0.021
852,743	10,919,103	787,457,546	72.12	0.014
187,816	1,169,839	81,395,389	69.58	0.014
644,254	6,596,110	517,113,574	78.40	0.013
182,034	1,393,867	77,665,662	55.72	0.018
191,383	2,331,440	83,724,649	35.91	0.028

146,577	2,387,130	56,117,277	23.51	0.043
445,014	8,549,204	296,866,128	34.72	0.029
200,417	1,971,811	89,722,692	45.50	0.022
162,231	1,351,475	65,343,048	48.35	0.021
469,189	4,882,936	321,382,232	65.82	0.015
961,544	17,111,414	942,873,813	55.10	0.018
265,652	2,321,253	136,920,769	58.99	0.017
163,677	1,589,112	66,218,913	41.67	0.024
1,231,586	20,018,878	1,366,775,904	68.27	0.015
303,090	2,849,900	166,861,703	58.55	0.017
899,343	14,695,477	852,880,389	58.04	0.017
455,967	5,193,865	307,893,310	59.28	0.017
259,034	2,573,175	131,836,501	51.23	0.020
1,143,225	17,670,506	1,222,355,609	69.17	0.014
413,664	6,153,992	266,055,131	43.23	0.023
678,490	7,603,477	558,875,713	73.50	0.014
368,510	3,806,532	223,704,455	58.77	0.017
567,534	10,302,020	427,550,337	41.50	0.024
1,596,070	23,052,380	2,016,404,922	87.47	0.011
839,445	12,840,048	769,109,329	59.90	0.017
913,502	11,203,064	873,101,072	77.93	0.013
1,234,676	14,456,013	1,371,922,906	94.90	0.011
1,355,195	19,931,380	1,577,621,245	79.15	0.013
438,696	5,762,442	290,566,697	50.42	0.020
338,574	3,435,355	197,005,996	57.35	0.017
588,468	7,067,722	451,423,259	63.87	0.016
481,841	5,616,753	334,469,170	59.55	0.017
1,162,165	16,630,742	1,252,856,723	75.33	0.013
689,492	8,050,240	572,523,731	71.12	0.014
1,337,338	23,628,718	1,546,541,776	65.45	0.015
567,857	5,649,939	427,915,527	75.74	0.013
979,880	15,219,898	969,972,973	63.73	0.016
584,336	13,273,270	446,677,171	33.65	0.030
656,811	8,979,122	532,304,491	59.28	0.017
345,260	2,626,080	202,870,816	77.25	0.013

Cretaceous mesocharcoal (measurements from Belcher et al., 2013b)				
Projected area (µm²)	**Volume (µm³)**	**Volume estimate where *C* = 1**	**Overestimate (where correct volume = 1)**	**Correct value of *C***
6,036	25,810	468,912	18.17	0.055
21,805	115,492	3,219,790	27.88	0.036
25,611	150,683	4,098,598	27.20	0.037

31,272	169,280	5,530,151	32.67	0.031
31,529	184,185	5,598,347	30.40	0.033
32,502	216,578	5,859,513	27.06	0.037
32,844	223,997	5,952,258	26.57	0.038
34,458	256,053	6,396,253	24.98	0.040
35,265	287,158	6,622,346	23.06	0.043
36,908	305,789	7,090,498	23.19	0.043
41,313	307,019	8,397,067	27.35	0.037
42,178	307,210	8,662,366	28.20	0.035
42,438	309,540	8,742,347	28.24	0.035
46,760	310,559	10,111,307	32.56	0.031
52,661	356,959	12,084,513	33.85	0.030
53,738	415,344	12,457,331	29.99	0.033
61,444	448,946	15,230,631	33.93	0.029
65,509	466,434	16,766,774	35.95	0.028
66,645	504,854	17,204,708	34.08	0.029
67,065	507,039	17,367,621	34.25	0.029
68,560	542,030	17,951,803	33.12	0.030
72,060	546,836	19,343,656	35.37	0.028
72,336	553,436	19,455,032	35.15	0.028
72,847	587,090	19,661,647	33.49	0.030
75,020	632,141	20,547,816	32.51	0.031
77,860	640,924	21,725,588	33.90	0.030
79,663	673,018	22,484,789	33.41	0.030
84,945	732,731	24,757,292	33.79	0.030
88,216	755,920	26,201,160	34.66	0.029
89,918	770,522	26,963,063	34.99	0.029
93,786	780,731	28,721,347	36.79	0.027
95,044	787,477	29,301,243	37.21	0.027
95,094	795,590	29,324,541	36.86	0.027
95,853	796,850	29,676,295	37.24	0.027
102,263	821,189	32,702,243	39.82	0.025
103,019	827,255	33,065,670	39.97	0.025
107,511	876,113	35,251,815	40.24	0.025
110,245	950,678	36,604,694	38.50	0.026
110,584	959,424	36,773,900	38.33	0.026
114,910	1,013,070	38,952,455	38.45	0.026
116,375	1,035,190	39,699,928	38.35	0.026
116,564	1,077,971	39,796,896	36.92	0.027
117,305	1,087,842	40,176,540	36.93	0.027
121,602	1,091,361	42,404,338	38.85	0.026
121,804	1,122,118	42,510,148	37.88	0.026
126,398	1,129,669	44,937,453	39.78	0.025
128,017	1,130,318	45,803,892	40.52	0.025

128,413	1,140,281	46,016,255	40.36	0.025
132,697	1,223,836	48,338,588	39.50	0.025
133,200	1,231,016	48,613,678	39.49	0.025
133,766	1,231,290	48,923,649	39.73	0.025
134,036	1,234,665	49,071,780	39.75	0.025
138,379	1,267,134	51,476,241	40.62	0.025
138,802	1,292,770	51,712,224	40.00	0.025
139,389	1,303,775	52,040,672	39.92	0.025
139,909	1,306,226	52,331,867	40.06	0.025
141,623	1,330,777	53,296,648	40.05	0.025
144,490	1,338,780	54,923,495	41.03	0.024
148,092	1,345,620	56,989,808	42.35	0.024
148,327	1,356,302	57,125,639	42.12	0.024
150,352	1,380,256	58,299,228	42.24	0.024
159,661	1,383,480	63,796,427	46.11	0.022
159,672	1,421,736	63,803,039	44.88	0.022
161,140	1,442,840	64,685,019	44.83	0.022
162,333	1,444,626	65,405,089	45.27	0.022
168,907	1,487,608	69,417,919	46.66	0.021
171,088	1,543,548	70,766,907	45.85	0.022
172,213	1,551,149	71,465,817	46.07	0.022
172,749	1,694,455	71,799,638	42.37	0.024
174,042	1,728,857	72,607,123	42.00	0.024
184,737	1,736,829	79,401,727	45.72	0.022
185,100	1,741,033	79,635,773	45.74	0.022
187,361	1,752,047	81,099,778	46.29	0.022
193,956	1,754,535	85,419,388	48.68	0.021
195,569	1,890,441	86,486,787	45.75	0.022
199,755	1,929,605	89,278,722	46.27	0.022
199,792	1,938,639	89,303,413	46.07	0.022
201,911	1,939,517	90,727,798	46.78	0.021
202,942	1,982,298	91,423,449	46.12	0.022
206,987	2,091,264	94,170,356	45.03	0.022
207,740	2,278,604	94,684,858	41.55	0.024
209,719	2,322,251	96,041,267	41.36	0.024
217,539	2,494,332	101,462,192	40.68	0.025
223,833	2,513,304	105,897,592	42.13	0.024
265,420	3,040,282	136,741,299	44.98	0.022
276,193	3,254,932	145,150,680	44.59	0.022
327,305	3,610,718	187,253,049	51.86	0.019
330,806	3,613,848	190,265,590	52.65	0.019
343,168	3,625,841	201,029,787	55.44	0.018
370,839	3,818,472	225,828,077	59.14	0.017
423,218	3,836,525	275,325,683	71.76	0.014

426,376	4,254,739	278,412,724	65.44	0.015
427,527	4,431,510	279,541,213	63.08	0.016
429,304	5,276,295	281,285,690	53.31	0.019
459,208	5,603,004	311,182,008	55.54	0.018
467,746	5,776,686	319,900,587	55.38	0.018
515,761	6,021,491	370,401,058	61.51	0.016
570,132	6,345,968	430,490,130	67.84	0.015
621,022	6,589,944	489,396,071	74.26	0.013
742,724	8,336,841	640,089,728	76.78	0.013

Holocene mesocharcoal				
Projected area (µm²)	**Volume (µm³)**	**Volume estimate where *C* = 1**	**Overestimate (where correct volume = 1)**	**Correct value of *C***
4,523	30,296	304,175	10.04	0.100
3,821	106,773	236,224	2.21	0.452
3,644	98,274	219,947	2.24	0.447
5,566	58,493	415,204	7.10	0.141
14,371	197,623	1,722,834	8.72	0.115
5,385	52,716	395,160	7.50	0.133
2,892	28,179	155,555	5.52	0.181
7,077	53,947	595,370	11.04	0.091
6,264	56,246	495,781	8.81	0.113
14,599	268,389	1,763,888	6.57	0.152
8,970	82,996	849,546	10.24	0.098
16,941	162,447	2,205,027	13.57	0.074
14,866	247,734	1,812,597	7.32	0.137
7,478	51,115	646,721	12.65	0.079
6,382	139,765	509,786	3.65	0.274
41,104	568,558	8,333,352	14.66	0.068
49,192	597,774	10,910,487	18.25	0.055
12,574	233,925	1,409,899	6.03	0.166
13,626	211,386	1,590,550	7.52	0.133
14,382	73,131	1,724,839	23.59	0.042
11,533	127,831	1,238,573	9.69	0.103
18,665	285,769	2,549,916	8.92	0.112
11,075	291,969	1,165,565	3.99	0.250
23,652	310,849	3,637,467	11.70	0.085
13,070	36,076	1,494,217	41.42	0.024
8,617	91,924	799,894	8.70	0.115
3,076	34,601	170,596	4.93	0.203
31,302	505,314	5,538,072	10.96	0.091
19,485	351,414	2,719,883	7.74	0.129

3,190	46,007	180,205	3.92	0.255
6,439	19,647	516,659	26.30	0.038
21,638	338,028	3,182,904	9.42	0.106
38,065	415,252	7,426,521	17.88	0.056
20,006	146,424	2,829,688	19.33	0.052
11,604	124,105	1,249,963	10.07	0.099
6,904	97,555	573,653	5.88	0.170
10,728	174,439	1,111,095	6.37	0.157
8,033	83,320	719,953	8.64	0.116
15,598	231,231	1,948,111	8.42	0.119
7,944	90,993	708,097	7.78	0.129
2,981	4,147	162,744	39.25	0.025
3,383	39,501	196,757	4.98	0.201
6,109	96,691	477,456	4.94	0.203
3,870	48,831	240,717	4.93	0.203
8,258	75,697	750,437	9.91	0.101

References

Ainsworth, A. & Kauffman, J.B. (2009) Response of native Hawaiian woody species to lava-ignited wildfires in tropical forests and shrublands. *Plant Ecology*, vol. 201, pp. 197-209.

Ainsworth, A. & Kaufman, J.B. (2013) Effects of repeated fires on native plant community
development at Hawaii Volcanoes National Park. *International Journal of Wildland Fire*, vol. 22, pp. 1044-1054.

Aleman, J.C., Blarquez, O., Bentaleb, I., Bonté, P., Brossier, B., Carcaillet, C., Gond, V., Gourlet-Fleury, S., Kpolita, A., Lefèvre, I., Oslisly, R., Power, M.J., Yongo, O., Bremond, L. & Favier, C. (2013) Tracking land-cover changes with sedimentary charcoal in the Afrotropics. *The Holocene*, vol. 23, no. 12, pp. 1853-1862.

Ali, A.A., Higuera, P.E., Bergeron, Y. & Carcaillet, C. (2009) Comparing fire-history interpretations based on area, number and estimated volume of macroscopic charcoal in lake sediments. *Quaternary Research*, vol. 72, pp. 462-468.

Andreae, M.O. (1983) Soot carbon and excess fine potassium: long-range transport of combustion-derived aerosols. *Science*, vol. 220, pp. 1148-1151.

Anon. (2000) *Munsell Soil Color Charts*, revised edition. Munsell Color, Grand Rapids, Michigan.

Antal, M.J., Jr. & Grønli, M. (2003) The Art, Science, and Technology of Charcoal Production. *Industrial & Engineering Chemistry Research*, vol. 42, pp. 1619-1640.

Ascough, P.L., Bird, M.I., Scott, A.C., Collinson, M.E., Cohen-Ofri, I., Snape, C.E. and Le Manquais, K. (2010) Charcoal reflectance measurements: implications for structural characterization and assessment of diagenetic alteration. *Journal of Archaeological Science*, vol. 37, pp. 1590-1599.

Asselin, H. & Payette, S. (2005a) Detecting local-scale fire episodes on pollen slides. *Review of Palaeobotany & Palynology*, vol. 137, pp. 31-40.

Asselin, H. & Payette, S. (2005b) Late Holocene deforestation of a tree line site: estimation of pre-fire vegetation composition and black spruce cover using soil charcoal. *Ecography*, vol. 28, pp. 801-805.

Baker, S.J., Belcher, C.M., Hesselbo, S.P., Lenton, T.M. & Duarte, L.V. (in review) Charcoal evidence that increased atmospheric oxygen helped terminate the Toarcian Oceanic Anoxic Event. *Geology*.

Belcher, C.M., Collinson, M.E., Sweet, A.R., Hildebrand, A.R. & Scott, A.C. (2003) Fireball passes and nothing burns – The role of thermal radiation in the Cretaceous-Tertiary event: Evidence from the charcoal

record of North America. *Geology*, vol. 31, pp. 1061-1064.

Belcher, C.M., Yearsley, J.M., Hadden, R.M., McElwain, J.C. & Rein, G. (2010a) Baseline intrinsic flammability of Earth's ecosystems estimated from paleoatmospheric oxygen over the past 350 million years. *PNAS*, vol. 107, no. 52, pp. 22448-22453.

Belcher, C.M., Mander, L., Rein, G., Jervis, F.X., Haworth, M., Hasselbo, S.P., Glasspool, I.J. & McElwain, J.C. (2010b) Increased fire activity at the Triassic/Jurassic boundary in Greenland due to climate-driven floral change. *Nature Geoscience*, vol. 3, pp. 426-429.

Belcher, C.M., Collinson, M.E. & Scott, A.C. (2013a) A 450-million-year history of fire. In: Belcher, C.M. (ed.) *Fire Phenomena and the Earth System: An Interdisciplinary Guide to Fire Science.* Wiley-Blackwell. pp. 229-249.

Belcher, C.M., Sivaguru, M. & Punyasena, S.W. (2013b) Novel application of laser scanning microscopy and image analysis to improve the resolution of the fossil record of wildfire activity. *PLoS One*, vol. 8: e72265.

Belcher, C.M. & Hudspith, V.A. (in review) The formation of charcoal reflectance and its potential use in post-fire assessments. Submitted to *International Journal of Wildland Fire*.

Blackford, J.J., Innes, J.B., Hatton, J.J. & Caseldine, C.J. (2006) Mid-Holocene environmental change at Black Ridge Brook, Dartmoor, SW England: A new appraisal based on fungal spore analysis. *Review of Palaeobotany & Palynology*, vol. 141, pp. 189-201.

Bookstein, F.L. (1978) The Measurement of Biological Shape and Shape Change. *Lecture Notes in Biomathematics*, vol. 24. Springer-Verlag. 191 pp.

Boulter, M.C. (1994) An approach to a standard terminology for palynodebris. In: Traverse, A. (ed.) *Sedimentation of Organic Particles*. Cambridge University Press. pp. 199-216.

Bouman, C.A. (2005) *CLUSTER: An Unsupervised Algorithm for Modeling Gaussian Mixtures*. Purdue University. 20 pp. Available at: https://engineering.purdue.edu/~bouman/software/cluster/manual.pdf. Accessed 8/5/2015.

Bowman, D.M.J.S., Balch, J.K., Artaxo, P., Bond, W.J., Carlson, J.M., Cochrane, M.A., D'Antonio, C.M., DeFries, R.S., Doyle, J.C., Harrison, S.P., Johnston, F.H., Keeley, J.E., Krawchuk, M.A., Kull, C.A., Marston, J.B., Moritz, M.A., Prentice, I.C., Roos, C.I., Scott, A.C., Swetnam, T.W., van der Werf, G.R. & Pyne, S.J. (2009) Fire in the Earth System. *Science*, vol. 324, pp. 481-484.

Braadbaart, F., Poole, I. & van Brussel, A.A. (2009) Preservation potential of charcoal in alkaline environments: an experimental approach and implications for the archaeological record. *Journal of Archaeological Science*, vol. 36, pp. 1672-1679.

Bruck, J., Johnston, R. & Wickstead, H. (2003) Excavations of Bronze Age field systems on Shovel Down, Dartmoor, 2003. *PAST*, no. 45, pp. 10-12.

Caldararo, N. (2002) Human ecological intervention and the role of forest fires in human ecology. *The Science of the Total Environment*, vol. 292, pp. 141–165.

Chatfield, C. (1980) *The Analysis of Time Series: An Introduction*, 2nd edition. Chapman and Hall, London / New York. 268pp.

Christenhusz, M.J.M., Reveal, J.L., Farjon, A., Gardner, M.F., Mill, R.R. & Chase, M.W. (2011) A new classification and linear sequence of extant gymnosperms. *Phytotaxa*, vol. 19, pp. 55-70.

Clark, R.L. (1982) Point count estimation of charcoal in pollen preparations and thin sections of sediments. *Pollen et Spores*, vol. 24, no. 3-4, pp. 523-535.

Clark, R.L. (1984) Effects on charcoal of pollen preparation procedures. *Pollen et Spores*, vol. 26, no. 3-4, pp. 559-576.

Clark, J.S. & Hussey, T.C. (1996) Estimating the mass flux of charcoal from sedimentary records: effects of particle size, morphology, and orientation. *The Holocene*, vol. 6, no. 2, pp. 129-144.

Clark, J.S. & Royall, P.D. (1996) Local and Regional Sediment Charcoal Evidence for Fire Regimes in Presettlement North-Eastern North America. *Journal of Ecology*, Vol. 84, No. 3, pp. 365-382.

Clark, J.S., Royall, P.D. & Chumbley, C. (1996) The Role of Fire During Climate Change in an Eastern Deciduous Forest at Devil's Bathtub, New York. *Ecology*, Vol. 77, No. 7, pp. 2148-2166.

Clarke, P.J., Lawes, M.J., Midgley, J.J., Lamont, B.B., Ojeda, F., Burrows, G.E., Enright, N.J. & Knox, K.J.E. (2013) Resprouting as a key functional trait: how buds, protection and resources drive persistence after fire. *New Phytologist*, vol. 197, pp. 19-35.

Cleveland, W.S. (1979) Robust Locally Weighted Regression and Smoothing Scatterplots. *Journal of the American Statistical Association*, Vol. 74, No. 368, pp. 829-836.

Cohen, A.D. (2009) Comparisons of pre-fire and post-fire peat thicknesses, petrography, and chemistry in the Okefenokee Swamp of Georgia following the fires of 2007. 58th Annual Meeting of the Southeastern Section, Geological Society of America. Paper No. 1–4.

Cohen, J., Cohen, P., West, S.G. & Aiken, L.S. (2003) *Applied Multiple Regression/Correlation Analysis for the Behavioural Sciences*, 3rd edition. Lawrence Erlbaum Associates. Mahwah. 703 pp.

Cohen-Ofri, I., Weiner, L., Boaretto, E., Mintz, G., Weiner, S. (2006) Modern and fossil charcoal: aspects of structure and diagenesis. *Journal of Archaeological Science 33*, pp. 428-439.

Collinson, M.E., Featherstone, C., Cripps, J.A., Nichols, G.J. & Scott, A.C. (1999) Charcoal-rich plant debris accumulations in the Lower Cretaceous of the Isle of Wight, England. *Acta Palaeobotanica*, Supplement 2, pp. 93-105.

Collinson, M.E., Steart, D.C., Scott, A.C., Glasspool, I.J. & Hooker, J.J. (2007) Episodic fire, runoff and deposition at the Palaeocene–Eocene boundary. *Journal of the Geological Society*, vol. 164, pp. 87-97.

Collinson, M.E., Steart, D.C., Harrington, G.J., Hooker, J.J., Scott, A.C., Allen, L.O., Glasspool, I.J. & Gibbons, S.J. (2009) Palynological evidence of vegetation dynamics in response to palaeoenvironmental change across the onset of the Paleocene-Eocene Thermal Maximum at Cobham, Southern England. *Grana*, vol. 48, pp. 38-66.

Colombaroli, D., Ssemmanda, I., Gelorini, V. & Verschuren, D. (2014) Contrasting long-term records of biomass burning in wet and dry savannas of equatorial East Africa. *Global Change Biology*, vol. 20, pp. 2903-2914.

Conedera, M., Tinner, W., Neff, C., Meurer, M., Dickens, A.F. & Krebs, P. (2009) Reconstructing past fire regimes: methods, applications, and relevance to fire management and conservation. *Quaternary Science Reviews*, vol. 28, pp. 555-576.

Costa, L. da F. & Cesar, R.M. Jr. (2001) *Shape Analysis and Classification: Theory and Practice*. CRC Press. 659 pp.

Crawford, A.J. & Belcher, C.M. (2014) Charcoal morphometry for paleoecological analysis: The effects of fuel type and transportation on morphological parameters. *Applications in Plant Sciences*, vol. 2, no. 8, doi: apps.1400004.

Cwynar, L.C. (1978) Recent history of fire and vegetation from laminated sediment of Greenleaf Lake, Algonquin Park, Ontario. *Canadian Journal of Botany*, vol. 56, pp. 10-21.

Daniau, A-L., Goñi, M.F.S., Martinez, P., Urrego, D.H., Bout-Roumazeilles, V., Desprat, S. & Marlon, J.R. (2013) Orbital-scale climate forcing of grassland burning in southern Africa. *PNAS*, vol. 110, pp. 5069-5073.

Davies, G.M. (2013) Understanding fire regimes and the ecological effects of fire. In: Belcher, C.M. (ed.) *Fire Phenomena and the Earth System: An Interdisciplinary Guide to Fire Science.* Wiley-Blackwell. pp. 97-124.
Doube M., Kłosowski, M.M., Arganda-Carreras, I., Cordeliéres, F., Dougherty, R.P., Jackson, J., Schmid, B., Hutchinson, J.R. & Shefelbine, S.J. (2010) BoneJ: free and extensible bone image analysis in ImageJ. *Bone*, vol. 47, pp. 1076-1079.

Drinnan, A.R., Crane, P.R., Friis, E.M. & Pedersen, K.R. (1991) Angiosperm Flowers and Tricolpate Pollen of Buxaceous Affinity from the Potomac Group (Mid-Cretaceous) of Eastern North America. *American Journal of Botany*, vol. 78, no. 2, pp. 153-176.

Earle, C.J., Brubaker, L.B. & Anderson, P.M. (1996) Charcoal in northcentral Alaskan lake sediments: relationships to fire and late-Quaternary vegetation history. *Review of Palaeobotany and Palynology*, vol. 92, pp. 83-95.

Eisenhauer, J.G. (2003) Regression through the origin. *Teaching Statistics*, vol. 25, no. 3, pp.
76-80.

Enache, M.D. & Cumming, B.F. (2006) Tracking recorded fires using charcoal morphology from the sedimentary sequence of Prosser Lake, British Columbia (Canada). *Quaternary Research*, vol. 65, pp. 282-292.

Enache, M.D. & Cumming, B.F. (2007) Charcoal morphotypes in lake sediments from British Columbia (Canada): an assessment of their utility for the reconstruction of past fire and precipitation. *Journal of Paleolimnology*, vol. 38, pp. 347-363.

Enache, M.D. & Cumming, B.F. (2009) Extreme fires under warmer and drier conditions inferred from sedimentary charcoal morphotypes from Opatcho Lake, central British Columbia, Canada. *The Holocene*, vol. 19, no. 6, pp. 835-846.

FAO (1985) *Industrial charcoal making. FAO Forestry Paper 63.* Food and Agriculture Organization of the United Nations. Rome.

Falcon-Lang , H. J. 1999. The Early Carboniferous (Courceyan–Arundian) monsoonal climate of the British Isles: Evidence from growth rings in fossil woods. Geological Magazine 136 : 177 – 187.

Fægri, K., Kaland, P.E. & Krzywinski, K. (1989) *Textbook of Pollen Analysis*, 4th edition. The Blackburn Press. Caldwell, New Jersey. p. 203.

Ferreira, T. & Rasband, W. (2012) *ImageJ User Guide: IJ 1.46r*. Available at: http://rsb.info.nih.gov/ij/docs/guide/index.html [Accessed 19/11/2012].

Finsinger, W. & Tinner, W. (2005) Minimum count sums for charcoal-concentration
estimates in pollen slides: accuracy and potential errors. *The Holocene*, vol. 15, pp. 293-297.

Finsinger, W., Kelly, R., Fevre, J. & Magyari, E.K. (2014) A guide to screening charcoal peaks in macrocharcoal-area records for fire-episode reconstructions. *The Holocene* Vol. 24, no. 8, pp. 1002-1008.

Flannigan, M.D., Krawchuk, M.A., de Groot, W.J., Wotton, B.M. & Gowman, L.M. (2009) Implications of changing climate for global wildland fire. *International Journal of Wildland Fire*, vol. 18, pp. 483-507.

Francus, P. & Pirard, E. (2004) Testing for sources of errors in quantitative image analysis. In: Francus, P. (ed.) *Image Analysis, Sediments and Paleoenvironments*. Springer. Dordrecht. pp. 87-102.

Francus, P., Bradley, R.S. & Thurow, J. (2004) An introduction to image analysis, sediments and paleoenvironments. In: Francus (ed.) *Image Analysis, Sediments and Paleoenvironments.* Springer. Dordrecht. pp. 1-7.

Franklin, R.E. (1950) The Interpretation of Diffuse X-ray Diagrams of Carbon. *Acta Crystallographica*, vol. 3, pp. 107-121.

Franklin, R.E. (1951) Crystallite Growth in Graphitizing and Non-Graphitizing Carbons. *Proceedings of the Royal Society of London. Series A, Mathematical and Physical Sciences*, vol. 209, no. 1097, pp. 196-218.

Friis, E.M., Crane, P.R. & Pedersen, K.R. (2011) *Early Flowers and Angiosperm Evolution*. Cambridge University Press. pp. 76-77.

Fyfe, R.M., Brück, J., Johnston, R., Lewis, H., Roland, T.P. & Wickstead, H. (2008) Historical context and chronology of Bronze Age land enclosure on Dartmoor, UK. Journal of Archaeological Science, vol. 35, pp. 2250-2261.

Gavin, D.G., Hu, F.S., Lertzman, K. & Corbett, P. (2006) Weak climatic control of stand-scale fire history during the late Holocene. *Ecology*, Vol. 87, No. 7, pp. 1722-1732.

Gavin, D.G., Hallett, D.J., Hu, F.S., Lertzman, K.P., Prichard, S.J., Brown, K.J., Lynch, J.A., Bartlein, P. & Peterson, D.L. (2007) Forest fire and climate change in western North America: insights from sediment charcoal records. *Frontiers in Ecology and the Environment*, vol. 5, pp. 499-506.

Gedye, S.J., Jones, R.T., Tinner, W., Ammann, B. & Oldfield, F. (2000) The use of mineral magnetism in the reconstruction of fire history: a case study from Lago di Origlio, Swiss Alps. *Palaeogeography, Palaeoclimatology, Palaeoecology*, vol. 164, pp. 101-110.

Glasbey, C.A. & Horgan, G.W. (1995) *Image Analysis for the Biological Sciences*. John Wiley & Sons. 218 pp.

Glasspool, I.J., Edwards, D. & Axe, L. (2004) Charcoal in the Silurian as evidence for the earliest wildfire. *Geology*, vol. 32, no. 5, pp. 381-383.

Glasspool, I.J. & Scott, A.C. (2010) Phanerozoic concentrations of atmospheric oxygen reconstructed from sedimentary charcoal. *Nature Geoscience* 3, pp. 627-630.

Glasspool, I.J. & Scott, A.C. (2013) Identifying past fire events. In: Belcher, C.M. (ed.) *Fire Phenomena and the Earth System: An Interdisciplinary Guide to Fire Science.* Wiley-Blackwell. pp. 179-206.

Gonzalez, R.C. & Woods, R.E. (2002) *Digital Image Processing*, 2nd edition. Prentice Hall. 793 pp.

Gutsell, S.L. & Johnson, E.A. (1996) How fire scars are formed: coupling a disturbance process to its ecological effect. *Canadian Journal of Forest Research*, vol. 26, pp. 166-174.

Hammes, K. & Abiven, S. (2013) Identification of black carbon in the earth system. In: Belcher, C.M. (ed.) *Fire Phenomena and the Earth System: An interdisciplinary guide to fire science.* Wiley-Blackwell. pp. 157-176.

Harris, P.J.F. (1999) On Charcoal. *Interdisciplinary Science Reviews*, vol. 24, no. 4, pp. 301-306.

Harris, P.J.F. (2013) Fullerene-like models for microporous carbon. *Journal of Materials Science*, vol. 48, pp. 565-577.

Hesselbo, S.P., Gröcke, D.R., Jenkyns, H.C., Bjerrum, C.J., Farrimond, P., Morgans Bell, H.S. & Green, O.R. (2000) Massive dissociation of gas hydrate during a Jurassic oceanic anoxic event. *Nature*, vol. 406, pp. 392-395.

Hesselbo, S.P., Jenkyns, H.C., Duarte, L.V. & Oliveira, L.C.V. (2007) Carbon-isotope record of the Early Jurassic (Toarcian) Oceanic Anoxic Event from fossil wood and marine carbonate (Lusitanian Basin, Portugal). *Earth and Planetary Science Letters*, vol. 253, pp. 455-470.

Higuera, P.E., Gavin, D.G., Bartlein, P.J. & Hallett, D.J. (2010) Peak detection in sediment–charcoal records: impacts of alternative data analysis methods on fire-history interpretations. *International Journal of Wildland Fire*, Vol. 19, pp. 996–1014.

Horn, S.P., Horn, R.D. & Byrne, R. (1992) An Automated Charcoal Scanner for Paleoecological Studies. *Palynology*, vol. 16, pp. 7-12.

Huang, C. & Hesselbo, S.P. (2014) Pacing of the Toarcian Oceanic Anoxic Event (Early Jurassic) from astronomical correlation of marine sections, *Gondwana Research*, vol. 25, no. 4, pp. 1348-1356.

Hudspith, V.A, Belcher, C.M. & Yearsley, J.M. (2014) Charring temperatures are driven by the fuel types burned in a peatland wildfire. *Frontiers in Plant Science*, Vol. 5, Article 714.

Hunt, M.A., Davidson, N.J., Unwin, G.L. & Close, D.C. (2002) Ecophysiology of the Soft Tree Fern, *Dicksonia antarctica* Labill. *Austral Ecology*, vol. 27, pp. 360-368.

Hykšová, M., Kalousová, A. & Saxl, I. (2012) Early history of geometric probability and stereology. *Image Analysis & Stereology*, vol. 31, pp. 1-16.

IBM Corp. (2012) IBM SPSS Statistics for Windows, Version 21.0 [Computer program]. IBM Corp., Armonk, NY, USA.

Innes, J.B., Blackford, J.J. & Simmons, I.G. (2004) Testing the integrity of fine spatial resolution palaeoecological records: microcharcoal data from near-duplicate peat profiles from the North York Moors, UK. *Palaeogeography, Palaeoclimatology, Palaeoecology*, vol. 214, pp. 295-307.

Iversen, J. (1964) Retrogressive vegetational succession in the post-glacial. *Journal of Animal Ecology*, vol. 33, pp. 59-70.

Jensen, K, Lynch, EA, Calcote, R & Hotchkiss, SC (2007) Interpretation of charcoal morphotypes in sediments from Ferry Lake, Wisconsin, USA: do different plant fuel sources produce distinctive charcoal morphotypes? *The Holocene*, vol. 17, no. 7, pp. 907-915.

Jones, T.P. & Chaloner, W.G. (1991) Fossil charcoal, its recognition and palaeoatmospheric significance. *Palaeogeography, Palaeoclimatology, Palaeoecology (Global and Planetary Change Section)*, vol. 97, pp. 39-50.

Jones, T.P., Chaloner, W.G. & Kuhlbusch, T.A.J. (1997) Proposed Bio-geological and Chemical Based Terminology for Fire-altered Plant Matter. In: Clark, J.S., Cachier, H., Goldammer, J.G. & Stocks, B. (eds.) *Sediment Records of Biomass Burning and Global Change*. NATO ASI Series. Series I: Global Environmental Change, vol. 51 (Proceedings of the NATO Advanced Study Institute "Biomass Burning Emissions and Global Change", held in Praia de Alvor, Algarve, Portugal, October 1994), pp. 9-22.

Jull, A.J.T. & Geertsema, M. (2006) Over 16,000 years of fire frequency determined from AMS radiocarbon dating of soil charcoal in an alluvial fan at Bear Flat, northeastern British Columbia. *Radiocarbon*, vol. 48, no. 3, pp. 435-450.

Keeley, J.E. (2009) Fire intensity, fire severity and burn severity: a brief review and suggested usage. *International Journal of Wildland Fire*, vol. 18, pp. 116-126.

Kelly, R.F., Higuera, P.E., Barrett, C.M. & Hu, F.S. (2011) A signal-to-noise index to quantify the potential for peak detection in sediment–charcoal records. *Quaternary Research*, Vol. 75, pp. 11–17.

Kendall, M. (1976) *Time-Series*, 2nd edition. Charles Griffin and Company Ltd., London / High Wycombe. 197pp.

Ketterings, Q.M. & Bigham, J.M. (2000) Soil Color as an Indicator of Slash-and-Burn Fire Severity and Soil Fertility in Sumatra, Indonesia. *Soil Science Society of America Journal*, vol. 64, pp. 1826-1833.

Kirchgeorg, T., Schüpbach, S., Kehrwald, N., McWethy, D.B. & Barbante, C. (2014) Method for the determination of specific molecular markers of biomass burning in lake sediments. *Organic Geochemistry*, vol. 71, pp. 1-6.

Kump, L.R. (1988) Terrestrial feedback in atmospheric oxygen regulation by fire and phosphorus. *Nature*, vol. 335, pp. 152-154.

Kurosaki, F., Ishimaru, K., Hata, T., Bronsveld, P., Kobayashi, E. & Imamura, Y. (2003) Microstructure of wood charcoal prepared by flash heating. *Carbon*, vol. 41, pp. 3057-3062.

Kurtz, A.C., Kump, L.R., Arthur, M.A., Zachos, J.C. & Paytan, A. (2003) Early Cenozoic decoupling of the global carbon and sulfur cycles. *Paleoceanography*, vol. 18, no. 4.

Lancelotti, C., Madella, M., Ajithprasad, P. & Petrie, C.A. (2010) Temperature, compression and fragmentation: an experimental analysis to assess the impact of taphonomic processes on charcoal preservation. *Archaeological and Anthropological Sciences*, vol. 2, pp. 307-320.

Lenton, T.M. (2001) The role of land plants, phosphorus weathering and fire in the rise and regulation of atmospheric oxygen. *Global Change Biology*, vol. 7, pp. 613-629.

Lenton, T.M. & Watson, A.J. (2000) Redfield revisited: 2. What regulates the oxygen content of the atmosphere? *Global Biogeochemical Cycles*, vol. 14, pp. 249-268.

Leys, B., Carcaillet, C., Dezileau, L., Ali, A.A. & Bradshaw, R.H.W. (2013) A comparison of charcoal measurements for reconstruction of Mediterranean paleo-fire frequency in the mountains of Corsica. *Quaternary Research*, vol. 79, pp. 337-349.

Lim, S., Ledru, M-P., Valdez, F., Devillers, B., Houngnon, A., Favier, C. & Bremond, L. (2014) Ecological effects of natural hazards and human activities on the Ecuadorian Pacific coast during the late Holocene. *Palaeogeography, Palaeoclimatology, Palaeoecology*, vol. 415, pp. 197–209.

Losiak, A., Wild, E.M., Huber, M.S., Wisniowski, T., Paavel, K., Jõeleht, A., Välja, R., Plado, J., Kriiska, A., Wilk, J., Zanetti, M., Geppert, W.D., Kulkov, A., Steier, P. & Pirkovic, I. (2015) Dating Kaali crater (Estonia) based on charcoal emplaced within proximal ejecta blanket. 46th Lunar and Planetary Science Conference. Abstract no. 1264.

Lovelock, J.E. (1988) *The Ages of Gaia: A Biography of our Living Earth*. Oxford University Press. 252 pp.

MacDonald, G.M., Larsen, C.P.S., Szeicz, J.M. & Moser, K.A. (1991) The reconstruction of boreal forest fire history from lake sediments: a comparison of charcoal, pollen, sedimentological, and geochemical indices. *Quaternary Science Reviews*, vol. 10, pp. 53-71.

Marlon, J.R., Bartlein, P.J., Walsh, M.K., Harrison, S.P., Brown, K.J., Edwards, M.E., Higuera, P.E., Power, M.J., Anderson, R.S., Briles, C., Brunelle, A., Carcaillet, C., Daniels, M., Hu, F.S., Lavoie, M., Long, C., Minckley, T., Ricard, P.J.H., Scott, A.C., Shafer, D.S., Tinner, W., Umbanhowar, C.E. & Whitlock, C. (2009) Wildfire responses to abrupt climate change in North America, *PNAS*, vol. 106, pp. 2519-2524.

Martill, D.M., Loveridge, R.F., Mohr, B.A.R. & Simmonds, E. (2012) A wildfire origin for terrestrial organic debris in the Cretaceous Santana Formation Fossil Lagerstätte (Araripe Basin) of north-east Brazil. *Cretaceous Research*, vol. 34, pp. 135-141.

McElwain , J. C. 1998. Do fossil plants signal palaeoatmospheric CO_2 concentration in the geological past? Philosophical Transactions of the Royal Society of London. Series B, Biological Sciences 353: 83– 96.

McElwain, J.C., Wade-Murphy, J. & Hesselbo, S.P. (2005) Changes in carbon dioxide during an oceanic anoxic event linked to intrusion into Gondwana coals. *Nature*, vol. 435, pp. 479-482.

McMichael, C.H., Bush, M.B., Piperno, D.R., Silman, M.R., Zimmerman, A.R. & Anderson, C. (2012a) Spatial and temporal scales of pre-Columbian disturbance associated with western Amazonian lakes. *The Holocene*, vol. 22. no. 2, pp. 131-141.

McMichael, C.H., Correa-Metrio, A. & Bush, M.B. (2012b) Pre-Columbian fire regimes in lowland tropical rainforests of southeastern Peru. *Palaeogeography, Palaeoclimatology, Palaeoecology*, vol. 342-343, pp. 73-83.

McParland, L.C., Collinson, M.E., Scott, A.C., Steart, D.C., Grassineau, N.V. & Gibbons, S.J. (2007) Ferns and fires: experimental charring of ferns compared to wood and implications for paleobiology, paleoecology, coal petrology, and isotope geochemistry. *Palaios*, vol. 22, pp. 528-538.

Mehlqvist, K., Vajda, V. & Larsson, L.M. (2009) A Jurassic (Pliensbachian) flora from Bornholm, Denmark – a study of a historic plant-fossil collection at Lund University, Sweden. *GFF*, vol. 131, pp. 137-146.

Millspaugh, S.H., Whitlock, C. & Bartlein, P.J. (2000) Variations in fire frequency and climate over the past 17 000 yr in central Yellowstone National Park. *Geology*, vol. 28, pp. 211-214.

Minnich, R.A. (2007) Climate, paleoclimate and paleovegetation. In: Barbour, M.G., Keeler-Wolf, T. & Schoenherr, A.A. (eds.) *Terrestrial Vegetation of California*, 3rd edition. University of California Press. pp. 43-70.

Mooney, S.D. & Tinner, W. (2011) The analysis of charcoal in peat and organic sediments. *Mires and Peat*, vol. 7, pp. 1-18.

Moore, P.D. (1989) No smoke without fire. *Nature*, vol. 342, pp. 226-227.

Moore, P.D., Chaloner, B. & Stott, P. (1996) *Global Environmental Change*. Wiley-Blackwell. 256 pp.

Moos, M.T. & Cumming, B.F. (2012) Climate–fire interactions during the Holocene: a test of the utility of charcoal morphotypes in a sediment core from the boreal region of north-western Ontario (Canada). *International Journal of Wildland Fire*, vol. 21, pp. 640-652.

Mustaphi, C.J.C. & Pisaric, M.F.J. (2014) A classification for macroscopic charcoal morphologies found in Holocene lacustrine sediments. *Progress in Physical Geography*, vol. 38, no. 6, pp. 734-754.

Nichols, G.J., Cripps, J.A., Collinson, M.E. & Scott, A.C. (2000) Experiments in waterlogging and sedimentology of charcoal: results and implications. *Palaeogeography, Palaeoclimatology, Palaeoecology*, vol. 164, pp. 43-56.

Orvis, K.H., Lane, C.S. & Horn, S.P. (2005) Laboratory production of vouchered reference charcoal from small wood samples and non-woody plant tissues. *Palynology*, vol. 29, pp. 1-11.

Ough, K. & Murphy, A. (2004) Decline in tree-fern abundance after clearfell harvesting. *Forest Ecology and Management*, vol. 199, pp. 153-163.

Patterson, W.A., III, Edwards, K.J. & Maguire, D.J. (1987) Microscopic Charcoal as a Fossil Indicator of Fire. *Quaternary Science Reviews*, vol. 6, pp. 3-23.

Perneger, T.V. (1998) What's wrong with Bonferroni adjustments. *BMJ*, vol. 316, pp. 1236-1238.

Pierce, J.L., Meyer, G.A. & Jull, A.J.T. (2004) Fire-induced erosion and millennial-scale climate change in northern ponderosa pine forests. *Nature*, vol. 432, pp. 87-90.

Pirard, E. (2004) Image Measurements. In: Francus, P. (ed.) *Image Analysis, Sediments and Paleoenvironments*. Springer. Dordrecht. pp. 59-86.

Preston, C.M. & Schmidt, M.W.I. (2006) Black (pyrogenic) carbon: a synthesis of current knowledge and uncertainties with special consideration of boreal regions. *Biogeosciences*, vol. 3, pp. 397-420.

Radley, J.D. & Allen, P. (2012) The non-marine Lower Cretaceous Wealden strata of southern England. *Proceedings of the Geologists' Association*, vol. 123, pp. 235-244.

Rasband, W.S. (2012) ImageJ [Computer program]. U. S. National Institutes of Health, Bethesda, Maryland, USA. Available at: http://imagej.nih.gov/ij/.

Rein, G. (2013) Smouldering Fires and Natural Fuels. In: Belcher, C.M. (ed.) *Fire Phenomena and the Earth System: An Interdisciplinary Guide to Fire Science.* Wiley-Blackwell. pp. 15-33.

Rhodes, A.N. (1998) A method for the preparation and quantification of microscopic charcoal from terrestrial and lacustrine sediment cores. *The Holocene*, vol. 8, no. 1, pp. 113-117.

Ridler, T.W. & Calvard, S. (1978) Picture thresholding using an iterative selection method. *IEEE Transactions on Systems, Man, and Cybernetics*, vol. 8, no. 8, pp. 630-632.

Rowe, J.S. & Scotter, G.W. (1973) Fire in the boreal forest. *Quaternary Research*, vol. 3, pp. 444-464.

Rummery, T.A. (1983) The use of magnetic measurements in interpreting the fire histories of lake drainage basins. *Hydrobiologia*, vol. 103, pp. 53-58.

Sander, P.M. & Gee, C.T. (1990) Fossil charcoal: techniques and applications. *Review of Palaeobotany and Palynology*, vol. 63, pp. 269-279.

Santín, C., Doerr, S.H., Kane, E.S., Masiello, C.A., Ohlson, M., de la Rosa, J.M., Preston, C.M. & Dittmar, T. (2015) Towards a global assessment of pyrogenic carbon from vegetation fires. *Global Change Biology*, doi: 10.1111/gcb.12985.

Scaramuzza dos Santos, Â.C., Holanda, E.C., de Souza, V., Guerra-Sommer, M., Manfroi, J., Uhl, D. & Jasper, A. (2016) Evidence of palaeo-wildfire from the upper Lower Cretaceous (Serra do Tucano Formation, Aptian-Albian) of Roraima (North Brazil). *Cretaceous Research*, vol. 57, pp. 46-49.

Schindelin, J., Arganda-Carreras, I., Frise, E., Kaynig, V., Longair, M., Pietzsch, T., Preibisch, S., Rueden, C., Saalfeld, S., Schmid, B., Tinevez, J.Y., White, D.J., Hartenstein, V., Eliceiri, K., Tomancak, P. & Cardona, A. (2012) Fiji: an open-source platform for biological-image analysis. *Nature Methods*, vol. 9, no. 7, pp. 676-682.

Scott, A.C & Glasspool, I.J. (2005) Charcoal reflectance as a proxy for the emplacement temperature of pyroclastic flow deposits. *Geology*, vol. 33, no. 7, pp. 589–592.

Scott, A.C. & Damblon, F. (2010) Charcoal: Taphonomy and significance in geology, botany and archaeology. *Palaeogeography, Palaeoclimatology, Palaeoecology*, vol. 291, pp. 1-10.

Scott, A.C. (2010) Charcoal recognition, taphonomy and uses in palaeoenvironmental analysis. *Palaeogeography, Palaeoclimatology, Palaeoecology*, vol. 1, pp. 11-39.

Shakesby, R.A. & Doerr, S.H. (2006) Wildfire as a hydrological and geomorphological agent. *Earth-Science Reviews*, vol. 74, pp. 269–307.

Sheskin, D.J. (2004) *Handbook of Parametric and Nonparametric Statistical Procedures*, 3rd edition. Chapman & Hall / CRC. 1184 pp.

Simmons, I.G. & Innes, J.B. (1988) Late Quaternary vegetational history of the North York Moors. X. Investigations on East Bilsdale Moor. *Journal of Biogeography*, vol. 15, pp. 299-324.

Singh, G., Kershaw, A.P. & Clark, R. (1981) Quaternary vegetation and fire history in Australia. In: Gill, A.M., Groves, R.H. & Noble, I.R. (eds.) *Fire and the Australian Biota*. Australian Academy of Science. Canberra. pp. 23-54.

Skog, J.E. (2001) Biogeography of Mesozoic Leptosporangiate Ferns Related to Extant Ferns. *Brittonia*, vol. 53, no. 2 (Papers from the Pteridophyte Biogeography Symposium, International Botanical Congress, April-June 2001), pp. 236-269.

Sonka, M., Hlavac, V. & Boyle, R. (1999) *Image Processing, Analysis, and Machine Vision*, 2nd edition. PWS Publishing. 770 pp.

Sporne, K.R. (1975) *The Morphology of Pteridophytes: The Structure of Ferns and Allied Plants*. Hutchinson & Co. London. 191 pp.

Summerfield, M.A. (1991) *Global Geomorphology: an introduction to the study of landforms*. Longman. Harlow. p. 199.

Svensen, H., Planke, S., Malthe-Sørenssen, A., Jamtveit, B., Myklebust, R., Eidem, T.R. & Rey, S.S. (2004) Release of methane from a volcanic basin as a mechanism for initial Eocene global warming. *Nature*, vol. 429, pp. 542-545.

Swain, A.M. (1973) A history of fire and vegetation in northeastern Minnesota as recorded in lake sediments. *Quaternary Research*, vol. 3, pp. 383-396.

Sweetman, S.C. & Insole, A.N. (2010) The plant debris beds of the Early Cretaceous (Barremian) Wessex Formation of the Isle of Wight, southern England: their genesis and palaeontological significance. *Palaeogeography, Palaeoclimatology, Palaeoecology*, vol. 292, pp. 409-424.

Théry-Parisot, I., Chabal, L. & Chrzavzez, J. (2010) Anthracology and taphonomy, from wood gathering to charcoal analysis. A review of the taphonomic processes modifying charcoal assemblages, in archaeological contexts. *Palaeogeography, Palaeoclimatology, Palaeoecology*, vol. 291, pp. 142-153.

Thevenon, F. & Anselmetti, F.S. (2007) Charcoal and fly-ash particles from Lake Lucerne sediments (Central Switzerland) characterized by image analysis: anthropologic, stratigraphic and environmental implications. *Quaternary Science Reviews*, vol. 26, pp. 2631-2643.

Tinner, W., Conedera, M., Ammann, B, Gaggeler, H.W., Gedye, S., Jones, R. & Sagesser, B. (1998) Pollen and charcoal in lake sediments compared with historically documented forest fires in southern Switzerland since AD 1920. *The Holocene*, vol. 8, no. 1, pp. 31-42.

Tinner, W. & Hu, F.S. (2003) Size parameters, size-class distribution and area-number relationship of microscopic charcoal: relevance for fire reconstruction. *The Holocene*, vol. 13, no. 4, pp. 499-505.

Tolonen, K. (1983) The post-glacial fire record. In: Wein, R.W. & MacLean, D.A. (eds.) *The Role of Fire in Northern Circumpolar Ecosystems.* John Wiley & Sons. pp. 21-44.

Tolonen, K. (1986) Charred particle analysis. In: Berglund, B.E. (ed.) *Handbook of Holocene Palaeoecology and Palaeohydrology.* John Wiley & Sons. pp. 485-496.

Tsai, W.-H. (1985) Moment-preserving thresholding: a new approach. *Computer Vision, Graphics, and Image Processing*, vol. 29, pp. 377-393.

Turney, C.S.M., Bird, M.I. & Roberts, R.G. (2001) Elemental $\delta^{13}C$ at Allen's Cave, Nullarbor Plain, Australia: assessing post-depositional disturbance and reconstructing past environments. *Journal of Quaternary Science* 16 (8) 779–784.

Umbanhowar, C.E., Jr. & McGrath, M.J. (1998) Experimental production and analysis of microscopic charcoal from wood, leaves and grasses. *The Holocene*, vol. 8, no. 3, pp. 341-346.

Umbanhowar, C.E. Jr., Camill, P., Geiss, C.E. & Teed, R. (2006) Asymmetric vegetation responses to mid-Holocene aridity at the prairie-forest ecotone in south-central Minnesota. *Quaternary Research*, vol. 66, pp. 53-66.

Vouk, V. (1948) Projected area of convex bodies. *Nature*, vol. 162, pp. 330-331.

Waddington, J.C.B. (1969) A stratigraphic record of the pollen influx to a lake in the Big Woods of Minnesota. *Geological Society of America Special Papers*, vol. 123, pp. 263-282.

Walsh, M.K., Pearl, C.A., Whitlock, C., Bartlein, P.J. & Worona, M.A. (2010) An 11 000-year-long record of fire and vegetation history at Beaver Lake, Oregon, central Willamette Valley. *Quaternary Science Reviews*, vol. 29, pp. 1093-1106.

Watson, A., Lovelock, J.E. & Margulis, L. (1978) Methanogenesis, fires and the regulation of atmospheric oxygen. *BioSystems*, vol. 10, pp. 293-298.

Watson, A.J. & Lovelock, J.E. (2013) The dependence of flame spread and probability of ignition on atmospheric oxygen: an experimental investigation. In: Belcher, C.M. (ed.) *Fire Phenomena and the Earth System: An Interdisciplinary Guide to Fire Science.* Wiley-Blackwell. pp. 273-287.

Weng, C. (2005) An improved method for quantifying sedimentary charcoal via a volume proxy. *The Holocene*, vol. 15, no. 2, pp. 298-301.

Willis, K.J. & McElwain, J.C. (2002) *The Evolution of Plants*. Oxford University Press. 378 pp.

Winkler, M.G. (1985) Charcoal analysis for paleoenvironmental interpretation: a chemical assay. *Quaternary Research*, vol. 23, pp. 313-326.

Whitlock, C. & Bartlein, P.J. (2004) Holocene fire activity as a record of past environmental change. *Development in Quaternary Science*, vol. 1, pp. 479-490.

Whitlock, C. & Larsen, C. (2001) Charcoal as a fire proxy. In: Smol, J.P., Birks, H.J.B. & Last, W.M. (eds.) *Tracking environmental change using lake sediments, Volume 3: Terrestrial, Algal, and Siliceous Indicators.* Kluwer Academic Publishers. pp. 75-97.

Wolbach, W.S., Gilmour, I. & Anders, E. (1990) Major wildfires at the Cretaceous/Tertiary boundary. In: Sharpton, V.L. & Ward, P.D. (eds.) Global catastrophes in Earth history. *Geological Society of America Special Papers*, vol. 247, pp. 391-400.

Zackrisson, O. (1977) Influence of forest fires on the North Swedish boreal forest. *Oikos*, vol. 29, pp. 22-32.

Zhang, D. & Lu, G. (2004) Review of shape representation and description techniques. *Pattern Recognition*, vol. 37, pp. 1-19.

Zimmerman, A.R. (2010) Abiotic and Microbial Oxidation of Laboratory-Produced Black Carbon (Biochar). *Environmental Science & Technology*, vol. 44, pp. 1295-1301.